

Archives
Closed
LD 1977
17546
A40K
Th
573

N94-4
4

MODELING OZONE CONCENTRATIONS USING METEOROLOGICAL VARIABLES

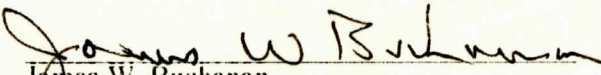
A Thesis

by


Terry Lee Thomas

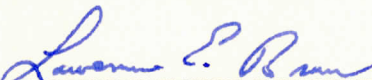
August 1990

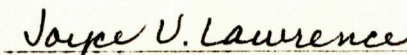
APPROVED BY:


James W. Buchanan
Chairperson, Thesis Committee


Thomas C. Rhyne
Member, Thesis Committee


Donald P. Olander
Member, Thesis Committee


Lawrence E. Brown
Chairperson, Department of Chemistry


Joyce V. Lawrence
Dean of Graduate Studies and Research

William Leonard Eury
Appalachian Collection

**MODELING OZONE CONCENTRATIONS
USING METEOROLOGICAL VARIABLES**

A Thesis

by

TERRY LEE THOMAS

Submitted to the Graduate School

Appalachian State University

in partial fulfillment of the requirements for the degree of

MASTER OF ARTS

August 1990

Major Department: Chemistry

ABSTRACT

Modeling Ozone Concentrations
Using Meteorological Variables. (August 1990)

Terry Lee Thomas

B. S., Campbell University

M. A., Appalachian State University

Thesis Chairperson: James W. Buchanan

Concern has been expressed in recent years concerning damage to vegetation, decline of forest growth, and human health problems that have been associated with tropospheric ozone. Because of this concern, it is important to have good estimates of ozone concentrations over wide geographic areas. Direct analysis for ozone is expensive, but meteorological data is low cost and universally available from local airports. It is therefore attractive to attempt to estimate ozone concentrations by means of these weather data in western North Carolina.

Average hourly ozone concentrations were 45 and 35 parts-per-billion (ppb) for 1988 and 1989, respectively. The maximum one-hour ozone concentration for 1988 occurred in mid-June with an average value of 78 ppb; while in 1989 the largest one-hour maximum occurred in April with an average value of 65 ppb. The mean daytime 12-hour ozone concentration averaged about 7 to 8 ppb higher than night time ozone concentration with the maxima occurring during June and April for 1988 and 1989, respectively. The year 1988 showed a typical seasonal variation in ozone, but 1989 had this largest ozone concentration at the beginning of the sampling season.

Those data were correlated with meteorological data obtained at the Hickory, NC airport. The statistical method used was a first order multiple linear regression model. A multiple linear regression equation was generated for each of the years 1988 and 1989. For both years, water vapor was a dominant, negatively correlated predictor of ozone. Temperature was also important,

and positively correlated. Cloud cover was not a significant predictor. Perhaps due to the high water content of the atmosphere during 1989, the equation generated for that year predicted ozone concentrations in Burke County, NC very well.

Acknowledgments

I wish to express my gratitude to my adviser, Dr. James Buchanan, without whose help and guidance this work would not have been possible. I also wish to express thanks to Dr. Thomas Rhyne for his valuable advice and assistance in the statistical and chemical aspects of this study and writing the thesis style sheet for the word processing program. I am also appreciative to Ms. Karen Callahan for her valuable assistance in the statistical aspects of this study. Deep appreciation is extended to the Duke Power Company, who provided instrumentation, technical assistance and a stipend for this project. Lastly many thanks to Ms. Evelyn Hess for the editorial work she performed. Thank you all.

Dedication

I would like to dedicate the following pages to my mother who has always supported me and encouraged me, and to those who follow in the path I have taken. Good luck.

Table of Contents

| | |
|---|----|
| Chapter 1 INTRODUCTION | 1 |
| 1.1 Photochemistry of the Troposphere | 2 |
| 1.1.1 Production and Destruction of Ozone | 2 |
| 1.1.2 The Role of Hydrocarbons | 4 |
| 1.2 Meteorological Modeling of Ozone Concentrations | 7 |
| 1.2.1 Utility of a Meteorological Model | 7 |
| 1.2.2 Previous Meteorological Models | 7 |
| 1.3 Purpose of this Study | 9 |
| Chapter 2 EXPERIMENTAL | 10 |
| 2.1 Overview | 10 |
| 2.2 Phase One: Sampling and Analysis | 10 |
| 2.2.1 Site | 11 |
| 2.2.2 Sampling System Configuration | 11 |
| 2.2.3 Analyzer Major Components and Operation | 13 |
| 2.2.3.1 Schematic Description and Operation of the Analyzer ... | 13 |
| 2.2.3.2 Radiation Source | 13 |
| 2.2.3.3 Absorption Cells | 15 |
| 2.2.3.4 Detectors | 15 |
| 2.2.3.5 Internal Calibration | 15 |
| 2.2.4 External Calibrator Major Components and Operation | 17 |
| 2.2.5 Treatment of Ozone Data | 17 |
| 2.2.5.1 Collection, Screening and Storage | 17 |

| | | |
|-----------|--|----|
| 2.2.5.2 | Quality Assurance | 17 |
| 2.2.5.3 | Meteorological Data | 18 |
| 2.3 | Phase Two: Statistical Analysis | 19 |
| 2.3.1 | Overview | 19 |
| 2.3.2 | Frequency | 19 |
| 2.3.3 | Multiple Linear Regression | 19 |
| 2.3.4 | Stepwise Search | 20 |
| 2.3.4.1 | Pearson Correlation | 20 |
| 2.3.4.2 | Coefficient of Determination | 20 |
| 2.3.4.3 | t Statistic and F statistic | 21 |
| 2.3.4.4 | Tolerance | 21 |
| 2.3.5 | Residual Statistic | 22 |
| 2.3.5.1 | Residual versus Predicted Residual Plots | 22 |
| 2.3.5.2 | Casewise plot | 22 |
| 2.3.5.3 | Histogram and Probability Residual Plots | 23 |
| 2.3.6 | Model Reliability | 23 |
| Chapter 3 | RESULTS | 24 |
| 3.1 | Descriptive Statistics for 1988 and 1989 Ozone Seasons | 24 |
| 3.1.1 | One-Hour Average Ozone Concentrations | 24 |
| 3.1.2 | Three-Hour Moving Averages | 27 |
| 3.1.3 | Twenty-Four-Hour Daily Averages and Moving Averages | 27 |
| 3.1.4 | Smoothing Techniques | 27 |
| 3.1.5 | Maximum One-Hour Ozone | 46 |
| 3.1.6 | One-Hour Maximum and 24-Hour Average Ozone | 46 |
| 3.1.7 | Twelve-Hour Day and Night Ozone Averages | 51 |
| 3.1.8 | Seven-Hour Ozone Averages | 51 |
| 3.1.9 | Diurnal Ozone | 56 |

| | |
|---|-----|
| 3.1.10 Monthly Average Ozone | 56 |
| 3.2 Meteorological Data for 1988 and 1989 | 63 |
| 3.2.1 Average Daily and 24-Hour Average Ambient Temperatures .. | 63 |
| 3.2.2 Twenty-four-Hour Average Water in the Atmosphere | 63 |
| 3.2.3 Twenty-four-Hour Average Cloud Cover | 67 |
| 3.3 Simple Linear Comparisons | 74 |
| 3.3.1 Twenty-Four-Hour Ozone versus Ambient Temperature, Water Vapor and Cloud Cover. | 74 |
| 3.4 Multiple Linear Regression to Predict Ozone | 74 |
| 3.4.1 1988 and 1989 MLR Equations as Predictor Model | 89 |
| Chapter 4 DISCUSSION AND CONCLUSIONS | 96 |
| References | 98 |
| Vita | 101 |

List of Figures

| | |
|---|----|
| Figure 2.1: Block diagram of site equipment and external flow. | 12 |
| Figure 2.2: Schematic of the Teco 49 UV spectrophotometer. | 14 |
| Figure 2.3: Daily Report and Daily three point calibration | 16 |
| Figure 3.1: One-hour ozone concentration frequency distribution for 1988. | 25 |
| Figure 3.2: One-hour ozone concentration frequency distribution for 1989. | 26 |
| Figure 3.3: Mean ozone three-hour moving average by day for 1988. | 28 |
| Figure 3.4: Mean ozone three-hour moving average by day for 1989. | 29 |
| Figure 3.5: Ozone three-hour moving averages frequency distribution for 1988. | 30 |
| Figure 3.6: Ozone three-hour moving averages frequency distribution for 1989. | 31 |
| Figure 3.7: Average 24-hour ozone for 1988. | 32 |
| Figure 3.8: Average 24-hour ozone for 1989. | 33 |
| Figure 3.9: Twenty-four-hour ozone averages frequency distribution for 1988. | 34 |
| Figure 3.10: Twenty-four-hour ozone averages frequency distribution for 1989. | 35 |
| Figure 3.11: Ozone 24-hour moving averages, computed from daily averages for 1988. | 36 |
| Figure 3.12: Ozone 24-hour moving averages, computed from daily averages for 1989. | 37 |
| Figure 3.13: Twenty-four-hour ozone averages for 1988, using a quadratic fit. | 38 |
| Figure 3.14: Twenty-four-hour ozone averages for 1989, using a quadratic fit. | 39 |

| | |
|---|----|
| Figure 3.15: Twenty-four-hour ozone averages for 1988, using a cubic fit. . . . | 40 |
| Figure 3.16: Twenty-four-hour ozone averages for 1989, using a cubic fit. . . . | 41 |
| Figure 3.17: Twenty-four-hour ozone averages for 1988, using a spline fit with Sm parameter 50. | 42 |
| Figure 3.18: Twenty-four-hour ozone averages for 1989, using a spline fit with Sm parameter 50. | 43 |
| Figure 3.19: Twenty-four-hour ozone averages for 1988, using a spline fit with Sm parameter 60. | 44 |
| Figure 3.20: Twenty-four-hour ozone averages for 1989, using a spline fit with Sm parameter 60. | 45 |
| Figure 3.21: Maximum one-hour ozone by day for 1988. | 47 |
| Figure 3.22: Maximum one-hour ozone by day for 1989. | 48 |
| Figure 3.23: One-hour maximum and 24-hour average ozone by day for 1988, using a spline fit with Sm parameter 60. | 49 |
| Figure 3.24: One-hour maximum and 24-hour average ozone by day for 1989, using a spline fit with Sm parameter 60. | 50 |
| Figure 3.25: Overlays of the ozone 12-hour averages, day (7 a.m.-6 p.m.) and night (7 p.m.-6 a.m.) for 1988, using a spline fit with Sm parameter 60. | 52 |
| Figure 3.26: Overlays of ozone 12-hour averages, day (7 a.m.-6 p.m.) and night (7 p.m.-6 a.m.) for 1989, using a spline fit with Sm parameter 60. | 53 |
| Figure 3.27: Seven-hour (10 a.m.-4 p.m.) ozone averages for 1988, using a spline fit with Sm parameter 60. | 54 |
| Figure 3.28: Seven-hour (10 a.m.-4 p.m.) ozone averages for 1989, using a spline fit with Sm parameter 60. | 55 |
| Figure 3.29: Seven-hour ozone averages frequency distribution for 1988. | 57 |
| Figure 3.30: Seven-hour ozone averages frequency distribution for 1989. | 58 |

| | |
|--|----|
| Figure 3.31: 1988 and 1989 Overlays of the mean diurnal cycles for Burke County, NC. | 59 |
| Figure 3.32: Mean diurnal ozone, by season, for 1988. | 60 |
| Figure 3.33: Mean diurnal ozone, by season, for 1989. | 61 |
| Figure 3.34: Monthly mean ozone concentrations for 1988 and 1989. | 62 |
| Figure 3.35: 1988 and 1989 average ambient temperatures by day. | 64 |
| Figure 3.36: Twenty-four-hour average ambient temperature for 1988, using a weighted least square smoothing curve with smoothing parameter 33.3. | 65 |
| Figure 3.37: Twenty-four-hour average ambient temperature for 1989, using a weighted least square smoothing curve with smoothing parameter 33.3. | 66 |
| Figure 3.38: Difference chart of average ambient and dewpoint temperatures for 1988. | 68 |
| Figure 3.39: Difference chart of average ambient and dewpoint temperatures for 1989. | 69 |
| Figure 3.40: Twenty-four-hour average water vapor for 1988, in torr, using a weighted least square smoothing curve with smoothing parameter 33.3. | 70 |
| Figure 3.41: Twenty-four-hour average water vapor for 1989, in torr, using a weighted least square smoothing curve with smoothing parameter 33.3. | 71 |
| Figure 3.42: Twenty-four-hour average cloud cover in percent by day, for 1988. | 72 |
| Figure 3.43: Twenty-four-hour average cloud cover in percent by day, for 1989. | 73 |
| Figure 3.44: Twenty-four-hour average ozone and ambient temperature by day, for 1988, using a spline fit with Sm parameter 1. | 76 |

| | |
|---|----|
| Figure 3.45: Twenty-four-hour average ozone and ambient temperature by day, for 1989, using a spline fit with Sm parameter 1. | 77 |
| Figure 3.46: Twenty-four-hour average ozone and water vapor by day, for 1988, using a spline fit with Sm parameter 1. | 78 |
| Figure 3.47: Twenty-four-hour average ozone and water vapor by day, for 1989, using a spline fit with Sm parameter 1. | 79 |
| Figure 3.48: Twenty-four-hour average ozone and cloud cover in percent by day, for 1988, using a spline fit with Sm parameter 1. | 80 |
| Figure 3.49: Twenty-four-hour average ozone and cloud cover in percent by day, for 1989, using a spline fit with Sm parameter 1. | 81 |
| Figure 3.50: Twenty-four-hour average ozone and average temperature by day, for 1988, with a weighted least square smoothing parameter of 33.3. | 82 |
| Figure 3.51: Twenty-four-hour average ozone and average temperature by day, for 1989, with a weighted least square smoothing parameter of 33.3. | 83 |
| Figure 3.52: Twenty-four-hour average ozone and average water vapor by day, for 1988, with a weighted least square smoothing parameter of 33.3. | 84 |
| Figure 3.53: Twenty-four-hour average ozone and water vapor by day, for 1989, using a weighted least square smoothing parameter of 33.3. | 85 |
| Figure 3.54: Twenty-four-hour average ozone and cloud cover by day, for 1988, with a weighted least square smoothing parameter of 33.3 | 86 |
| Figure 3.55: Twenty-four-hour average ozone and cloud cover by day, for 1989, using a weighted least square smoothing parameter of 33.3. | 87 |
| Figure 3.56: Daytime mean and predicted ozone for 1988, with a weighted least square smoothing parameter of 33.3. | 90 |

| | |
|---|----|
| Figure 3.57: Daytime mean and predicted ozone for 1989, with a weighted least square smoothing parameter of 33.3. | 91 |
| Figure 3.58: Twenty-four-hour mean and predicted ozone for 1988, with a weighted least square smoothing parameter of 33.3. | 92 |
| Figure 3.59: Twenty-four-hour mean and predicted ozone for 1989, with a weighted least square smoothing parameter of 33.3. | 93 |
| Figure 3.60: Comparison plots of the 1989 24-hour ozone and predicted ozone, computed with the 1988 multiple linear regression equation and using 1989 weather data. A weighted least square smoothing parameter of 33.3 is used. | 94 |
| Figure 3.61: Comparison plots of the 1988 24-hour ozone and predicted ozone, computed with the 1989 multiple linear regression equation and using 1988 weather data. A weighted least square smoothing parameter of 33.3 is used. | 95 |

List of Tables

| | |
|---|----|
| Table 3.1: Number of One-Hour Average Ozone Concentrations above 70, 80, 90, 100, and 110 ppb. | 24 |
| Table 3.2: Mean Day and Night Averages (6 a.m.-6 p.m., 6 p.m.-6 a.m., in ppb). | 51 |
| Table 3.3: Monthly Mean and Maximum 24-Hour Ozone for 1988 and 1989, in ppb. | 56 |
| Table 3.4: Seasonal Coefficients of Determination (R squared) for 1988 and 1989 Daytime and 24-Hour Seasonal Periods. | 88 |
| Table 3.5: Independent Variable Coefficients and Intercept Terms for 1988 and 1989. | 88 |
| Table 4.1: Reduction in Hourly Ozone from the Annual Mean, as a Function of Days when the Mean Atmosphere was saturated with Water Vapor. .96 | |

Chapter 1

INTRODUCTION

Concern has been expressed in recent years concerning damage to vegetation and decline of forest growth due to air pollutants. Lefohn and coworkers^{1,2,3}, Yang and colleagues⁴, and Peterson and Arbaugh⁵ attribute this damage to the major photochemical oxidant ozone. The term "photochemical oxidant" refers to a group of compounds that are formed during reactions of certain moieties which act as oxidant precursors in sunlight. Such precursors include nitric oxide and nitrogen dioxide, carbon monoxide, and hydrocarbons⁶.

Studies have shown that ozone is the leading contributor to about 1.8 billion dollars annual damage in crop loss and decline in forest production worldwide⁷. The National Ambient Air Quality Standard for ozone, set by the United States Environmental Protection Agency for the protection of human health, specifies that no single hourly average concentration should exceed 120 parts per billion (ppb)^{8,9,10}

Rural ozone levels are thought to be influenced by three major processes: stratospheric injection^{1,7,11}, long range transport¹¹, and photochemical production¹². Stratospheric injection is usually seen only during night time periods¹³. Stratospheric and tropospheric air are mixed during late winter and early spring¹. Since ozone sampling generally occurs from April to November, stratospheric injection is probably not a major factor in determining ozone concentrations during the sampling season.

Long range transport of ozone and oxidant precursors from the urban environment to the rural environment is possible under appropriate meteorological conditions. Under such conditions, high levels of pollutants can be transported several hundred miles, affecting rural

ozone concentrations¹³. The most important process, photochemical production, is dealt with in some detail below.

1.1 Photochemistry of the Troposphere

The chemistry of the troposphere vis-a-vis ozone concentrations has been a subject of considerable debate. The primary reactions for formation and destruction of ozone will be discussed below.

1.1.1 Production and Destruction of Ozone

Ozone is produced and destroyed in the troposphere by several mechanisms. Chameides and Davis¹² have outlined the essential components of the chemistry of the troposphere as a variety of biological and geological processes which result in the emission of gases from the earth's surface to the atmosphere. In spite of the complexity of biospheric surface emissions, the vast majority of gaseous trace species emitted into the atmosphere are in a reduced oxidation state. Materials returning to the earth, usually by dissolution in raindrops or by dry deposition, are highly oxidized. Highly reactive free radical species are recognized as being responsible for these oxidations. Because free radicals have an unpaired electron and an affinity for adding a second electron, they can act as strong oxidizers of atmospheric trace gases. Of the free radicals present in the atmosphere, the hydroxyl species appears to be the most significant in tropospheric photochemistry¹¹.

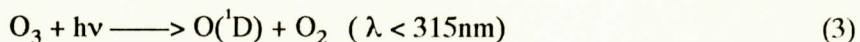
The production of hydroxyl radical occurs primarily by photolysis of ozone. Photons of wavelengths between 315 and 1200 nanometers (nm) dissociate ozone and produce molecular oxygen and atomic oxygen^{12,14,15,16} via reaction 1.



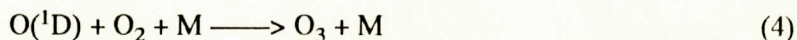
Regeneration of ozone can rapidly occur, with ground state atomic oxygen (³P) atoms immediately combining with molecular oxygen and a third body energy sink, M^{12,15}.



This yields a null (net zero ozone) cycle. When ozone absorbs radiation of wavelengths shorter than 315 nm, metastable atomic oxygen $\text{O}({}^1\text{D})$ is produced.



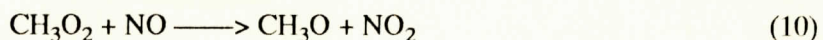
In the lower atmosphere $\text{O}({}^1\text{D})$ most often collides with nitrogen or oxygen molecules and is converted to $\text{O}({}^3\text{P})$. Singlet-D atomic oxygen may also combine with O_2 as in reaction 4, yielding another null cycle.



Most importantly, singlet-D atomic oxygen also reacts directly with water to produce the hydroxyl (OH) radical, this being the primary source of production of OH in the troposphere.



Chameides and Davis¹² suggest that the photochemistry of the unpolluted troposphere develops around a chain reaction sequence involving methane (CH_4), carbon monoxide (CO), and oxides of nitrogen (NO_x). Hydroxyl radicals react in the clean troposphere to yield hydroperoxyl (HO_2) and methyl peroxy (CH_3O_2) radicals, as in the following reactions:



According to Finlayson-Pitts and Pitts¹⁴, the major atmospheric sink for CH_4 is reaction 6. The chemistry of the methyl peroxy radical (CH_3O_2) and its products is complex and mechanisms are not fully understood¹².

Chemical reactions initiated by the photolysis of nitrogen dioxide (NO_2) provide the basis for the tropospheric synthesis of ozone¹⁷. The reaction sequence for ozone production involves oxidizing nitric oxide (NO) to NO_2 . Reactions which contribute to formation and destruction of ozone are:



Reactions 12-15 govern ozone concentration levels present in the sunlight-irradiated atmosphere. Because of reaction 15 an ozone concentration buildup occurs only after NO has fallen to a low concentration¹⁸. Worth and Ripperton¹⁸ suggest that reactions 13-15 are cyclic in nature and yield no net ozone. However, in the dark the destruction of ozone by NO continues. Studies indicate that in rural environments concentrations of NO_x are not high enough to materially affect ozone^{9,18}.

By using fossil fuels and wood as sources of heat, society produces large quantities of CO and NO. Although a buildup of CO causes a decrease in OH radical (reaction 7), nitric oxide tends to increase the concentration of OH, affecting ozone concentrations¹² (reactions 12-15).

In a polluted atmosphere OH radical derives from several reactions, including the photolysis of nitrous acid (HONO) and hydrogen peroxide (H₂O₂).



Some researchers suggest that the OH produced in reaction 17 can lead to the chain termination reaction^{12,15,19,20}



In summation in the rural troposphere, ozone formation occurs by photolysis of NO₂ with subsequent combination of molecular and atomic oxygen, either O(³P) or O(¹D), as in reaction 13 and 14. The primary path for destruction of ozone is via reaction 1 and 15.

1.1.2 The Role of Hydrocarbons

Uncertainty exists concerning the contribution that natural organic emissions make to the photochemical ozone production cycle. Methane is the single most important naturally-produced organic compound emitted by vegetation¹⁴. However, Graedel cites 367 other organics which are

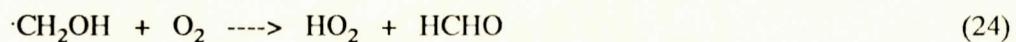
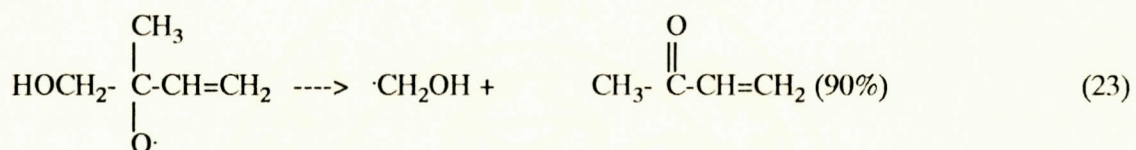
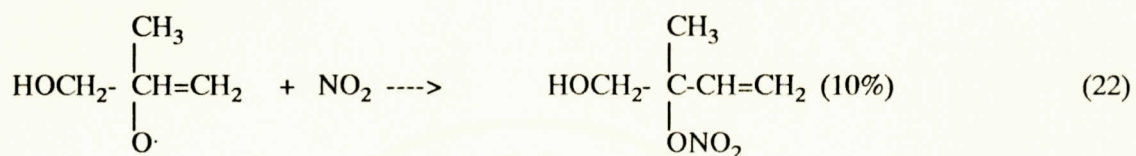
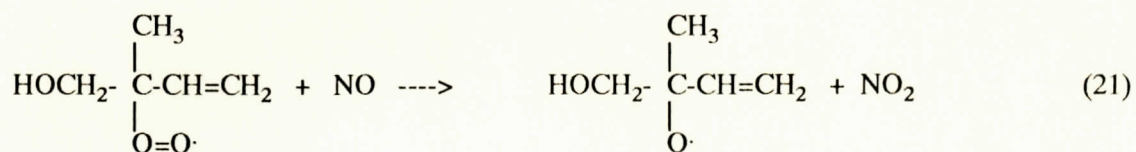
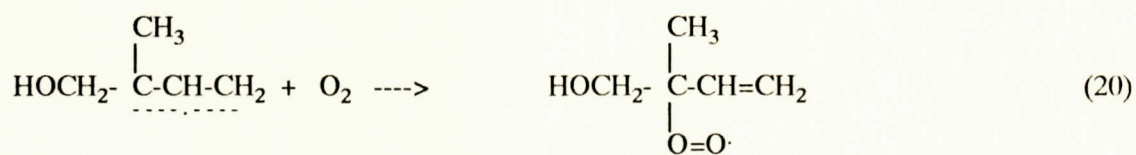
emitted by vegetation²¹. In the presence of olefins such as isoprene and monoterpenes, higher ozone concentrations may be produced¹⁴. The hydrocarbons are not themselves photoreactive, but are highly reactive with other photochemical products. These products interfere with ozone decomposition reactions, yielding an increase in ozone concentrations^{17,22}.

The natural decomposition of vegetation through microbial action appears to contribute significantly to production of ozone precursors. Decomposing vegetation is considered to be the largest natural source of hydrocarbons⁷. Isoprenes and monoterpenes are emitted by a variety of plants and trees, with the emission rates governed by temperature, amount of water vapor, and other daily and seasonal factors. Monoterpenes, emitted primarily by conifers, occur in greater concentrations as temperature and water vapor increase^{9,17,23}. Altshuller²⁴ suggests that the highest emission rates for monoterpenes occur in the southeastern part of the United States during midsummer. Concentrations of monoterpenes in the atmosphere have been found to be in the range of 10-100 ppb in forested areas^{16,23,24}.

Isoprenes, emitted primarily by deciduous trees during the daytime, tend to increase with temperature and decrease with water vapor. Studies indicate that isoprenes react much faster with OH radicals than do other terpenes¹⁴. Trainer and coworkers²² used a one-dimensional planetary boundary layer model that includes isoprene photochemistry to evaluate the effects of natural hydrocarbons on the formation of rural ozone. Their results suggest that if isoprene emission is included, concentrations of HO₂ and organic peroxy radicals are increased, resulting in a strong buildup of ozone. Although mechanisms for the reactions of isoprene and monoterpenes are not fully understood, a proposed mechanism includes oxidation of isoprene by addition of OH radical



The free electron is delocalized over the adjacent bonds, and addition of oxygen followed by reaction with NO is expected under atmospheric conditions, yielding a variety of products¹⁴.



As a result of this oxidation, nitric oxide concentrations are reduced and ozone concentrations are increased.

Trainer and coworkers²² have made a case that terpenes are a consumer of ozone rather than a producer, forming aerosols which scavenge ozone. Other studies have also suggested that these hydrocarbons act as sinks for ozone²³. Chameides and Davis¹² state that a small amount of ozone reacts directly with higher olefinic hydrocarbons. Various products can be formed from these reactions. Ozonolysis of the compounds can occur, as well as production of biradicals formed by the Criegee mechanism²³.

1.2 Meteorological Modeling of Ozone Concentrations

Ozone concentrations in rural areas have been estimated by several approaches, including limited measurements at rural sites and calculated results from tropospheric photochemical models²⁴. Due to the high cost of ozone monitoring and the necessarily limited number of monitoring sites, modeling techniques have become the usual means of estimating ozone concentrations over wide rural areas.

1.2.1 Utility of a Meteorological Model

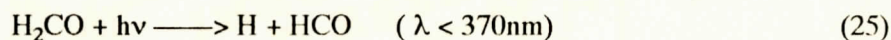
The objective of any statistical model is to provide the user with the means of predicting natural variables with reasonable accuracy, relative ease, and some degree of generality. It is attractive to attempt to predict rural ozone concentrations by means of weather variables, since these parameters are low cost, universally reported and recorded, and are easily obtained from the National Weather Service. Recently the use of meteorology in modeling ozone concentration has had limited application.

1.2.2 Previous Meteorological Models

W. D. Bach²⁵ correlated ozone and meteorological parameters on a day-to-day basis. He found that ozone concentrations rose steadily prior to frontal passage, then decreased rapidly. Bach and other researchers found that high ozone concentrations were associated with slower moving air generally found in an area of high pressure^{15,18,25}. The weather conditions under a high-pressure system are characterized as having disorganized wind flow, little movement of air into or out of a given geographical region, and clear to partly cloudy skies. These are optimum conditions for photochemical generation of ozone¹⁸. His findings, along with those of other researchers, suggest that the best correlations exist among ozone concentration, water vapor content of the air, and ambient temperatures^{17,18,25}.

Pagnotti statistically correlated ozone and upper air temperatures above an urban environment. His findings suggest that long periods of elevated temperatures are accompanied by long periods of high ozone. Results indicate that elevated temperatures occurred during years with high ozone concentrations, such as in 1983, 1987, and 1988. He suggests that chronic high ozone concentrations can appear when prolonged conducive meteorological air patterns develop²⁶.

In spite of the small volume of condensed water in the atmosphere¹⁹, reactions occurring in the aqueous phase may be important to tropospheric chemistry. Model calculations conducted by Lelieveld and Crutzen²⁰, suggest that aqueous-phase reactions in clouds strongly affect the ozone budget in the troposphere. Their findings indicate that when models do not consider aqueous-phase reactions, an overestimation of 60-70 percent in ozone concentrations occurs. They suggest that formaldehyde is an important precursor of HO₂ and CO in gas phase reactions, through photodissociation as in reaction 25, and subsequently via reactions 9 and 26.



The HO₂ radical, which is very soluble in water, reacts with OH in clouds via reaction 27.



Reaction 27 significantly reduces OH and HO₂ concentrations in the gas phase. Also, dissolved ozone can react with high concentrations of hydrogen peroxide existing in cloud vapor²⁰ as in reaction 28.



Other studies using meteorological parameters have been attempted. For example, some studies have used upper air measurements obtained by airplanes, sampling and monitoring ozone concentrations and upper air weather data^{13,18}. One study used weather balloon instruments to measure water vapor and temperature profiles vertically in the atmosphere¹⁵, and another used a UV Differential Absorption Lidar System. This latter system provides simultaneous, range

resolved ozone concentrations and aerosol back scatter profiles in the upper troposphere²⁷. The methodologies these researchers used cannot be applied directly to this project.

1.3 Purpose of this Study

There is growing concern regarding forest decline, crop loss, and human health problem attributable to ozone. Because ozone concentrations appear to fluctuate with prevailing weather patterns, it is important that the relationships between weather and ozone concentrations be better understood. Direct measurements of ozone are expensive so extensive ozone concentration profiles over rural areas are not available. Weather data are relatively inexpensive and are available from regional airports. The purpose of this project then is to attempt to discover weather parameters that may correlate with ozone concentrations and use these to quantitatively model ozone concentrations at a rural site.

Chapter 2

EXPERIMENTAL

2.1 Overview

The experiment consisted of two phases. Phase One dealt with air sample collection and analysis, and data storage and retrieval. Ambient air was sampled and analyzed at a rural site in Burke County, North Carolina, from April to November of 1988 and 1989. Data were stored on-site by a data logger. Retrieval was accomplished by telemetric link to a microcomputer, using an automated data retrieval program.

Phase Two involved statistical treatment of the data by the Statistical Package for the Social Sciences (SPSS), mounted on the mainframe computer at Appalachian State University. Ozone concentrations were correlated with meteorological data. The statistical method used was a multiple linear regression (MLR) model.

2.2 Phase One: Sampling and Analysis

The following section will detail various aspects by which the data were collected and a description of the instruments used to measure ambient ozone concentrations. Siting and various components of the instrumentation will be discussed in detail.

2.2.1 Site

The site was located in a rural area of Burke County, North Carolina, just off Highway 126, approximately 5 miles west of Morganton, NC. The building was located approximately 46 meters from the highway. Siting criteria for continuous monitoring of ozone met requirements dictated by the United States Environmental Protection Agency (US-EPA)²⁸. Instruments were housed in a mobile 12'X12' thermostatically controlled building. The inside temperature was kept at about 25 °C during the sampling period.

The sample inlet was mounted on a hollow telescoping aluminum pole approximately 11 meters above ground level, providing continuous sampling at the top of the tree canopy. Air flow was unrestricted around the inlet. The inlet was an inverted plastic funnel attached to the top of the mast with 0.25 inch o.d. FEP Teflon tubing.

2.2.2 Sampling System Configuration

A Thomas Industries Vacuum Pump Model 2107B420 was used to pull ambient air into the inlet and to a manifold positioned on the back interior wall of the building. The manifold provided a dump by-pass to allow the gas to equilibrate to atmospheric pressure. (A dump by-pass is a large bell jar into which ambient air flows). Heated 0.25 inch o.d. FEP Teflon tubing was used to prevent condensation of water. In-line to the analyzer was a 5-10 micron Teflon particle filter. The air passed into the sample inlet located on the back of the Thermo Electron Model 49 Ultraviolet Photometric Ozone Analyzer (Teco 49). Exhaust was vented to the outside of the building. Figure 2.1 is a flow diagram for the system.

Zero air for calibration was produced by irradiating ambient air with UV radiation to convert NO to NO₂, then passing the air through a system of scrubbing filters to remove NO₂, SO₂, and hydrocarbons. The filter system consisted of a Perma-Pure dryer followed by a column of indicating silica gel and a large column of activated charcoal. A quartz filter removed any particles which originated from the scrubbing filters. The air then passed through the ozone catalytic converter filter system, which converts ozone to oxygen by surface contact. A capillary

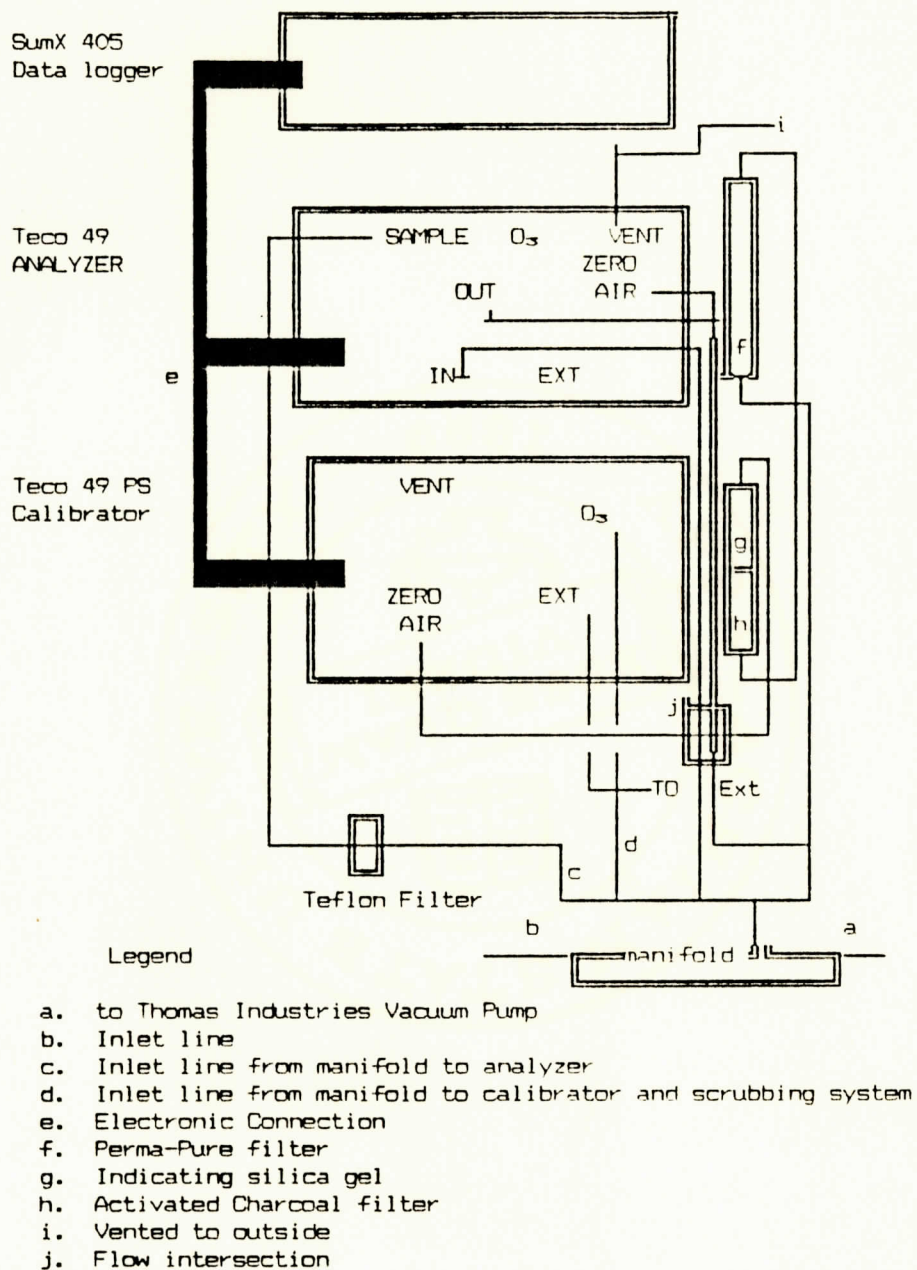


Figure 2.1: Block diagram of site equipment and external flow.

reduced the flow to 1 liter-per-minute to ensure sufficient residence time in the converter. Flow was monitored by a rotameter.

2.2.3 Analyzer Major Components and Operation

2.2.3.1 Schematic Description and Operation of the Analyzer

Ozone displays a strong absorption in the UV region between 200-300 nanometers (nm), with peak absorption occurring between 250-260 nm²⁸. The Teco 49 determines ozone concentrations

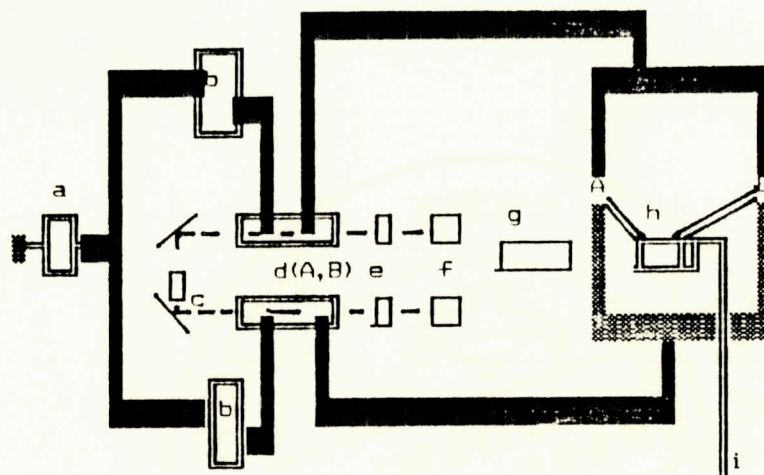
in ambient air every 10 seconds in the following way: the attenuation of 254 nm radiation by zero air in absorption cell A establishes a zero light intensity (I_0) (See Figure 2.2). The ambient sample passes through absorption cell B to establish a sample light intensity (I). The ratio (I/I_0) is the attenuation of 254 nm radiation by ozone in the sample. Ozone concentration is directly proportional to the magnitude of this attenuation, as given by the Beer-Lambert Law.

$$\log (I_0/I) = abC \quad (29)$$

where $\log (I_0/I)$ is the absorbance of the species, a is the absorptivity of the absorbing species, b is the pathlength of the cell, and C is the concentration of the ambient ozone. The photometer's cells and detectors operate 180 degrees out of phase but synchronously; that is, when cell A contains the reference, cell B contains the ambient sample and vice versa²⁸.

2.2.3.2 Radiation Source

The Teco 49 uses a low pressure mercury vapor lamp which has 99.5 percent of its intensity at the 254 nm line, and no output at the ozone forming line of 185 nm. The lamp is driven by a precisely regulated power supply, and is mounted in a temperature controlled insulated aluminum block to provide thermal stability.



Legend

- a. Pump leading to exhaust
- b. Flow meters
- c. Source
- d. Absorption Cell A and B
- e. Detectors
- f. Voltage to frequency converter
- g. Digital Electronics
- h. Converter
- i. Sample inlet
- A. Solenoid A
- B. Solenoid B

Figure 2.2: Schematic of the Teco 49 UV spectrophotometer.

2.2.3.3 Absorption Cells

Dual absorption cells are used, with each cell having a pathlength of 37.84 centimeters. The cells are coated with polyvinylidene fluoride to ensure that no ozone undergoes decomposition upon exposure to the surfaces of the cells²⁸.

2.2.3.4 Detectors

Dual detectors share the same source. "Solar blind" vacuum photodiodes are used. (The photodiode is sensitive to UV light but not to visible radiation with wavelength greater than 300 nm). To ensure that the detector signal maintains a high degree of stability, it and its associated electronics are mounted in an insulated enclosure. All electrical lines are shielded and held to minimum length.

2.2.3.5 Internal Calibration

The Teco 49 has an internal ozonator which generates ozone for a nightly three-point calibration. Ozone concentrations generated were typically 0, 80, and 800 parts-per-billion (ppb). Response by the analyzer was reported on the daily ozone report. If the response differed by five percent or more from the generated concentrations, corrective action was taken. Figure 2.3 displays an example of this calibration report. Where O₃ is the ozone concentration in ppb; TMP is the ambient temperature inside the building in °C; and VDC is a reference voltage. THEORETICAL values are generated by the internal ozonator and ACTUAL values are those measured by the analyzer.

PREVIOUS DAILY SUMMARY 04/12/89 102 (WP)MORGANTON

| COLUMN NUMBER | 01 | 02 | 03 |
|----------------|----|-----|-----|
| CHANNEL NUMBER | 01 | 02 | 03 |
| CHANNEL NAME | 03 | TMP | VDC |

| | | | |
|-------|-----|------|-------|
| 01:00 | 33 | 24.9 | 1.475 |
| 02:00 | 34 | 25.3 | 1.475 |
| 03:00 | 33 | 25.1 | 1.475 |
| 04:00 | 32 | 25.1 | 1.475 |
| 05:00 | 28 | 25.2 | 1.475 |
| 06:00 | 25 | 25.2 | 1.475 |
| 07:00 | 21 | 25.3 | 1.475 |
| 08:00 | 23 | 25.4 | 1.475 |
| 09:00 | 24 | 25.4 | 1.475 |
| 10:00 | 32 | 25.2 | 1.475 |
| 11:00 | 42 | 26.1 | 1.475 |
| 12:00 | 44 | 27.4 | 1.473 |
| 13:00 | 52 | 28.5 | 1.473 |
| 14:00 | 58 | 28.2 | 1.473 |
| 15:00 | 60 | 28.0 | 1.473 |
| 16:00 | 59 | 28.0 | 1.473 |
| 17:00 | 60 | 27.9 | 1.473 |
| 18:00 | 63 | 28.0 | 1.473 |
| 19:00 | 62 | 28.0 | 1.473 |
| 20:00 | 58 | 28.1 | 1.473 |
| 21:00 | 58 | 28.0 | 1.473 |
| 22:00 | 51 | 28.1 | 1.473 |
| 23:00 | 49< | 27.6 | 1.473 |
| 00:00 | 44< | 27.1 | 1.473 |

AVERAGE 44< 26.7 1.473

CALIBRATION-RESULTS

| COLUMNS # & NAME | LEVEL 0 | LEVEL 1 | LEVEL 2 | LEVEL 3 |
|------------------|---------|---------|---------|---------|
|------------------|---------|---------|---------|---------|

| | | | | |
|--------------|-------------|-----|------|-----|
| 01 03 ACTUAL | -1B | 83B | 797B | |
| | THEORETICAL | -1 | 78 | 794 |

>

Figure 2.3: Daily Report and Daily three point calibration

2.2.4 External Calibrator Major Components and Operation

The Teco 49 Primary Standard (PS) is the companion external calibration unit for the Teco 49 analyzer. It operates on the photolytic principle that the ozone concentration produced is a direct proportion of the radiation intensity at 185 nm. The radiation intensity is changed by varying the current into the UV mercury vapor lamp. The Teco 49 and Teco 49 PS are absorption photometers with internal ozonators. Both have identical system configurations. During a multipoint calibration the Teco 49 PS generates and analyzes a sample with known ozone concentration, then transfers this sample to the analyzer.

2.2.5 Treatment of Ozone Data

2.2.5.1 Collection, Screening and Storage

A SumX-405 data logger was used for storage of the hourly ozone averages. The SumX-405 is a self-contained data storage processor. The data can be accessed either through a real time printer at the site, or through telemetric link with a microcomputer. The data logger performs an editing function, flagging and invalidating data.

Flags used were: (F), to indicate that there was a power failure for the system; (D), a parameter marked down as system maintenance was performed; (B), bad status due to some internal problem with the instrumentation; and (<), to indicate an average has missing data.

Figure 2.3 is an example of the daily reports generated by the SumX-405²⁹.

Data were stored in the internal memory of the SumX-405 for fifteen consecutive days. Additional storage for the sampling season was on a backup DC 100 magnetic data cartridge produced by the 3M Company, designed for harsh environments.

2.2.5.2 Quality Assurance

a. Multi-point Calibration

Calibrations were performed at the beginning and end of the sampling period, and at least every 60 days during the period. A calibration was required when the system was removed for maintenance. Calibrator and analyzer output were subjected to a linear regression analysis. Acceptable results of a regression were: slope within ± 15 percent of unity, intercept within three percent of analyzers' range, and correlation coefficient greater than 0.9950³⁰. All calibrations were well within acceptable limits.

b. Audit Calibration

An independent calibration audit was performed each year by the ZEDEK Corporation. The analyzer was audited against a Dasibi 1003-AH photometric certified transfer standard instrument. All external calibrations were within acceptable limits.

c. Spike Removal

The data were scanned visually and by the computer to check for spikes. A spike was defined in this study as an hourly average which was 25 ppb greater than both the previous and succeeding averages. Spikes were removed from 1988 data, but on recommendation from Duke Power Company, the funding organization for this study, they were retained in 1989 data. Duke Power was concerned that some exceedances from US-EPA upper limit concentrations could inadvertently be removed from the data base.

2.2.5.3 Meteorological Data

Meteorological data were furnished by the National Weather Service Climatological Center located at Asheville, North Carolina. The data consisted of hourly weather observations reported by the regional airport at Hickory, North Carolina. Air temperature, dewpoint temperature, and total cloud cover were the variables originally chosen to be correlated with the ozone data.

2.3 Phase Two: Statistical Analysis

2.3.1 Overview

The data were analyzed using the Statistical Package for the Social Sciences (SPSS) and SAS. A multiple linear regression (MLR) ozone prediction statistical model was developed using meteorological parameters as independent variables. Standard statistical procedures were used to check for data characteristics. A stepwise search was used to select the best variables to be included in the model. Various standard diagnostic plots and statistics were used to identify departures from the model. The final statistical model was generated and tested for its predicting ability.

2.3.2 Frequency

A frequency distribution provided the mean, standard deviation, and nature of distribution of the data base. The distribution was determined, and transformation of variables was computed, if necessary, to establish normality (Gaussian distribution). Scatter plots were generated to determine any evident relationships.

2.3.3 Multiple Linear Regression

A first order multiple linear regression statistical model was used to determine the variability in the ozone accounted for by the independent variables. The MLR equation generated was

$$\text{OZONE} = \beta_0 + \beta_1 \text{temp} + \beta_2 \text{VP} + \beta_3 \% \text{cloud} \quad (30)$$

where ozone is the dependent variable, and the independent variables are ambient air temperature, dewpoint temperature, and %cloud cover. β_0 is the intercept and $\beta_{1,2,3}$ are the coefficients. The method of least-squares was used to fit the independent variables to the regression line. A coefficient of determination was used to indicate the ozone variability

accounted for by the equation. To obtain the best fit a variable search and test procedure was conducted. Analysis of residuals was used to test how well the calculated regression fit the data. The statistical regression model chosen was then subjected to a different data base to test for generality.

2.3.4 Stepwise Search

An “all possible regressions” stepwise search on the independent variables was conducted to determine which variables to include in the MLR equation. Several tests used by the stepwise search for variable addition or removal ensured that no regression assumptions had been violated³¹.

2.3.4.1 Pearson Correlation

A Pearson correlation matrix was computed to display the correlation between the dependent and independent variables. The matrix also provided an indication of the amount of correlation among the independent variables. Highly correlated independent variables tend to inflate the variance of the model. The relative importance of each variable can be obtained from the correlation matrix. The first variable used was the variable with the largest positive or negative correlation.

2.3.4.2 Coefficient of Determination

The coefficient of determination, which is the square of the correlation coefficient R , is a measure of the goodness of fit of the independent variables in the equation. Coefficients of determination provide an estimate of how well the model fits the data population, and provides an indication of the amount of variability in the dependent variable that is explained by the independent variable.

2.3.4.3 t Statistic and F statistic

The t statistic tests for linearity. All independent variables in the equation were analyzed by the t statistic to test the hypothesis that there was no linear relationship between pairs of the variables. If a variable displayed a small level of significance or confidence level of the t statistic test, a linear relationship existed.

The F statistic is defined as a linearity test between the dependent and all independent variables. The F statistic tested the hypothesis that the coefficients of the entered variables are equal to 0 i.e., $\beta_1=\beta_2=\beta_3=0$, where β is defined as the partial regression coefficient or the coefficients of the variables. If the regression assumptions were met, the probability associated with the F statistic was small so the null hypothesis that the coefficient of determination equals zero was rejected.

The first variable was entered into the equation based on its correlation value. The F statistic test was calculated. This variable and any remaining variables were entered only if the F and t tests indicated linearity of the dependent variable with respect to the added independent variable. The second variable was selected based on the next highest partial correlation. Next, the first variable was examined to see if it should now be removed. All variables not in the equation were also re-examined for entry or removal. Variable selection terminated when no variables met entry or removal criteria.

2.3.4.4 Tolerance

Several measures were taken to warn of correlation of independent variables. The Pearson correlation matrix indicates correlation of the independent variables. Large values of the Pearson correlation coefficients for two independent variables indicate a high degree of correlation. For cases where the correlation coefficients are small but there is still correlation, the variables must pass both a tolerance and a minimum tolerance test. Tolerance is the proportion of variability in an independent variable not explained by the other independent variables. It is

calculated by $1 - (\text{coefficient of determination})$. If the tolerance of the variable was less than 0.0001, a warning was issued and the variable was not entered into the equation. Minimum tolerance of a variable is the smallest tolerance any variable already in the analysis would have if that variable were included in the analysis. A variable must pass both tolerance and minimum tolerance tests in order to enter a regression equation³².

2.3.5 Residual Statistic

Analysis of the residuals by analysis of variance provided an idea of how well the calculated regression line actually fit the data. In statistical model building, residuals are defined as what is left after the model is fitted. Four temporary variables were computed and analyzed: predicted ozone, residual ozone, standardized residual ozone, and standardized predicted ozone. A standardized variable is a variable divided by the standard deviation of the residuals. Standard residuals have a mean of zero and a standard deviation of one. Several plots were produced using these variables to determine whether the assumptions of linearity, homogeneity of variance (that the variances are equal), and normality had been violated.

2.3.5.1 Residual versus Predicted Residual Plots

Residuals were plotted versus predicted ozone, providing indications of linearity and homogeneity of variance. If the hypothesis of linearity and homogeneity of variance are met, no trends will be seen in the plots. For linearity the variance of Y for all Xs is constant. If the spread of the residuals increases or decreases with values of the independent variable, or with the predicted ozone values, the hypothesis of homogeneity of variance is suspect.

2.3.5.2 Casewise plot

A casewise plot of standardized residuals by sequence provided an indication of the independence of error terms. Since time is not considered a variable in the model, it could influence the residuals. If sequence and residual are independent, a pattern is not seen in the

casewise plot. The plot also provides a measure of how much the residuals deviate from the mean.

2.3.5.3 Histogram and Probability Residual Plots

A histogram of the standardized residuals was plotted to determine distribution. The plot of the observed residuals versus the expected residual's probability was an indicator for normality. A plot displaying a straight diagonal line verified the assumption of normality.

2.3.6 Model Reliability

The ability of the statistical model to predict ozone concentration was tested against experimentally measured concentrations obtained during the 1988 and 1989 sampling seasons.

Chapter 3

RESULTS

3.1 Descriptive Statistics for 1988 and 1989 Ozone Seasons

Data were collected from April 1 to November 1, 1988, and from April 3 to November 13, 1989. There were 5,019 and 4,692 hourly averages collected in 1988 and 1989, respectively. The ozone data were broken down in a variety of ways and analyzed statistically. Each type of analysis will be discussed individually.

3.1.1 One-Hour Average Ozone Concentrations

Figures 3.1 and 3.2 display the average one-hour ozone concentration frequency distributions. During the two years of sampling there were no valid exceedances of the National Ambient Air Quality Standard unacceptable hourly maximum of 120 ppb. Table 3.1 shows the number of hourly average cases above 70, 80, 90, 100, and 110 ppb for 1988 and 1989. The most frequent hourly averages for 1988 were between 30 and 39 ppb, while for 1989 they were between 20 and 29 ppb. Mean hourly ozone was 45 and 35 ppb in 1988 and 1989, respectively.

Table 3.1: Number of One-Hour Average Ozone Concentrations above 70, 80, 90, 100, and 110 ppb.

| <u>Ozone (ppb)</u> | <u>1988</u> | <u>1989</u> |
|--------------------|-------------|-------------|
| ≥70 | 546 | 32 |
| ≥80 | 226 | 5 |
| ≥90 | 91 | 2 |
| ≥100 | 49 | 0 |
| ≥110 | 16 | 0 |

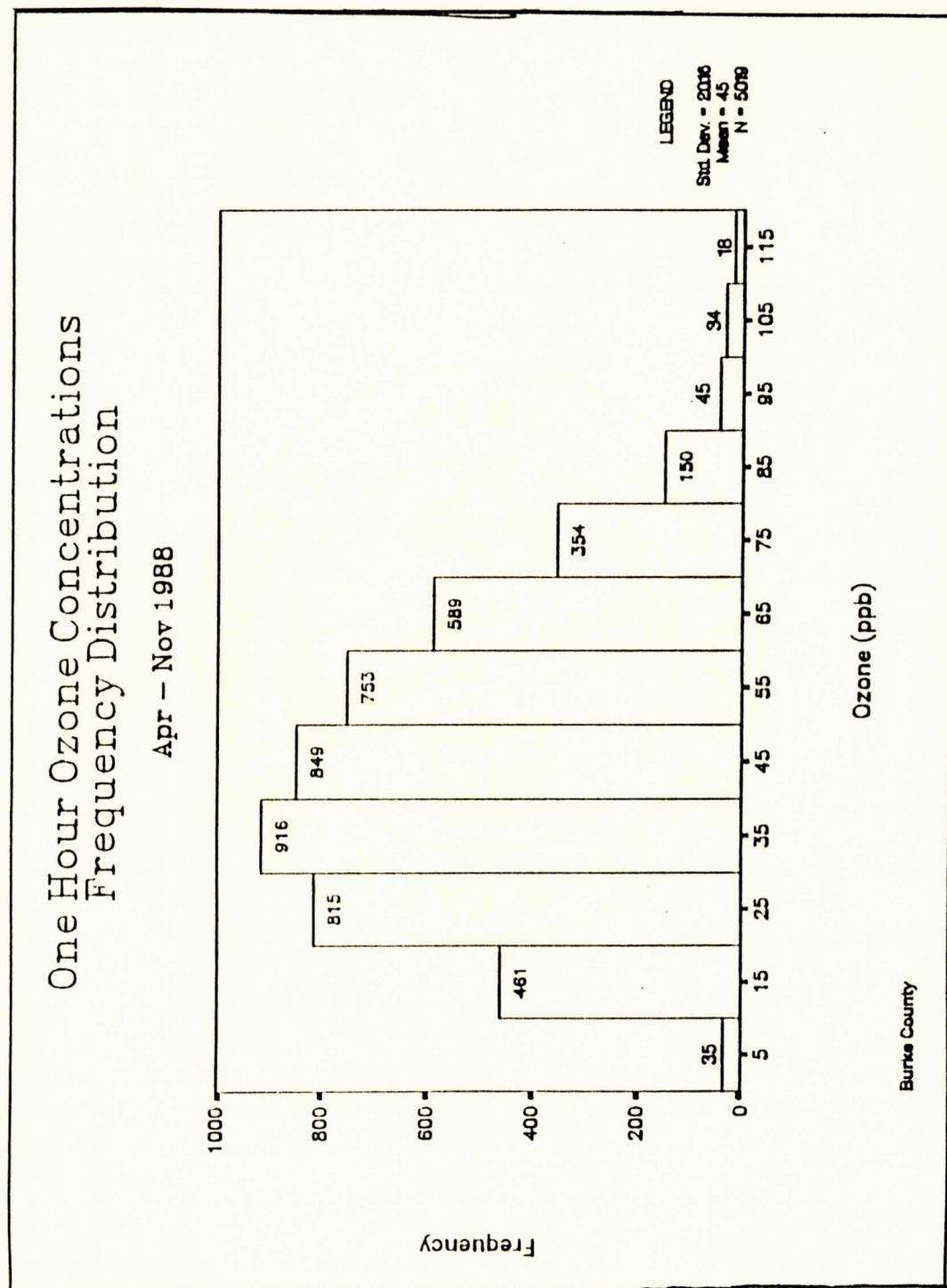


Figure 3.1: One-hour ozone concentration frequency distribution for 1988.

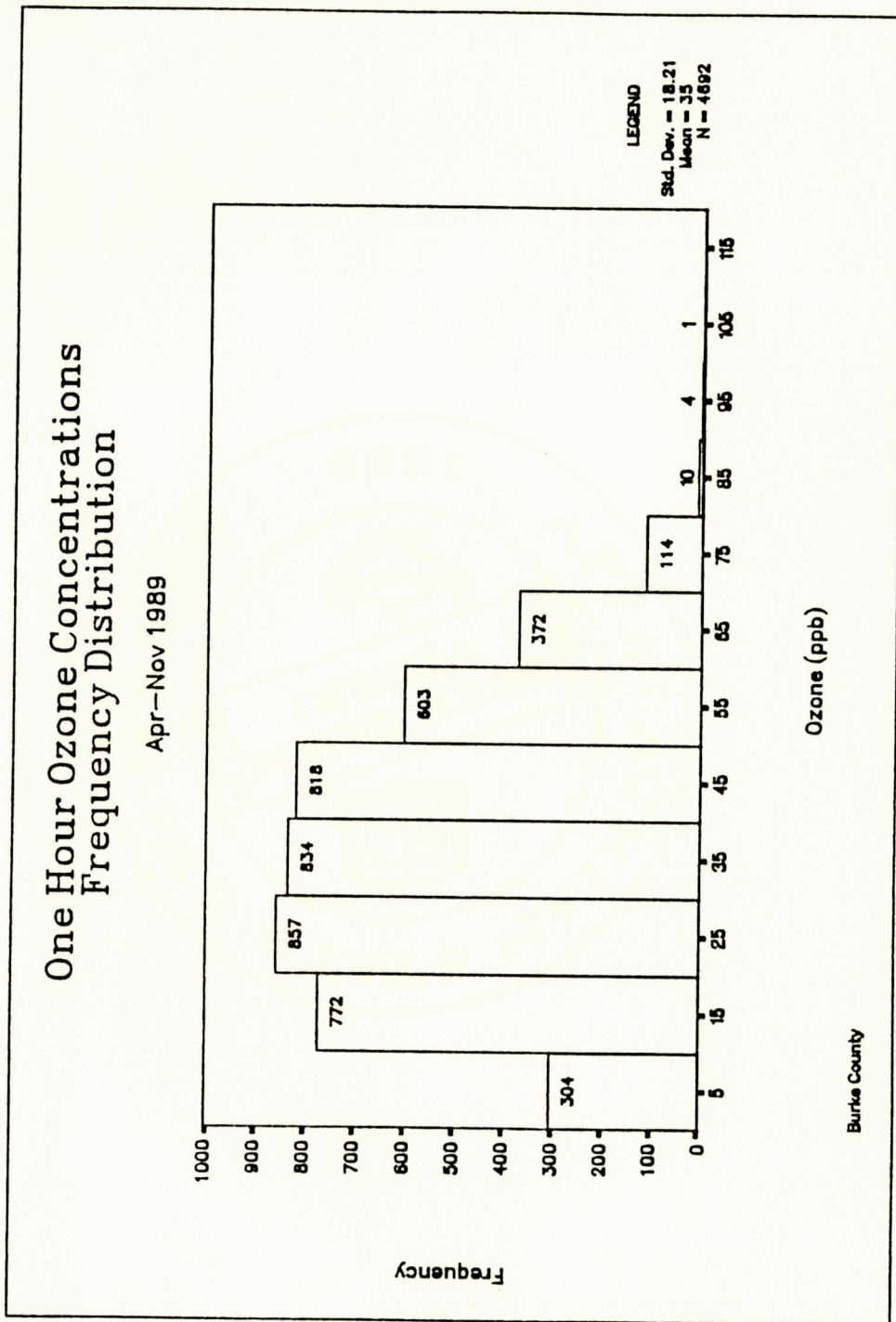


Figure 3.2: One-hour ozone concentration frequency distribution for 1989.

3.1.2 Three-Hour Moving Averages

Figures 3.3, 3.4, 3.5, and 3.6 display three-hour moving average data, plotted by Julian day and frequency distributions. Moving average plots were used to attempt to smooth the data and determine trends. Figures 3.3 and 3.4 are time series plots of the 1988 and 1989 three-hour moving averages. Both plots retain the high variability shown in Figures 3.7 and 3.8, where moving averages were not used. Figures 3.7 and 3.8 are discussed later in this section. Figures 3.5 and 3.6 are the three-hour moving average frequency distributions. In the 1989 plot, for the period Julian day 227 through 251 (August 15 to September 7), all data are missing due to analyzer failure.

3.1.3 Twenty-Four-Hour Daily Averages and Moving Averages

Figures 3.7, 3.8, 3.9, 3.10, 3.11, and 3.12 display 24-hour ozone data. Figures 3.7 and 3.8 are 24-hour ozone averages plotted over time. Figures 3.9 and 3.10 are the 24-hour average frequency distributions. The most frequent 24-hour averages occurred between 30-39 ppb for both years, but the mean daily value was 45 ppb for 1988 and 35 ppb in 1989. Figures 3.11 and 3.12 are 24-hour three-day moving averages. The moving averages did not appreciably alter the appearance of the data, reinforcing the results of section 3.1.2; i.e., the hourly and the daily moving averages cannot noticeably smooth the data.

3.1.4 Smoothing Techniques

Figures 3.13-3.20 display the various more sophisticated data smoothing methods used. The first method tested was a quadratic fit of the data. The quadratic fit for 1988 is too stiff (does not follow the data variation sufficiently well, Figure 3.13), while the cubic fit displays an upward trend in ozone during the fall season (Figure 3.15). The cubic fit is not consistent with the expectation that ozone concentrations decrease during colder periods.

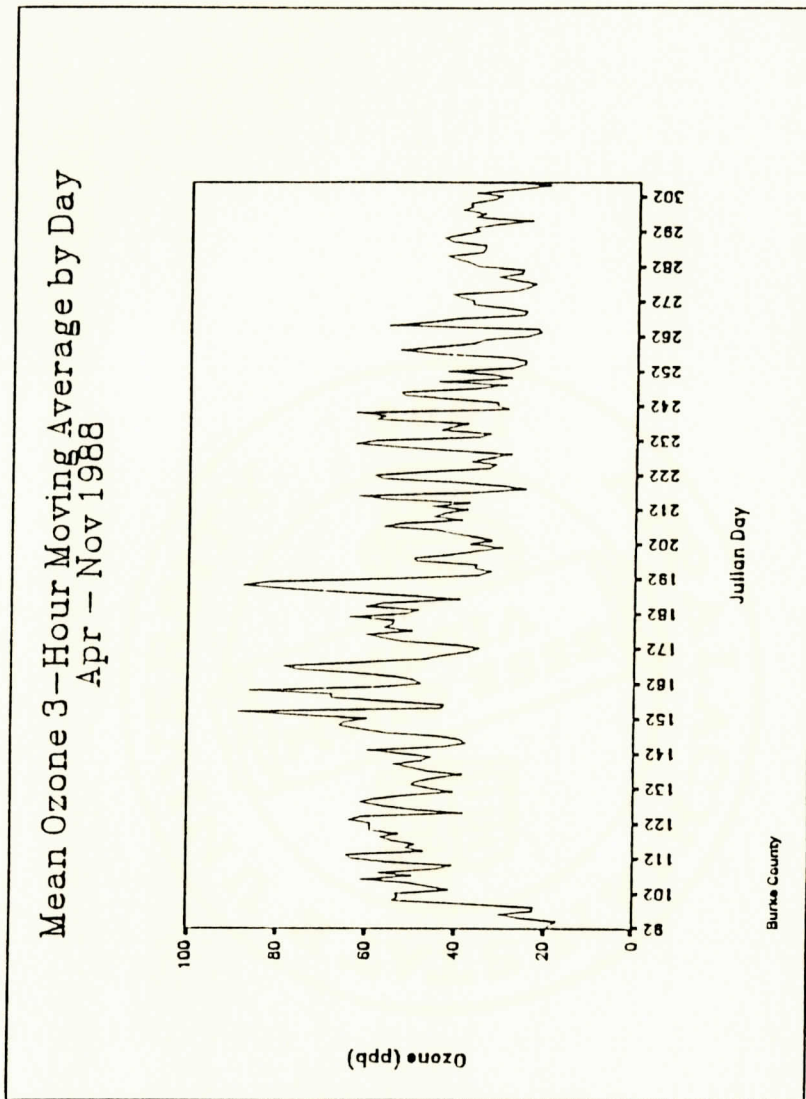


Figure 3.3: Mean ozone three-hour moving average by day for 1988.

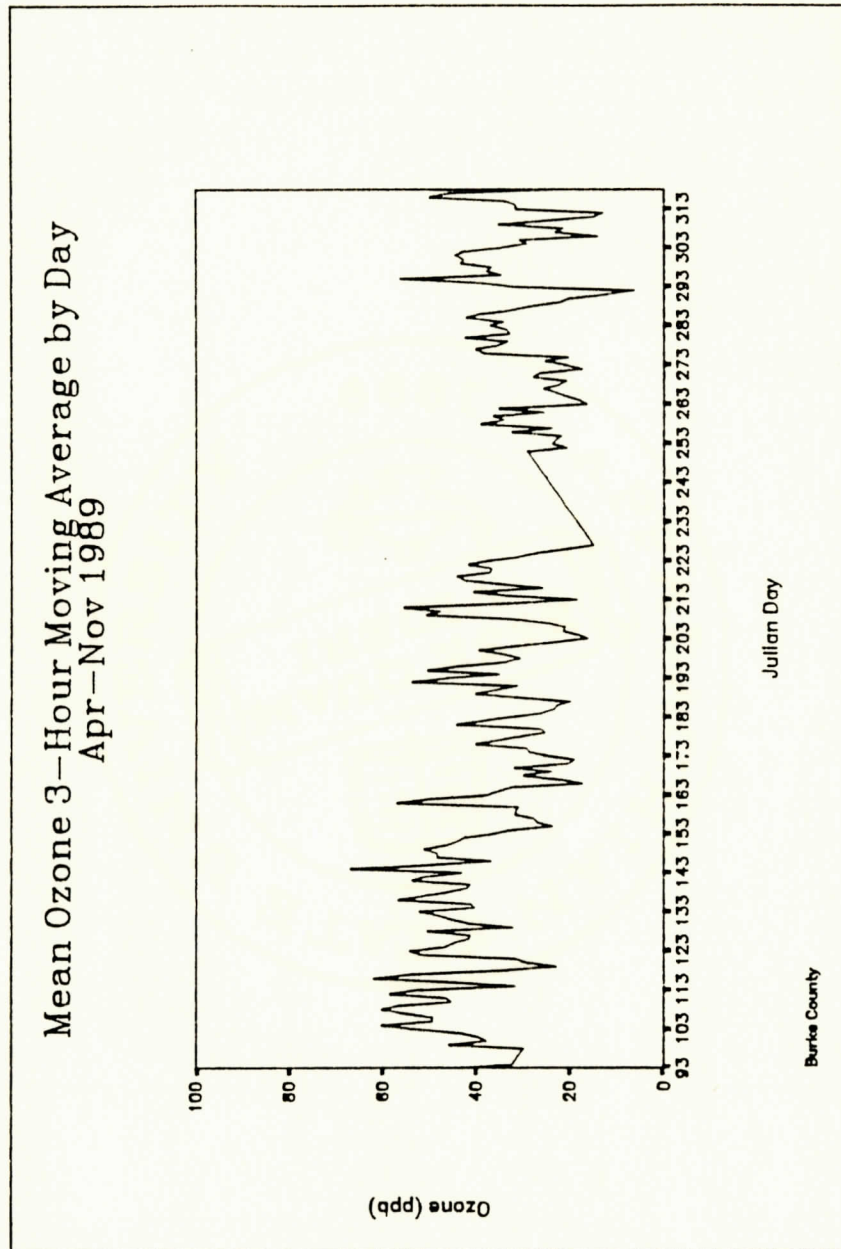


Figure 3.4: Mean ozone three-hour moving average by day for 1989.

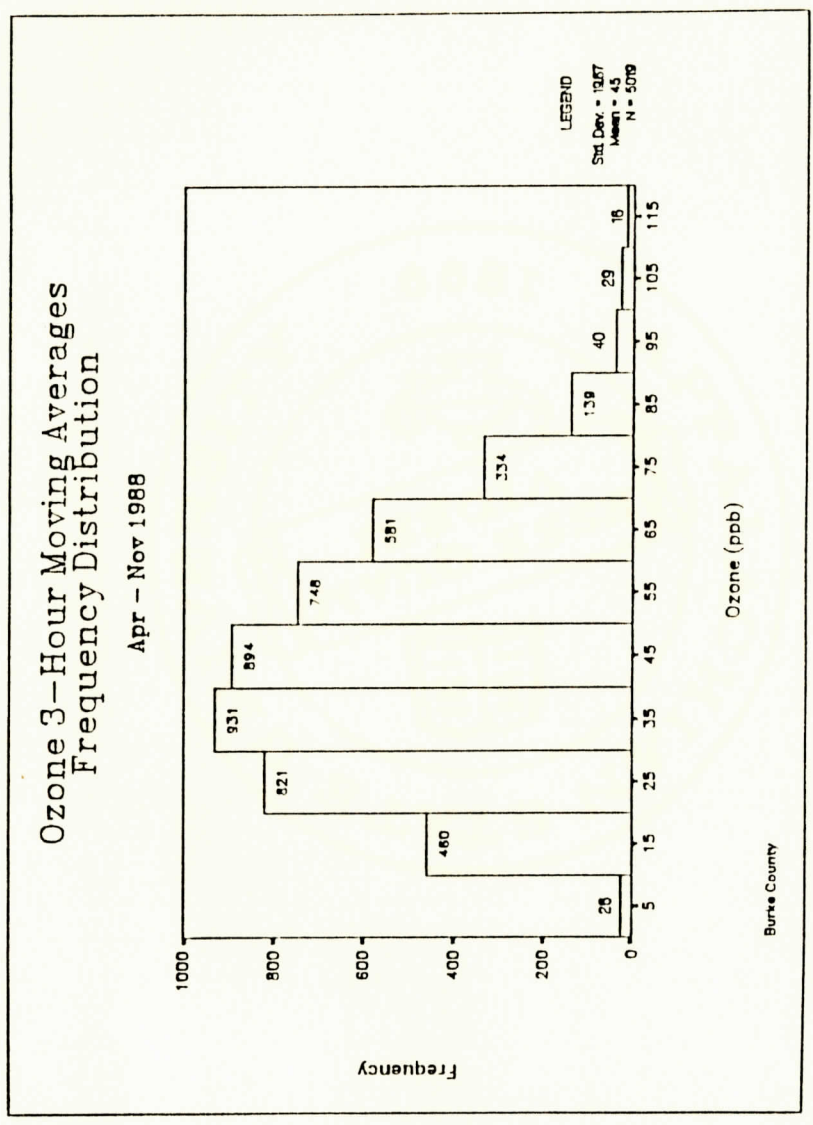


Figure 3.5: Ozone three-hour moving averages frequency distribution for 1988.

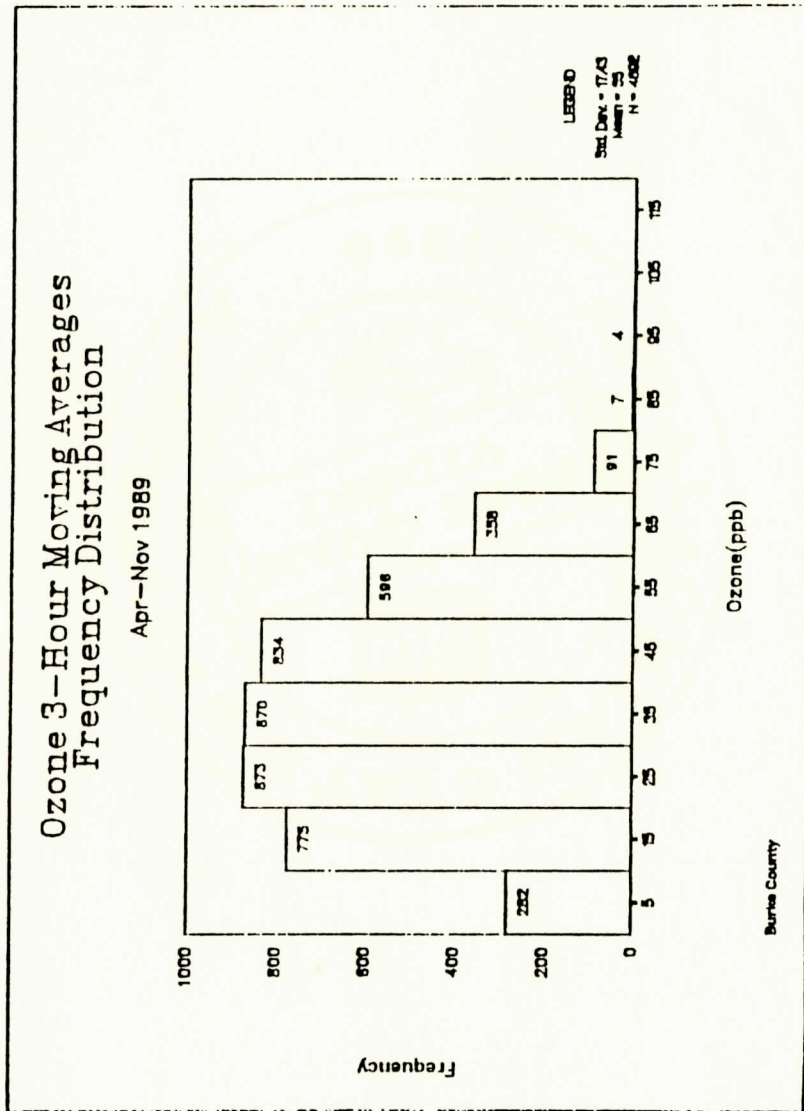


Figure 3.6: Ozone three-hour moving averages frequency distribution for 1989.

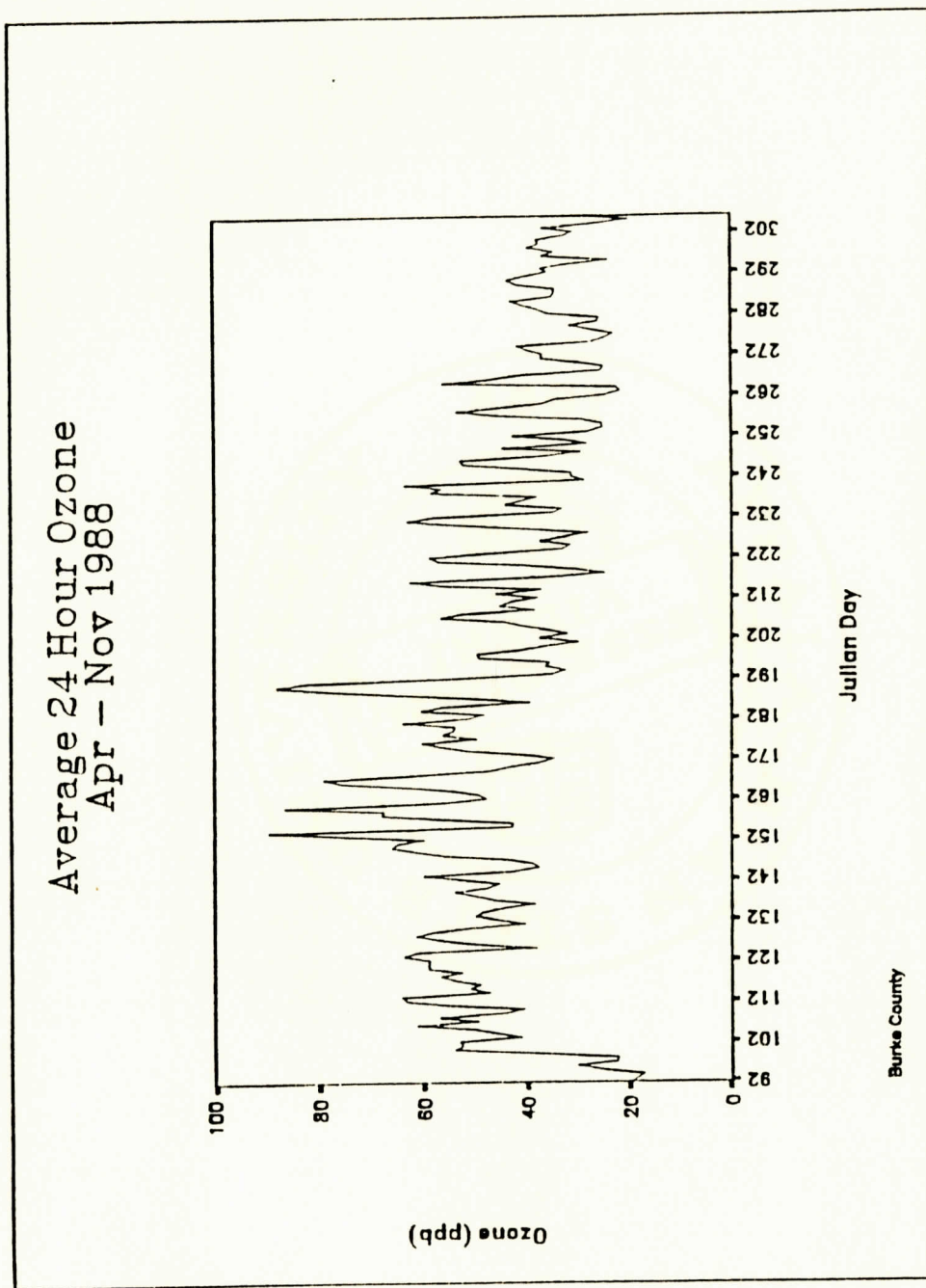


Figure 3.7: Average 24-hour ozone for 1988.

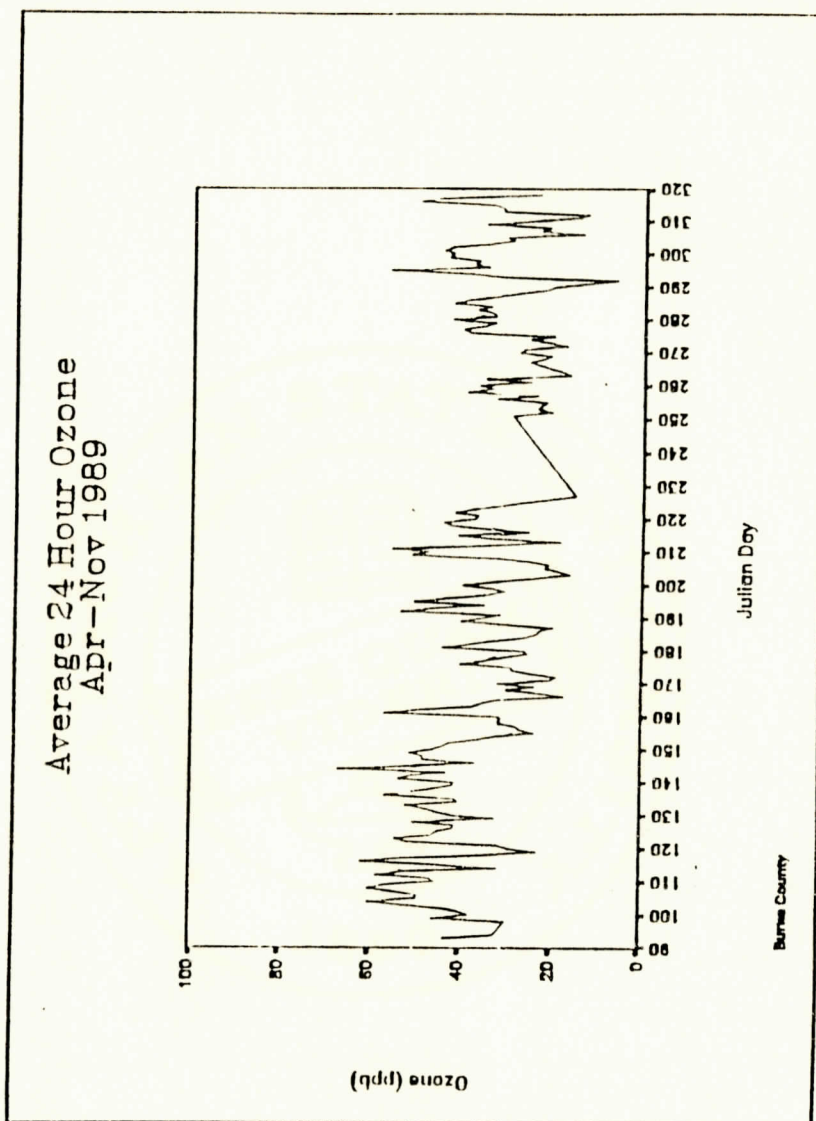


Figure 3.8: Average 24-hour ozone for 1989.

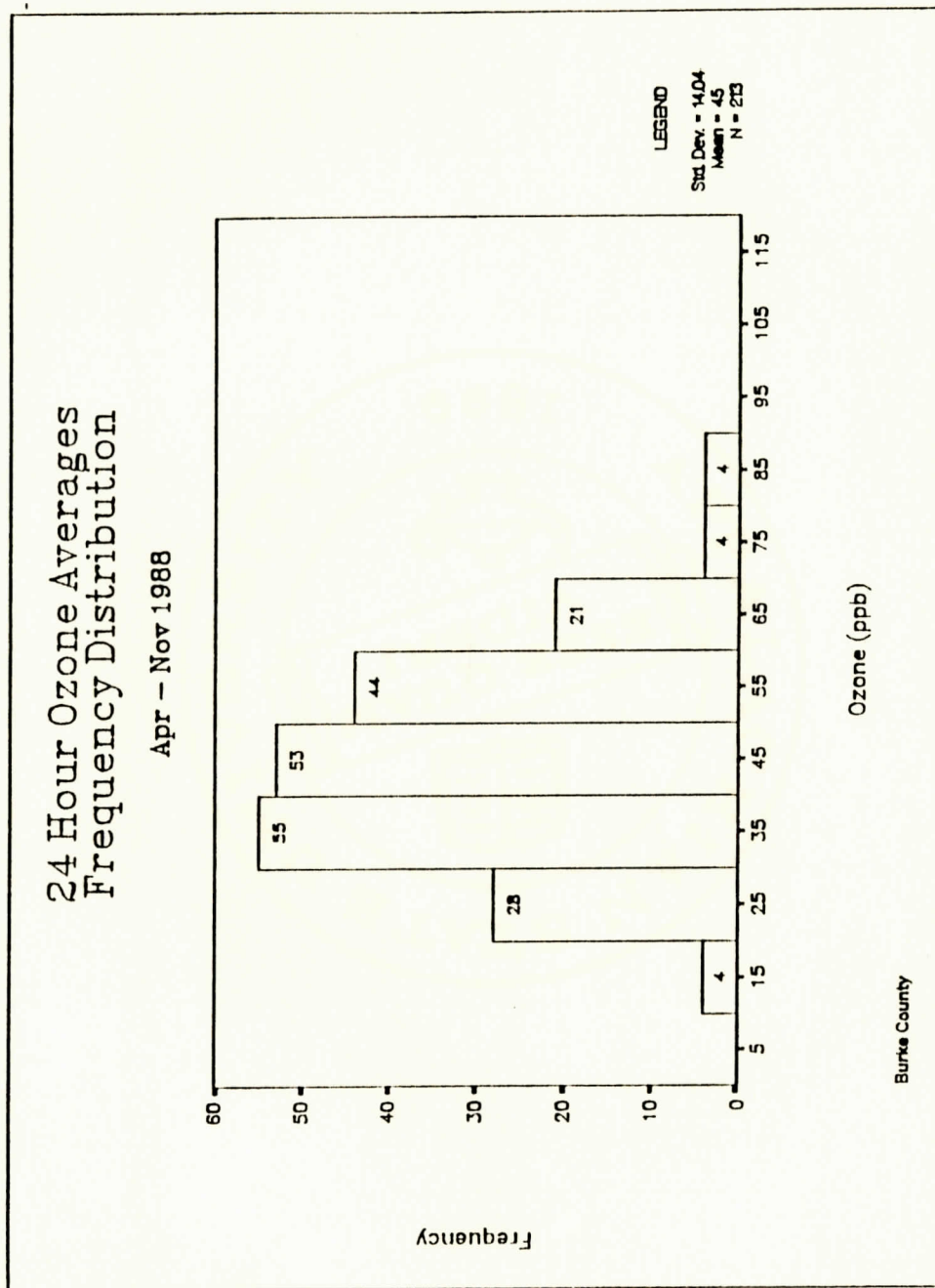


Figure 3.9: Twenty-four-hour ozone averages frequency distribution for 1988.

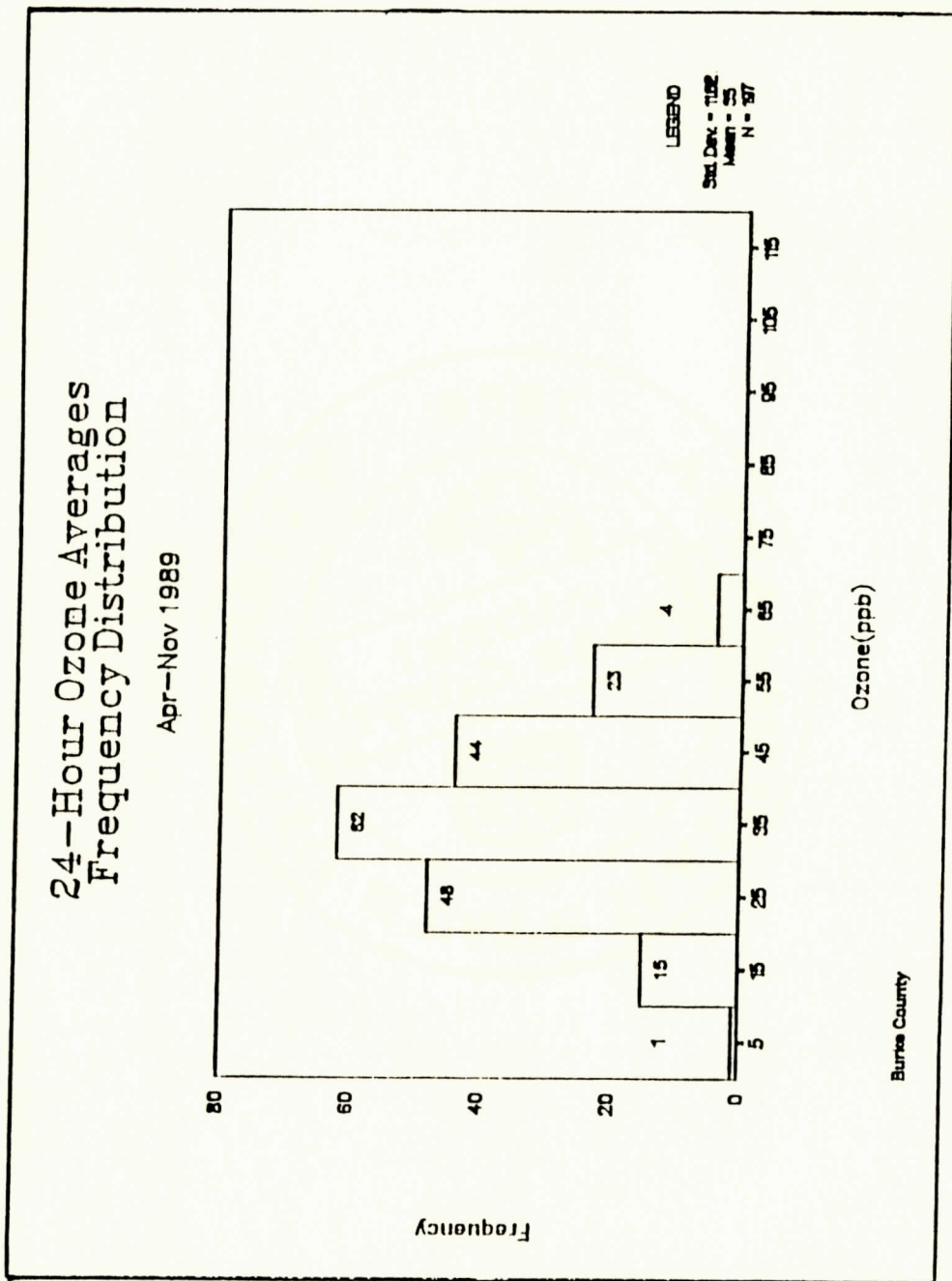


Figure 3.10: Twenty-four-hour ozone averages frequency distribution for 1989.

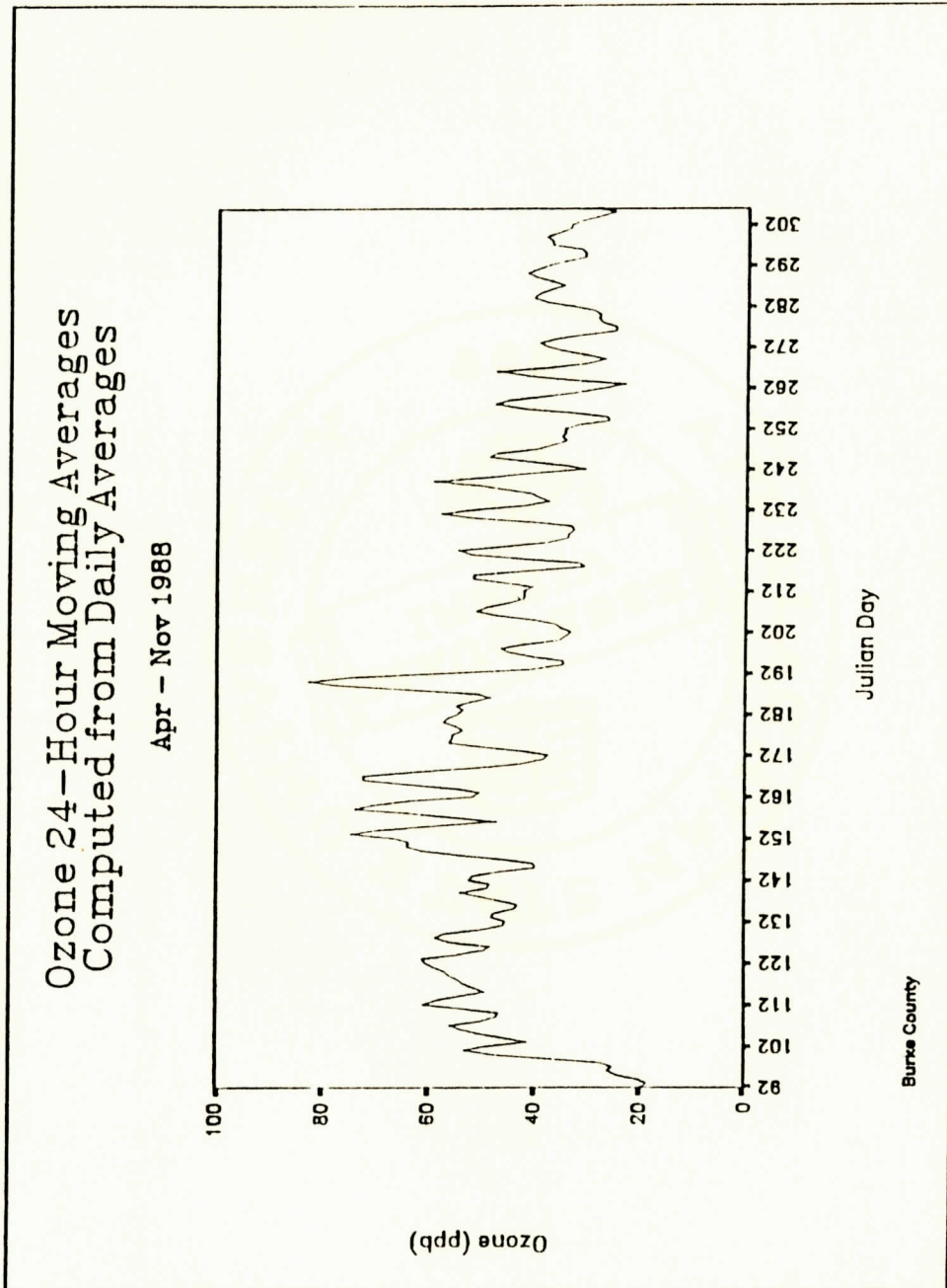


Figure 3.11: Ozone 24-hour moving averages, computed from daily averages for 1988.

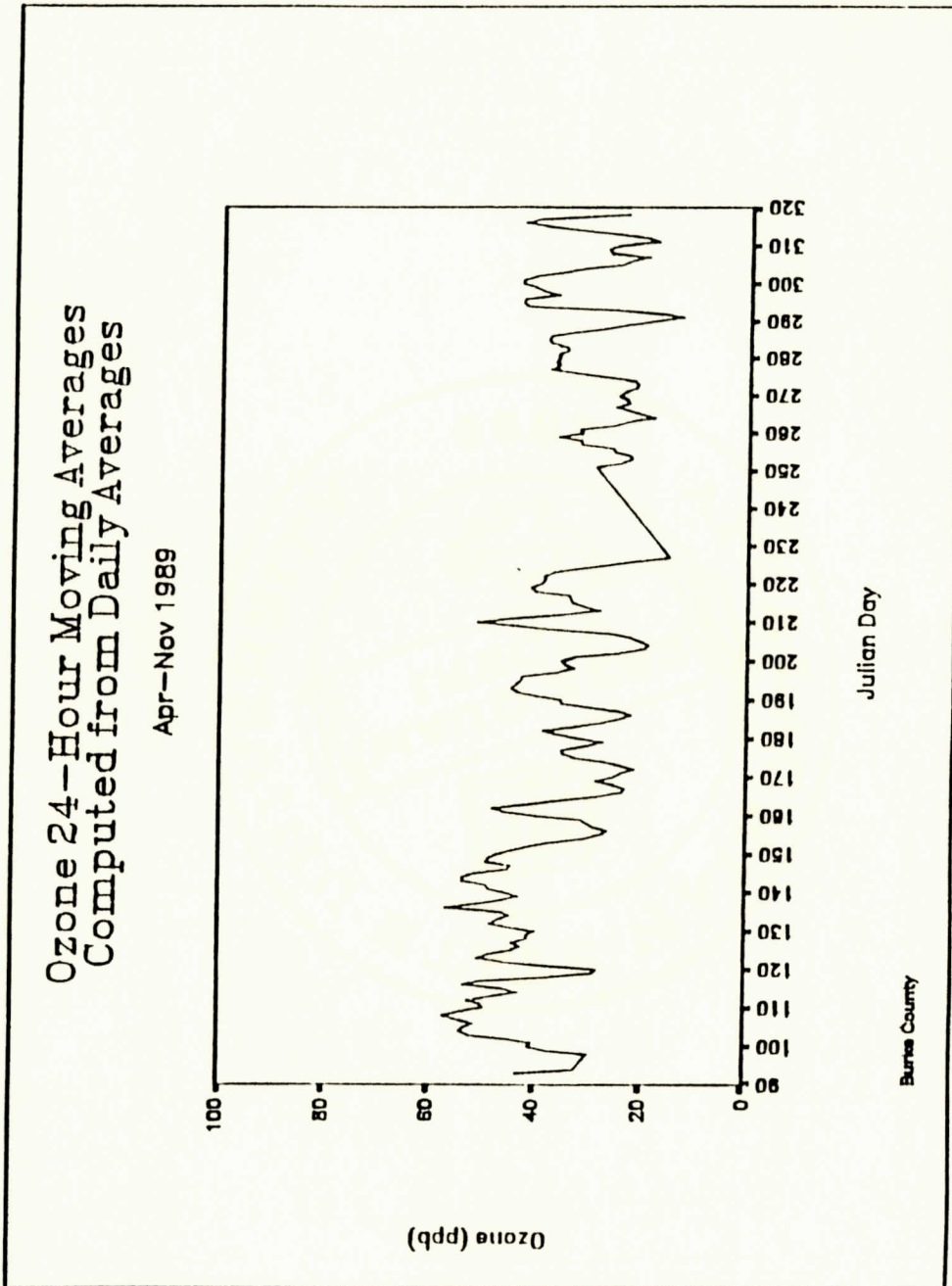


Figure 3.12: Ozone 24-hour moving averages, computed from daily averages for 1989.

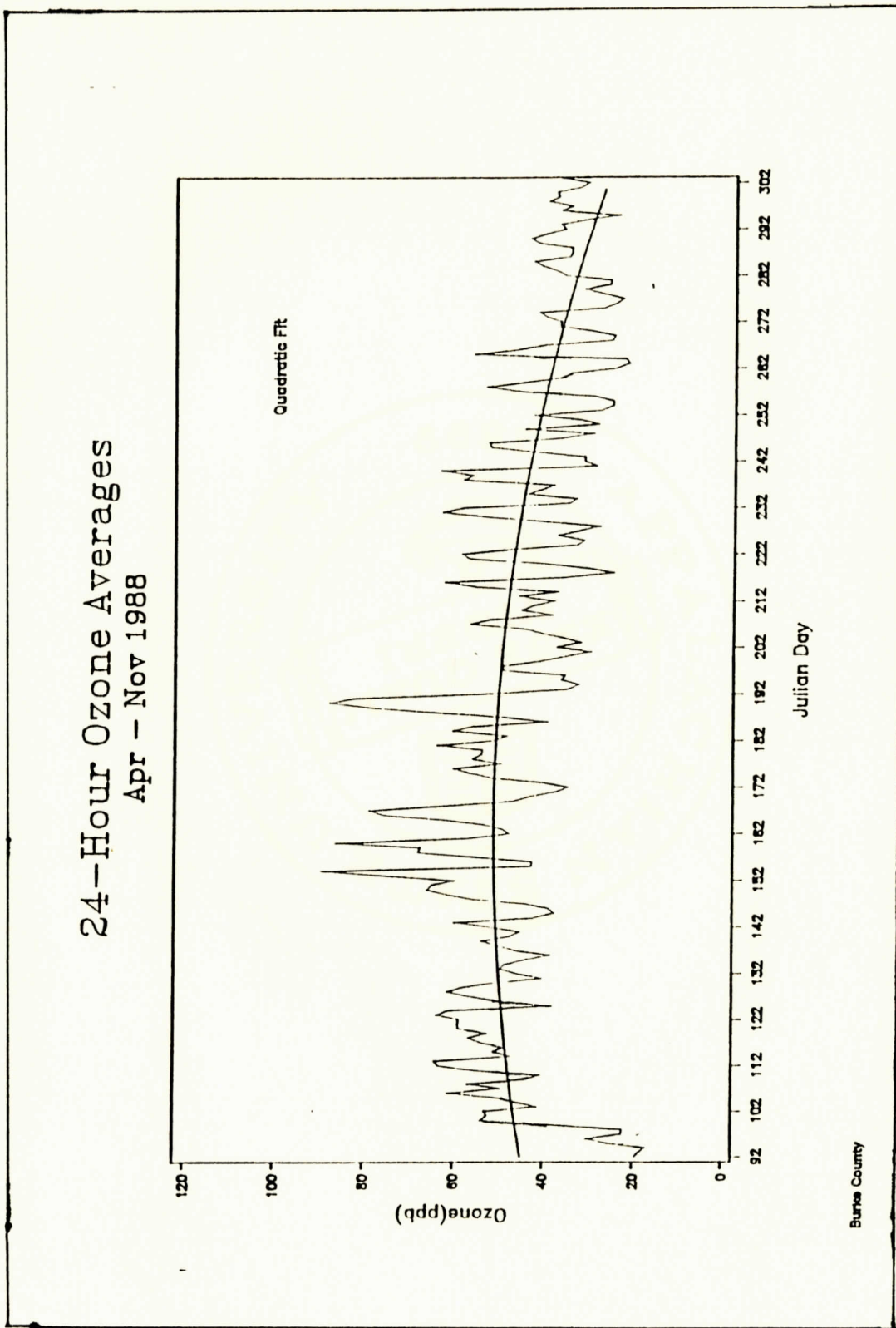


Figure 3.13: Twenty-four-hour ozone averages for 1988, using a quadratic fit.

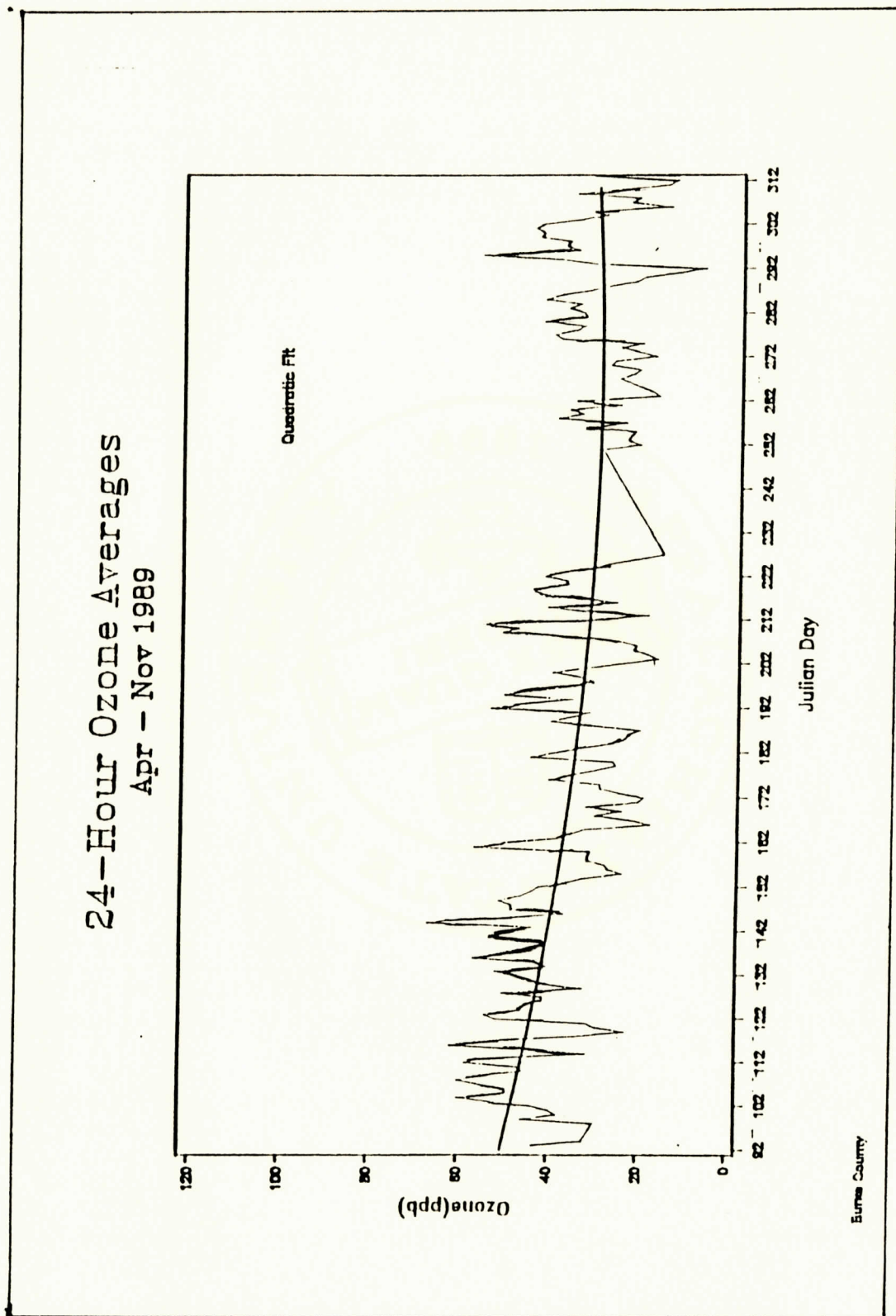


Figure 3.14: Twenty-four-hour ozone averages for 1989, using a quadratic fit.

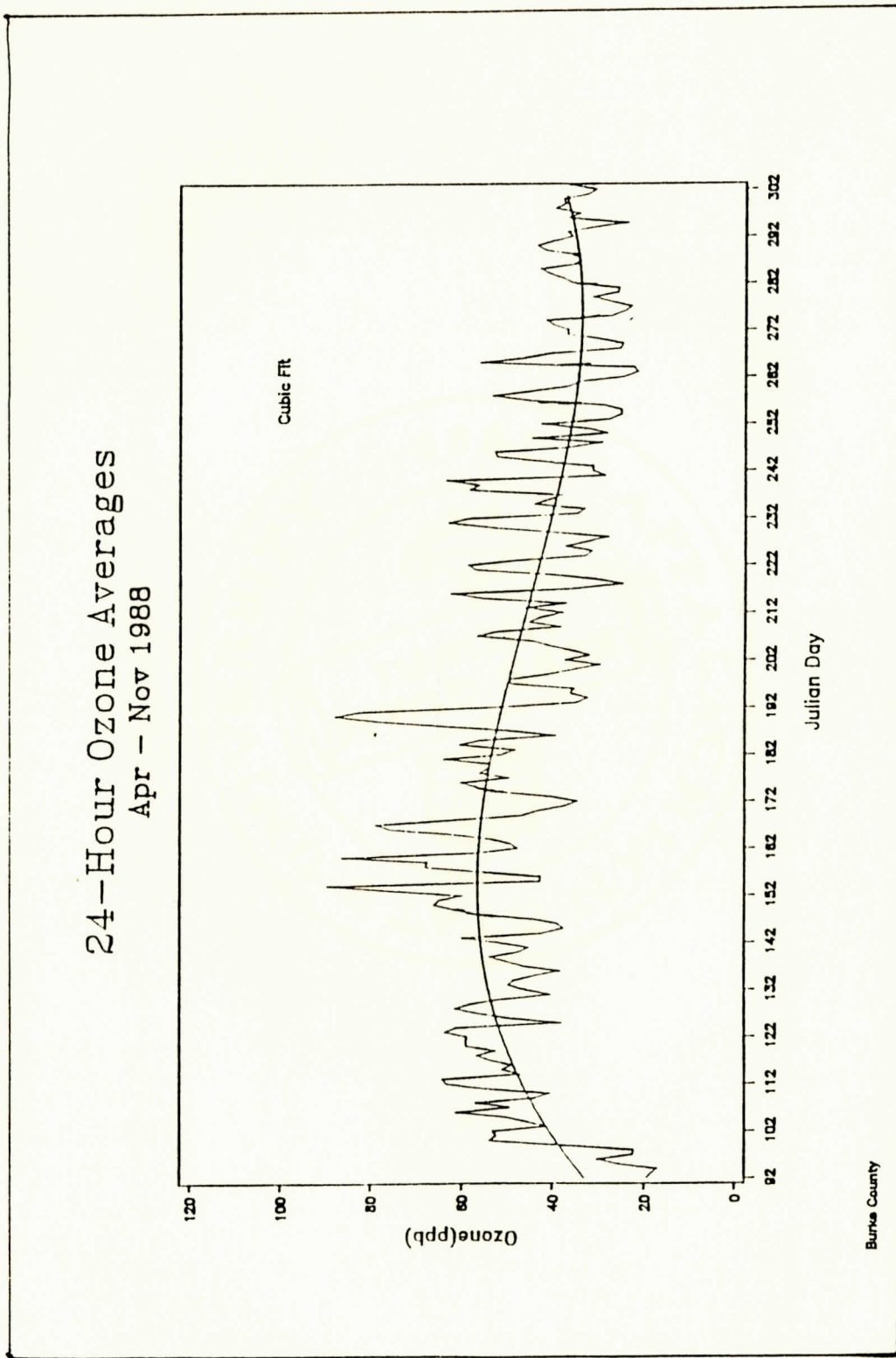


Figure 3.15: Twenty-four-hour ozone averages for 1988, using a cubic fit.

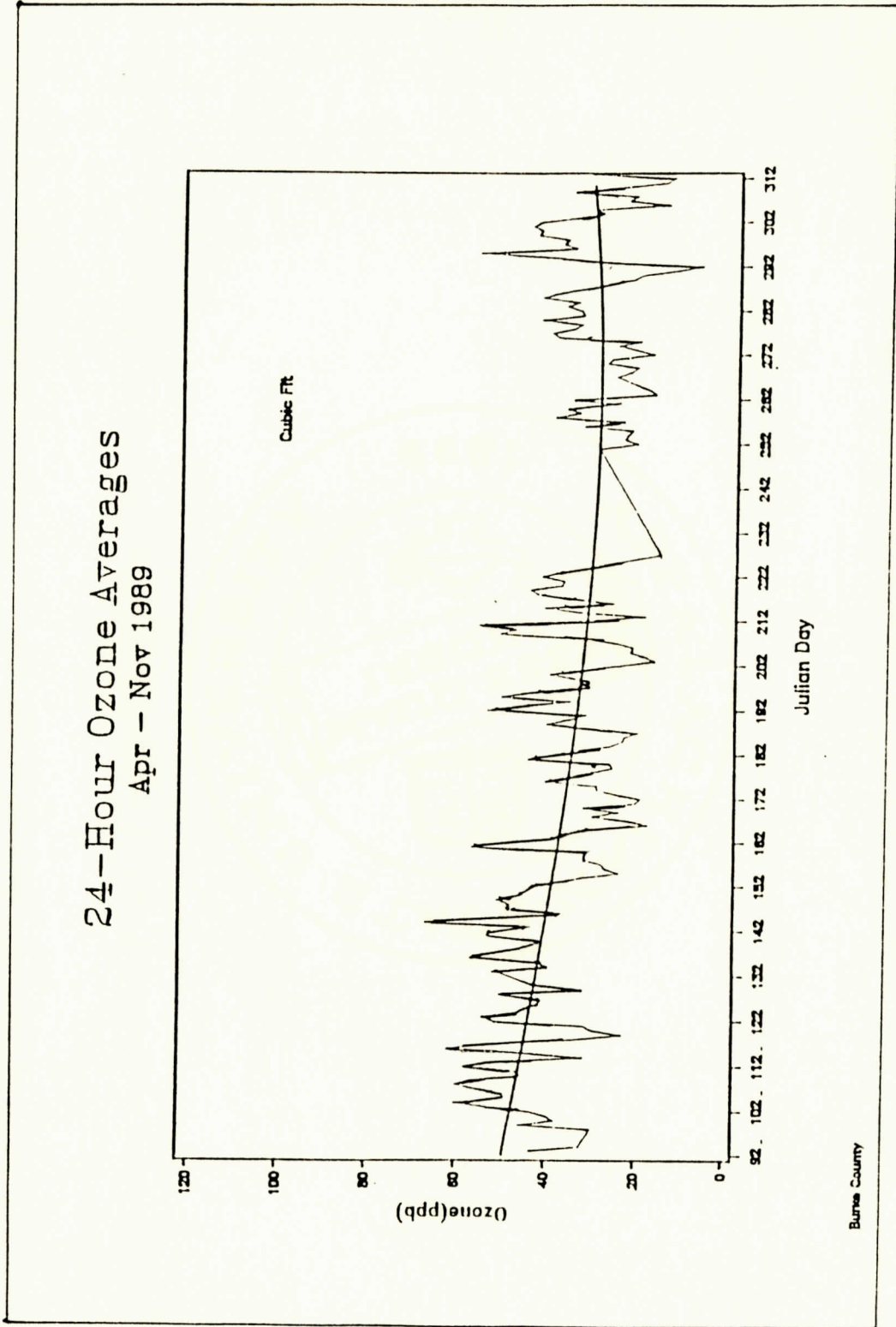


Figure 3.16: Twenty-four-hour ozone averages for 1989, using a cubic fit.

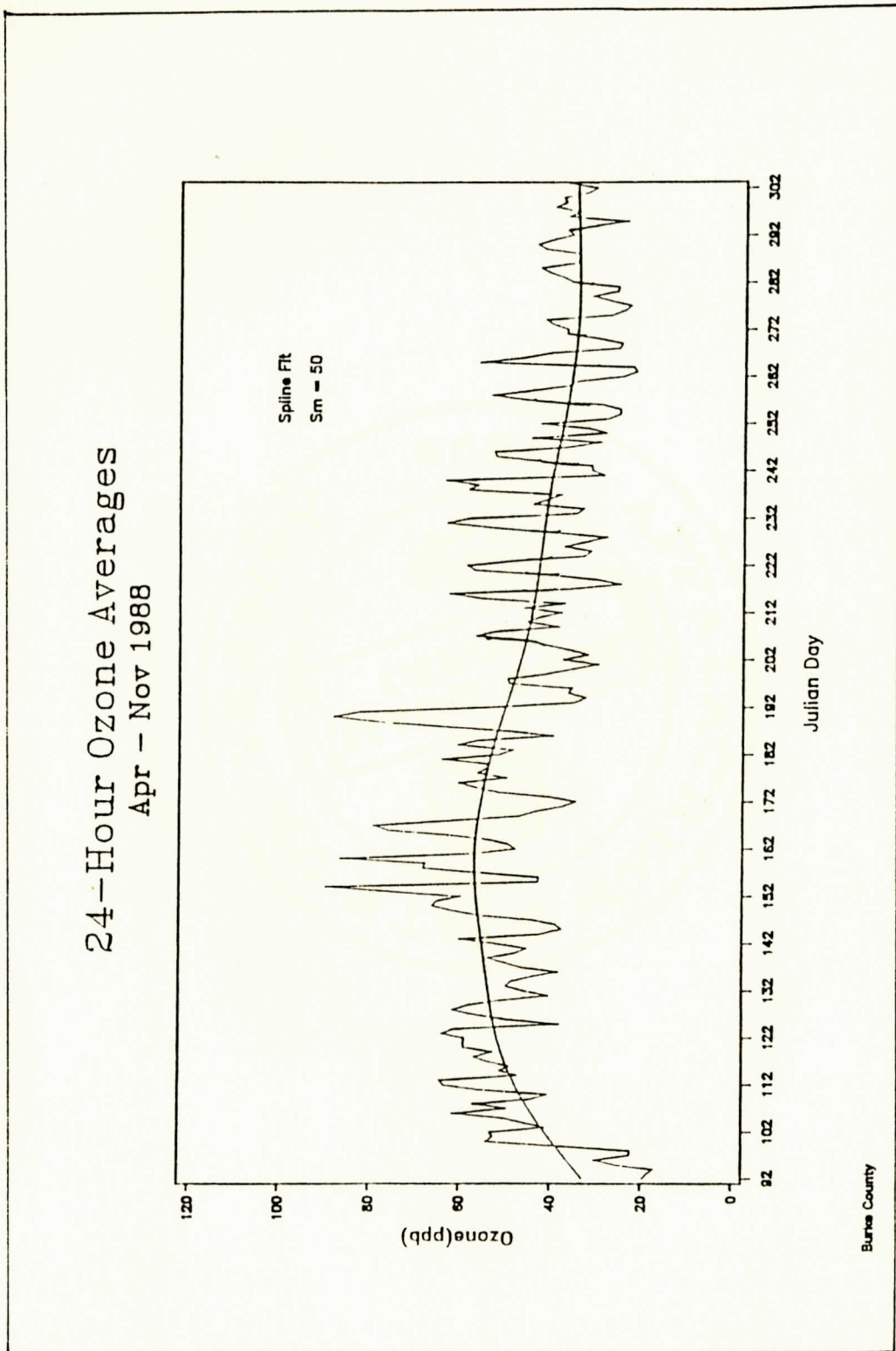


Figure 3.17: Twenty-four-hour ozone averages for 1988, using a spline fit with Sm parameter 50.

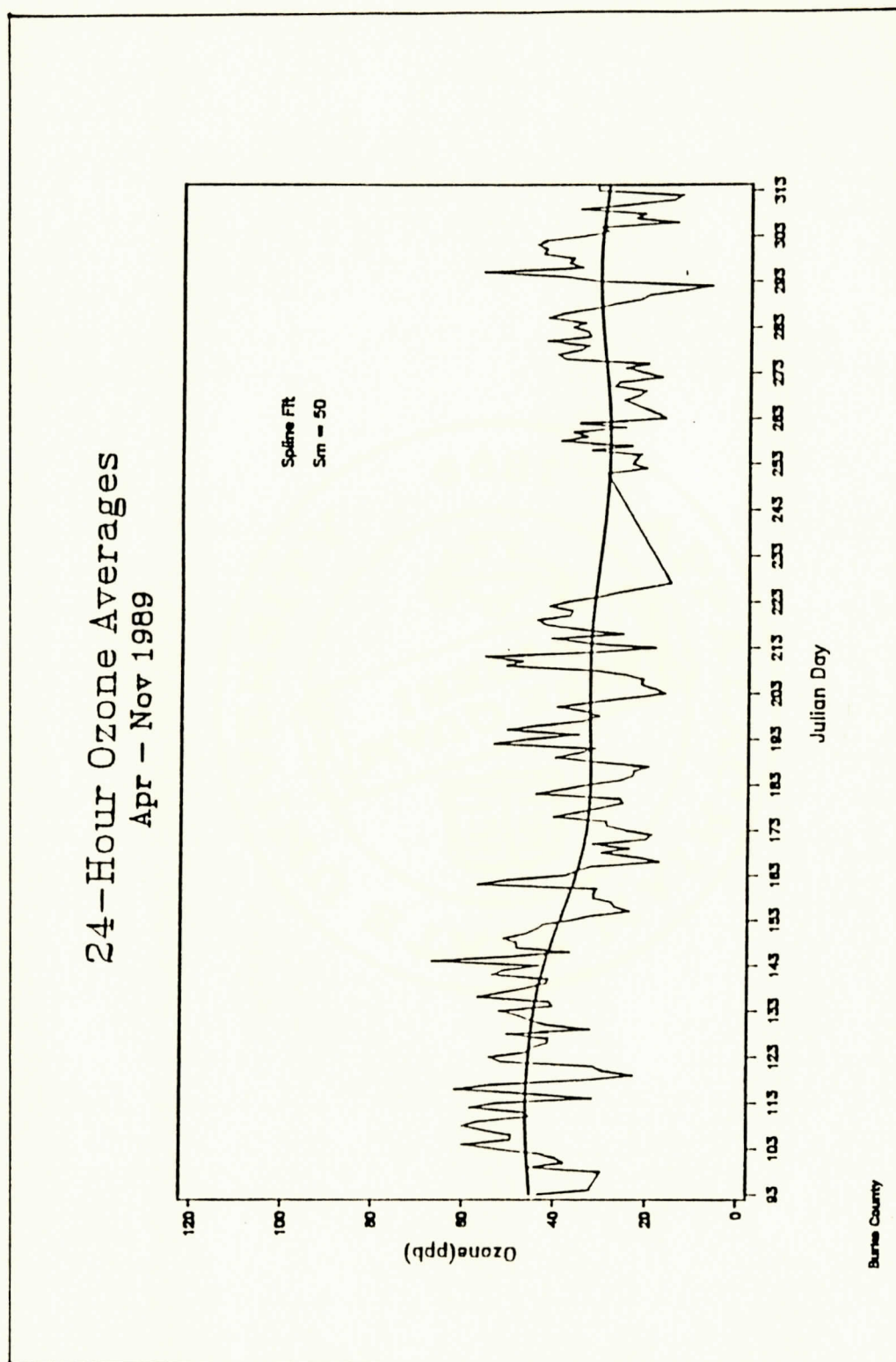


Figure 3.18: Twenty-four-hour ozone averages for 1989, using a spline fit with Sm parameter 50.

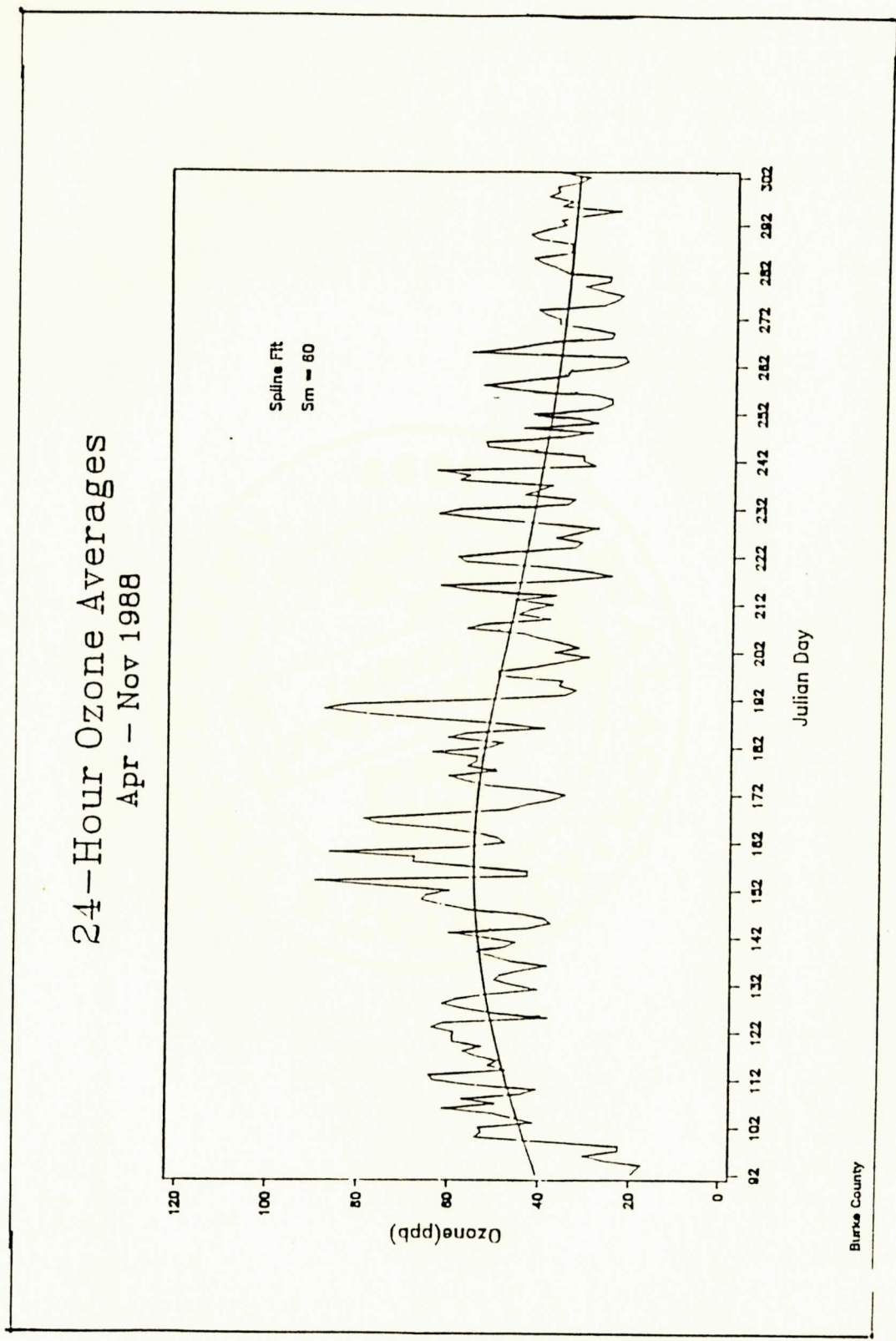


Figure 3.19: Twenty-four-hour ozone averages for 1988, using a spline fit with Sm parameter 60.

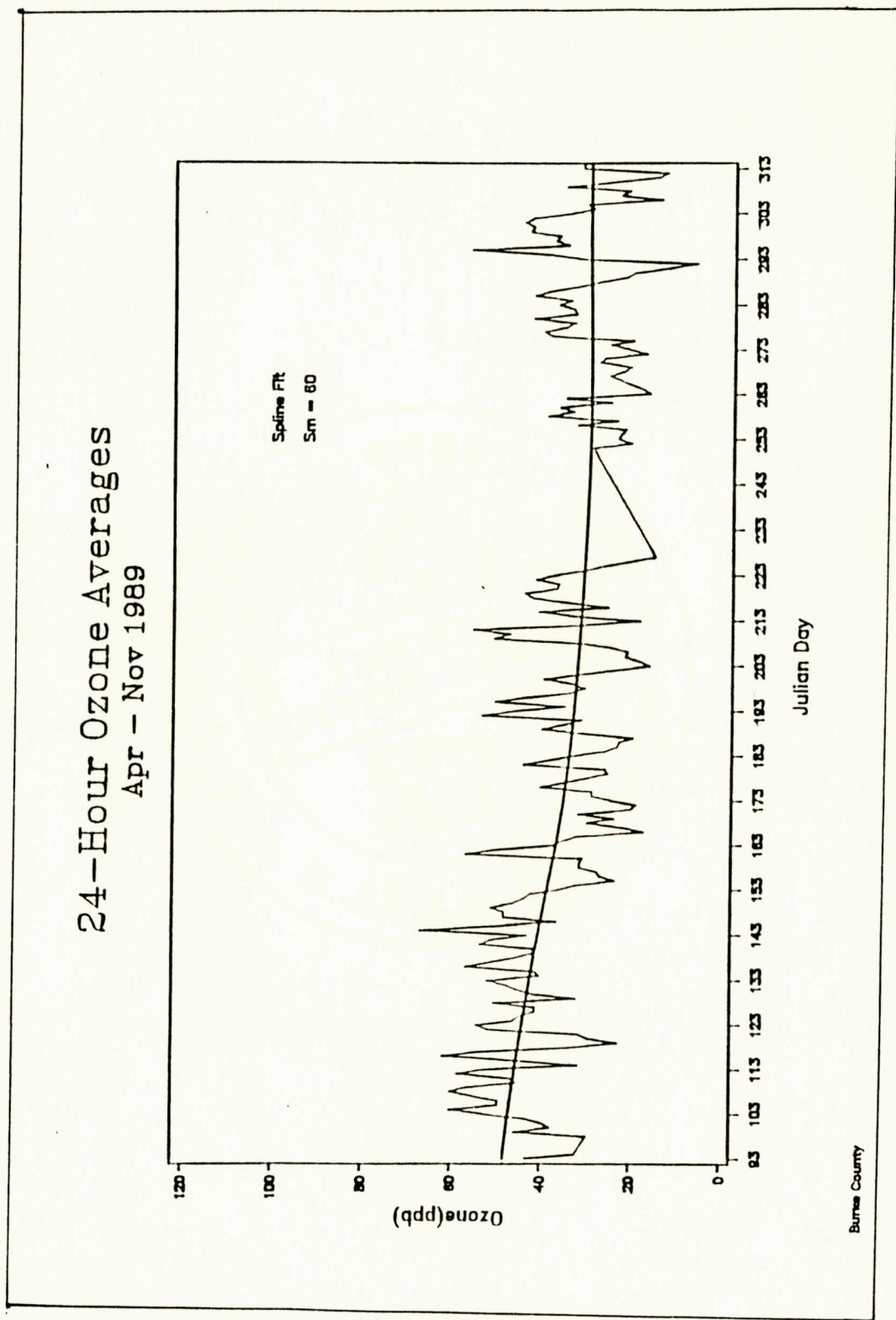


Figure 3.20: Twenty-four-hour ozone averages for 1989, using a spline fit with Sm parameter 60.

The method chosen to best represent the data was a spline interpolation. This procedure, designed to smooth noisy data, minimizes a linear combination of the sum of squares of the residuals of fit and the integral of the square of the second derivative³¹. The adjustable spline parameter (S_m) selected was 60, from a possible range of 1 to 99, with 1 producing the tightest fit to the data, and 99 producing a line with the least variation, a straight line³⁰. Figures 3.17 and 3.18 display the data with a S_m parameter of 50. While the parameter of 50 gives more detail it does not exhibit the smooth long-range trend desired. Figures 3.19 and 3.20 display the data with a spline fit and S_m parameter of 60. This provides a continuous smooth curve which follows the data long-range trends. These plots indicate that 1988 and 1989 peak ozone concentrations occurred during June and April, respectively.

For 1989 the quadratic and cubic fits are very similar to the spline fit (see Figures 3.14 and 3.16). This reinforces the impression that the 1989 data are best described as continuously decreasing ozone concentrations from beginning to end of the sampling season³³.

3.1.5 Maximum One-Hour Ozone

Figures 3.21 and 3.22 are the maximum one-hour ozone concentrations by day. The largest maximum for 1988 occurred in mid-June, with an average value of 78 ppb; in 1989 the largest one-hour maximum occurred in April, with an average value of about 65 ppb. The most striking difference between the two sampling seasons is that the 1988 plot is typical of ozone trends throughout a season, but 1989 does not show this pattern. A typical seasonal plot shows high ozone concentrations during hotter periods. The 1989 plot of one-hour maximum ozone is atypical, with the peak ozone period found in mid-April.

3.1.6 One-Hour Maximum and Twenty-Four-Hour Average Ozone

Figures 3.23 and 3.24 are overlays of the one-hour maximum and twenty-four-hour average ozone concentrations, by day. The spline fits for the maxima and the average

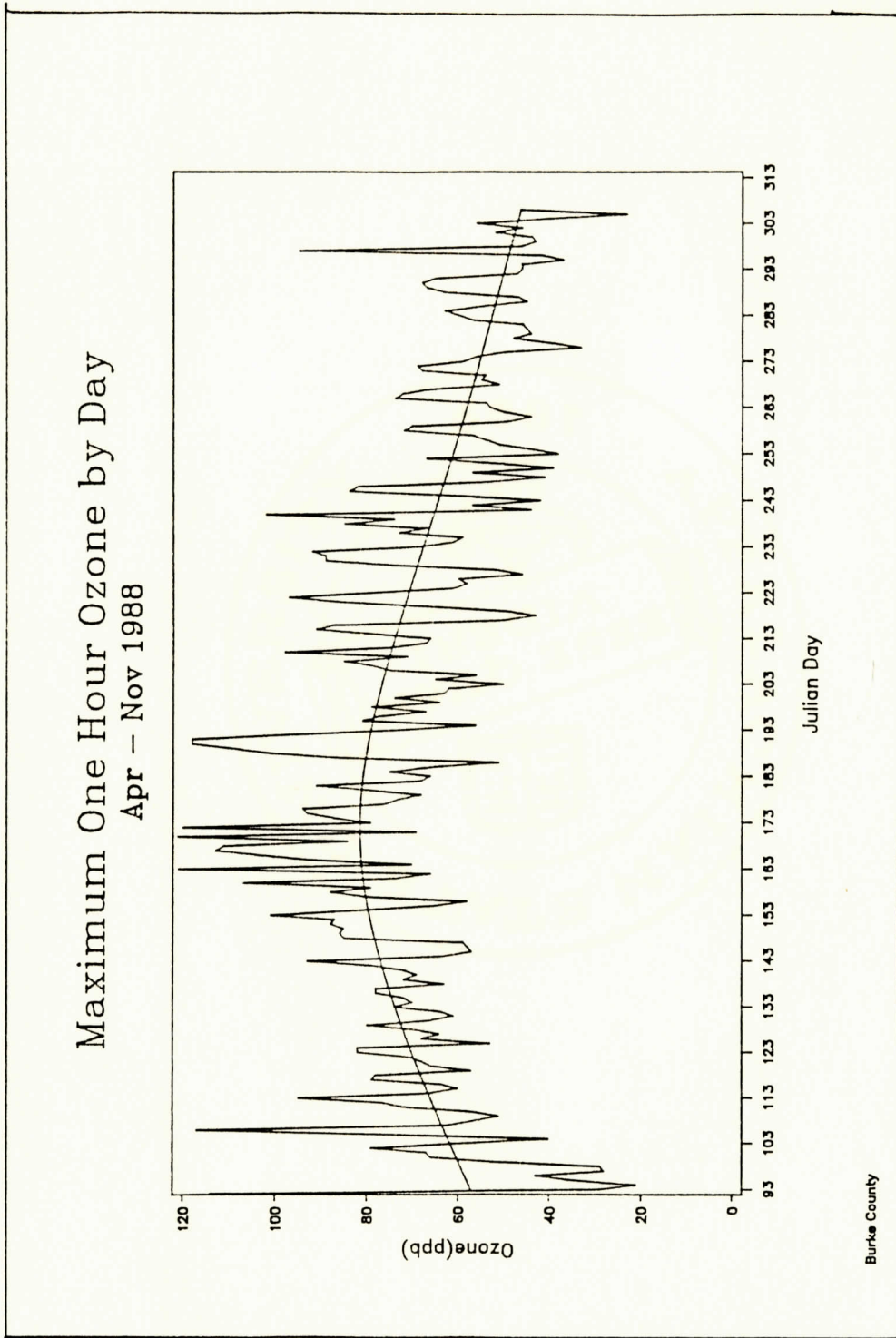


Figure 3.21: Maximum one-hour ozone by day for 1988.

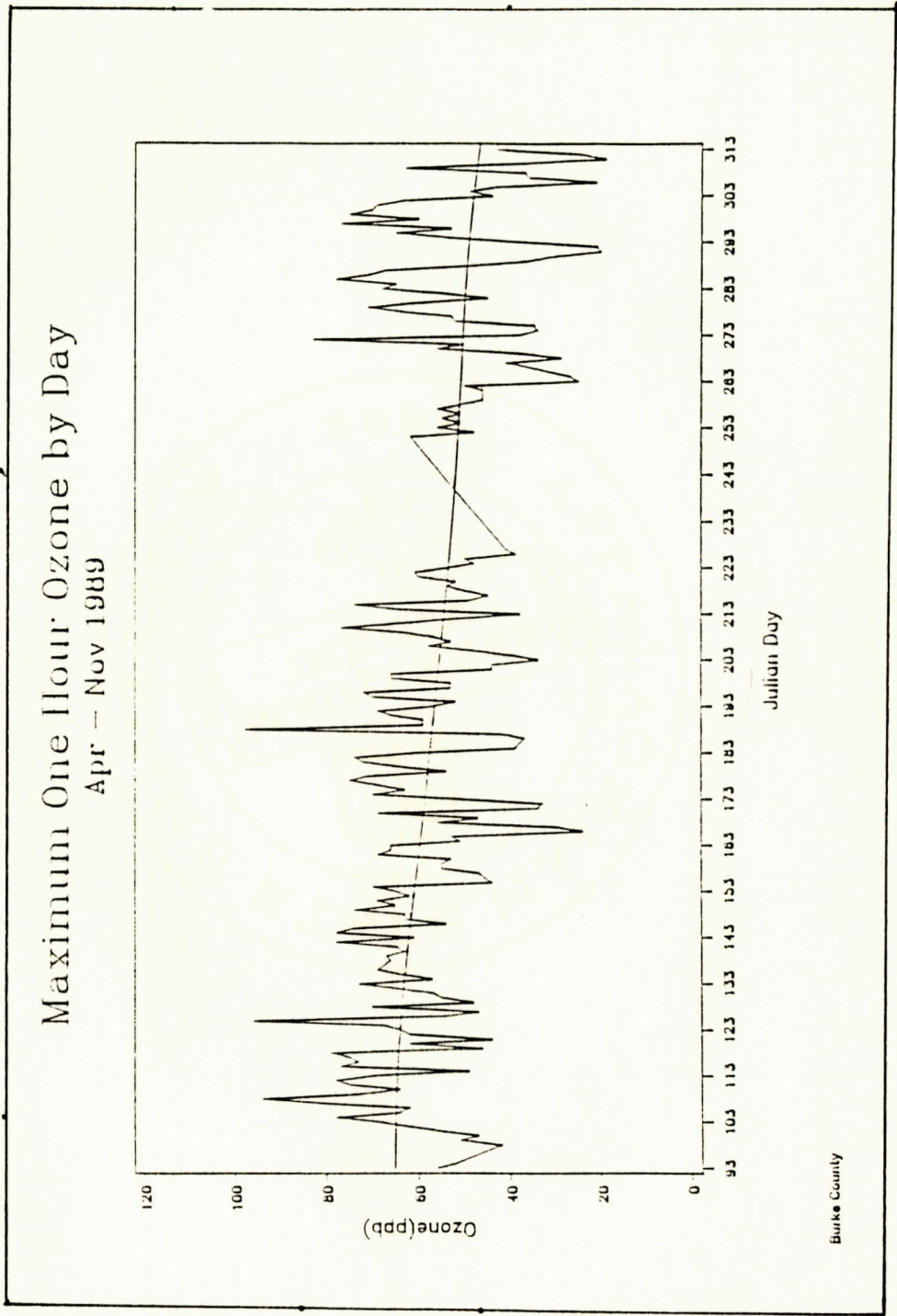


Figure 3.22: Maximum one-hour ozone by day for 1989.

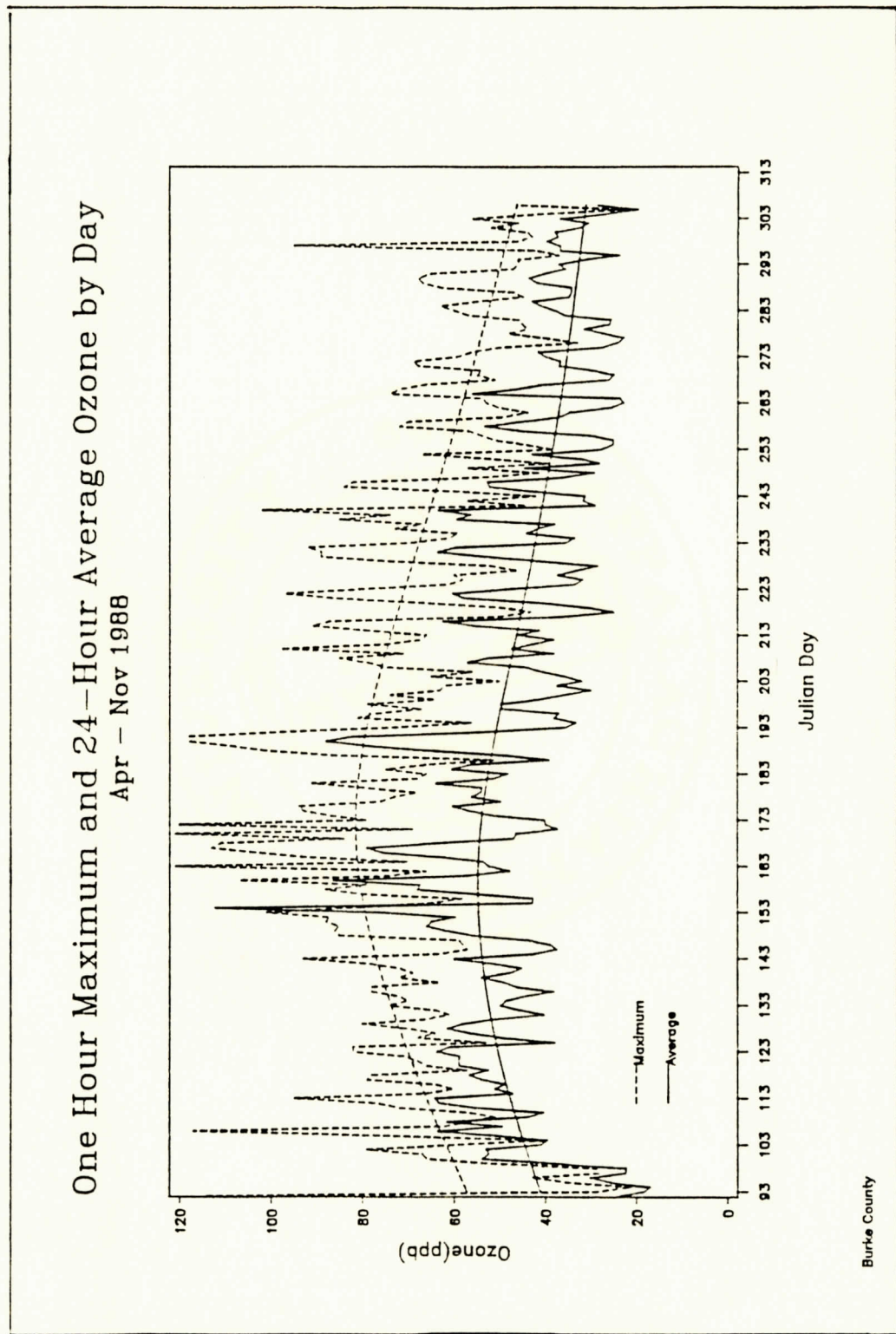


Figure 3.23: One-hour maximum and 24-hour average ozone by day for 1988, using a spline fit with S_m parameter 60.

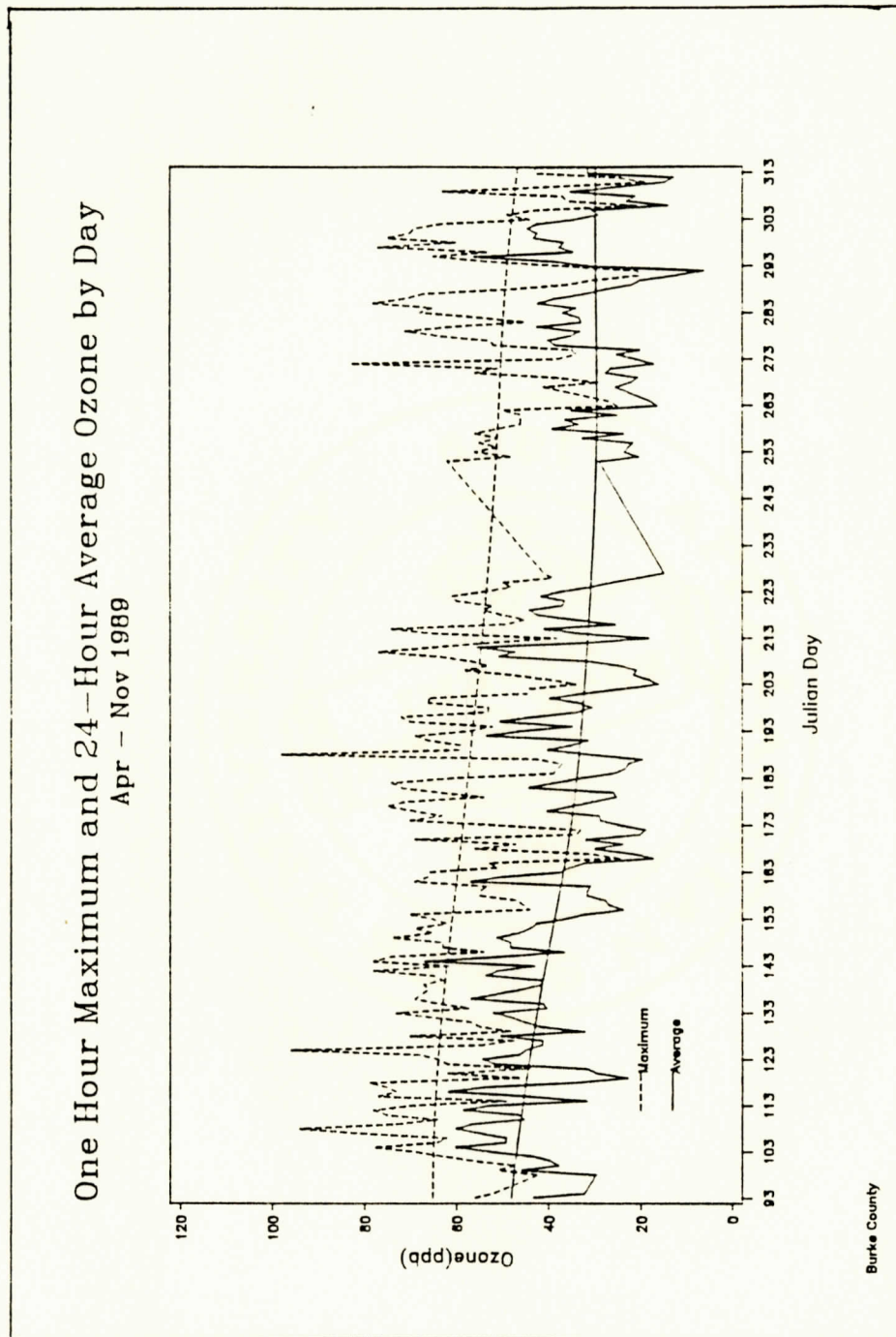


Figure 3.24: One-hour maximum and 24-hour average ozone by day for 1989, using a spline fit with S_m parameter 60.

concentrations are very similar in form. Figure 3.23 shows the largest ozone maximum occurring in late June in 1988, and averaging of about 78 ppb. The largest 24-hour averages for 1988 occurred in early June with an average of about 56 ppb. In 1989, the largest maximum occurred in April and averaged in the mid 60s ppb range. Largest 24-hour averages were in the high 40s, in April. During both years the maximum one-hour values were 20-40 ppb higher than the average 24-hour ozone, throughout the sampling season.

3.1.7 Twelve-Hour Day and Night Ozone Averages

Figures 3.25 and 3.26 are overlays of the 12-hour daytime and nighttime ozone data. The 24-hour day was broken into 6 a.m. to 6 p.m. and 6 p.m. and to 6 a.m. periods. The plots are labeled 7 a.m. and 7 p.m., since the data from 6 a.m./p.m. to 7 a.m./p.m. were averaged and recorded at 7 a.m./p.m.. The mean daytime and nighttime ozone concentrations are displayed in Table 3.2. For both years the daytime average is higher than nighttime. Peak ozone periods occurred in June and April for 1988 and 1989, respectively. The superimposed spline fits show that the largest differences in day and night averages were during hot daytime summer periods for both 1988 and 1989.

Table 3.2: Mean Day and Night Averages (6 a.m.-6 p.m., 6 p.m.-6 a.m., in ppb).

| 1988 | | 1989 | |
|------------|--------------|------------|--------------|
| <u>Day</u> | <u>Night</u> | <u>Day</u> | <u>Night</u> |
| 48 | 41 | 39 | 31 |

3.1.8 Seven-Hour Ozone Averages

Figures 3.27-3.28 display the seven-hour ozone averages with a Sm parameter of 60. The seven-hour period is from 9 a.m. to 4 p.m.* , which constitutes the hottest part of the day. The most striking differences are in the ozone concentrations during the predominantly hot days of summer for 1988 and 1989. In 1989 these values decreased throughout the sampling season, and

* 9 a.m. to 10 a.m. data are reported at 10 a.m., hence the graphs were labeled 10 a.m.-4 p.m.

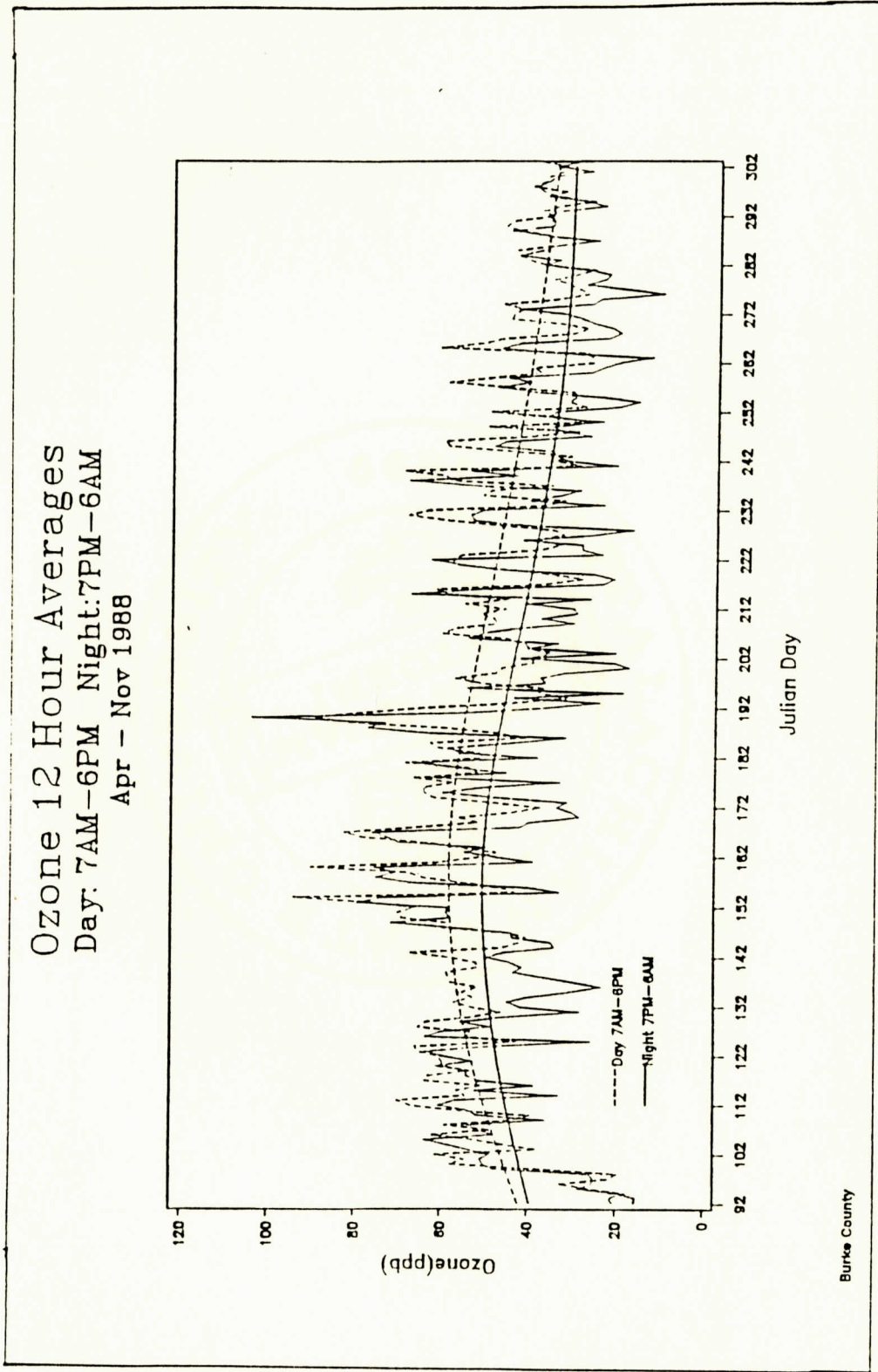


Figure 3.25: Overlays of the ozone 12-hour averages, day (7 a.m.-6 p.m.) and night (7 p.m.-6 a.m.) for 1988, using a spline fit with Sm parameter 60.

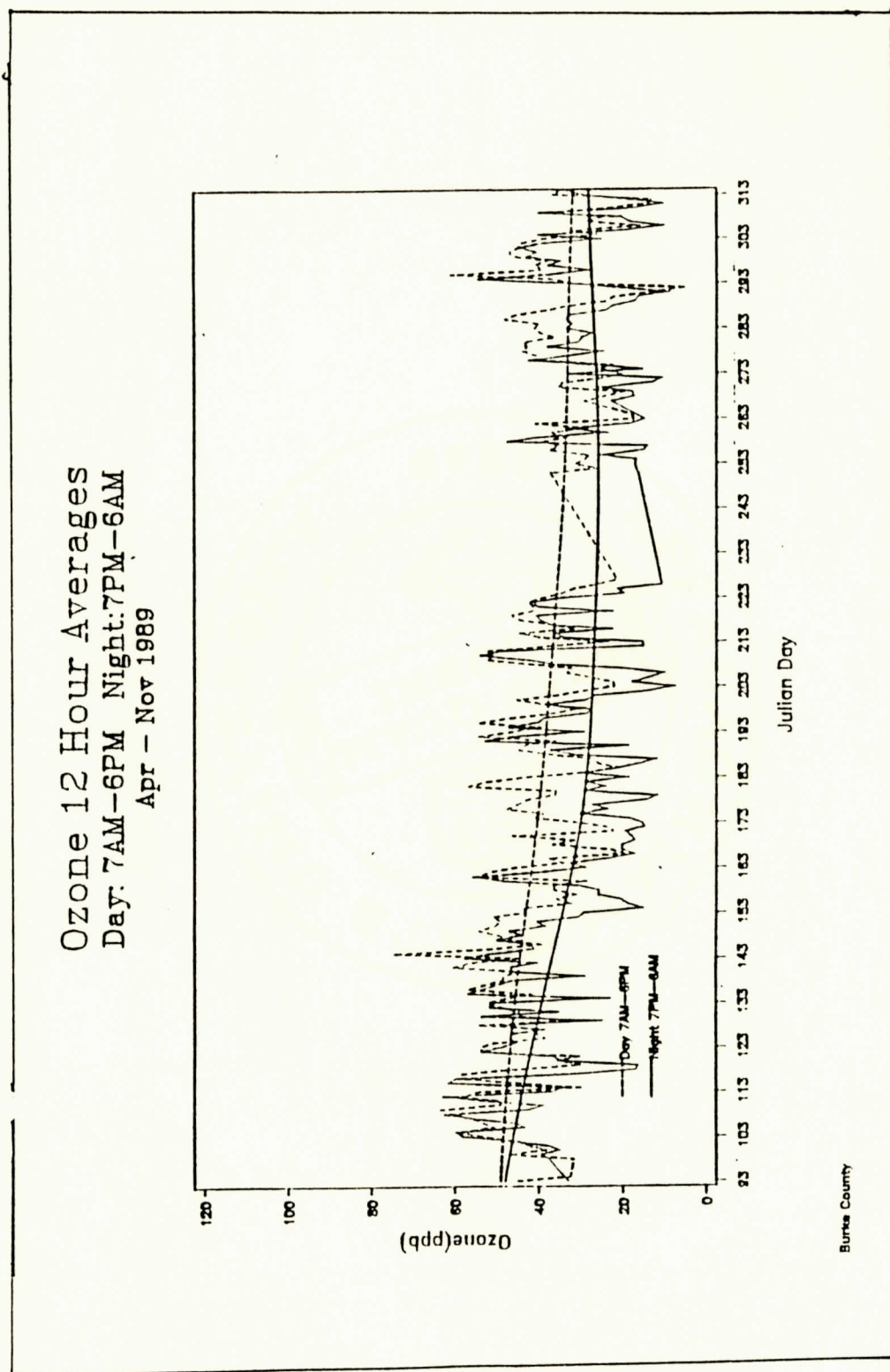


Figure 3.26: Overlays of ozone 12-hour averages, day (7 a.m.-6 p.m.) and night (7 p.m.-6 a.m.) for 1989, using a spline fit with Sm parameter 60.

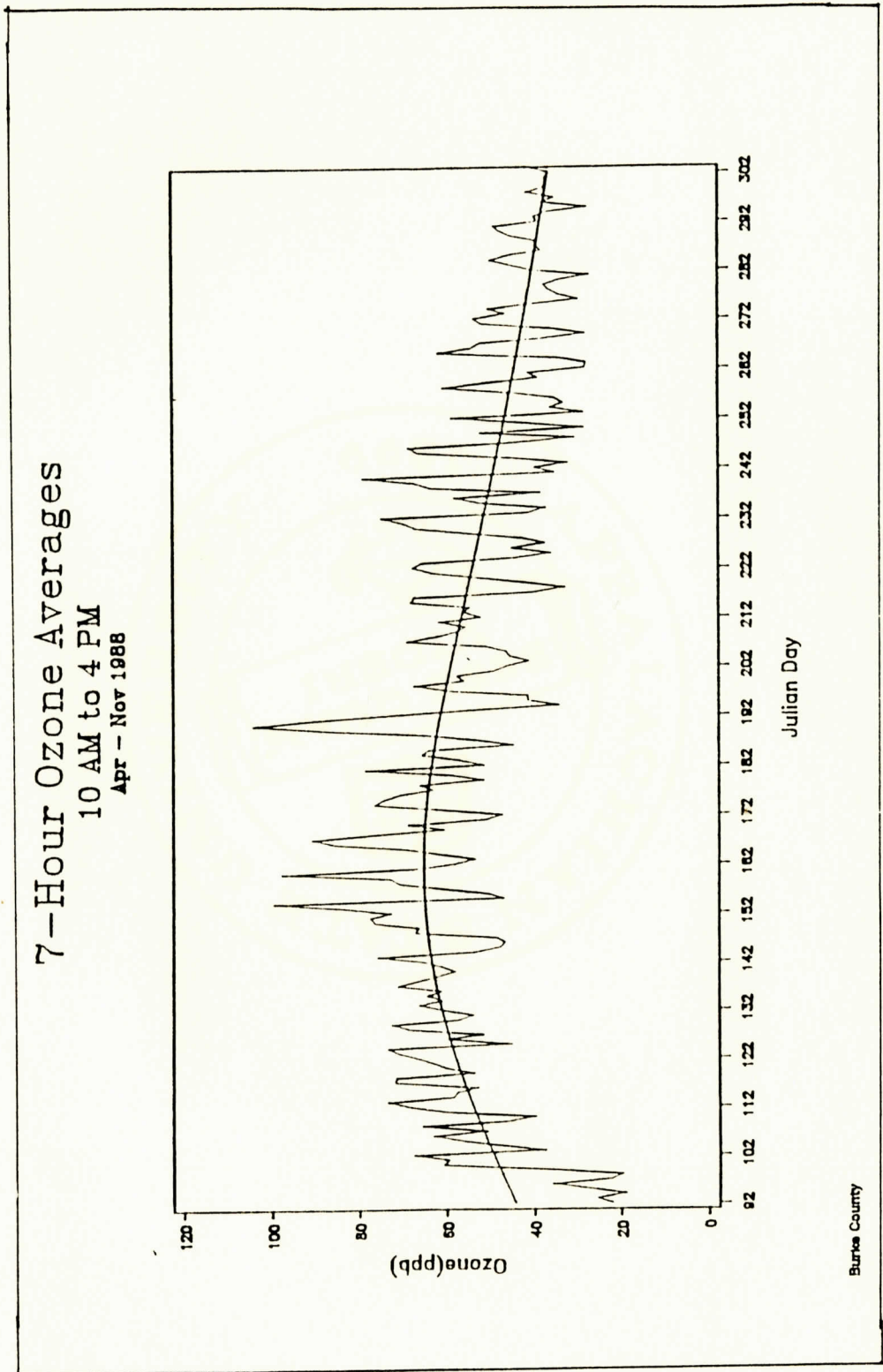


Figure 3.27: Seven-hour (10 a.m.-4 p.m.) ozone averages for 1988, using a spline fit with Sm parameter 60.

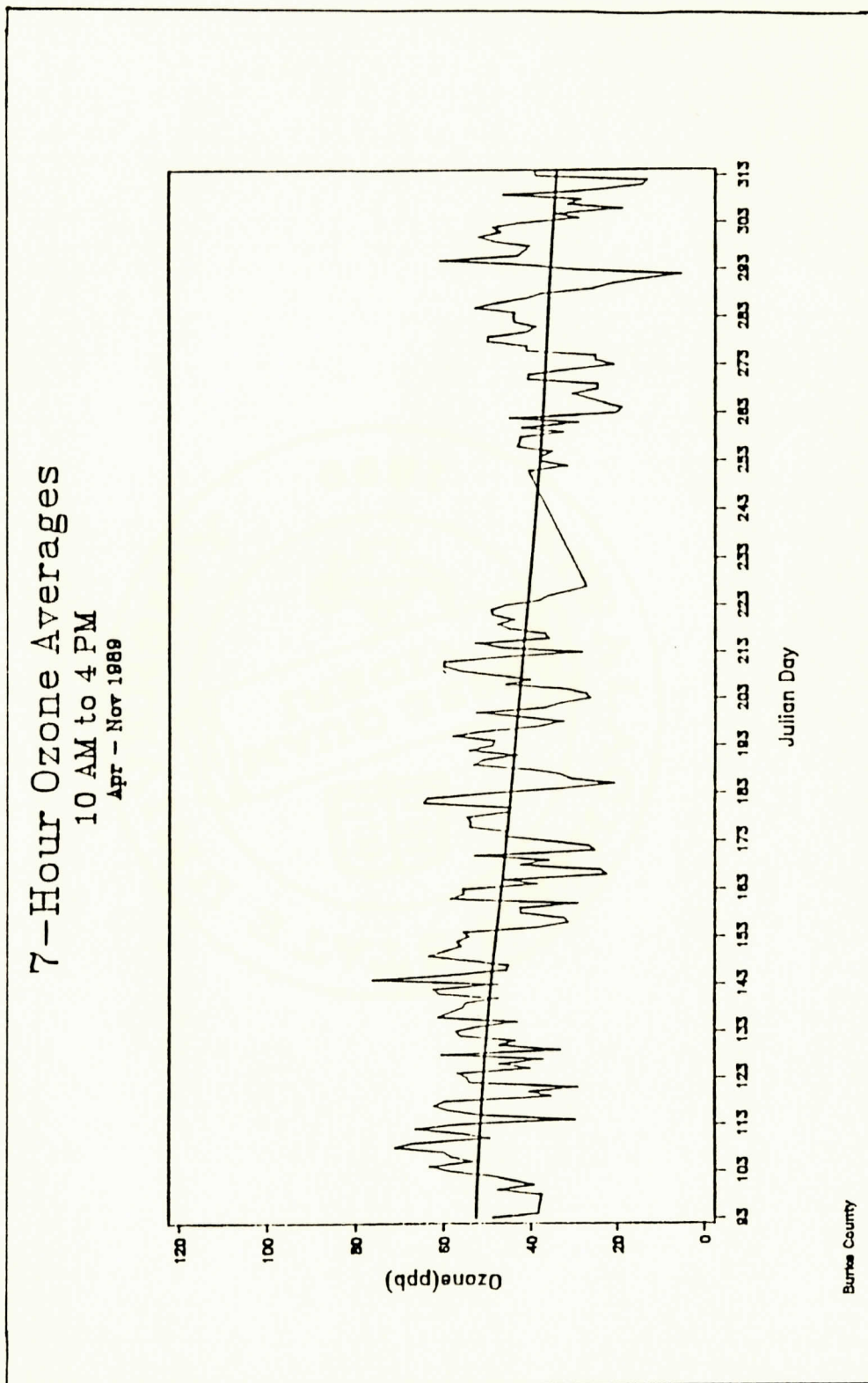


Figure 3.28: Seven-hour (10 a.m.-4 p.m.) ozone averages for 1989, using a spline fit with Sm parameter 60.

were also lower than the values occurring in 1988 during the same time period. Figures 3.29-3.30 are the seven-hour frequency distributions for 1988 and 1989, respectively. The mean values obtained were 53 ppb and 43 ppb in 1988 and 1989, respectively. Data from all plots indicate that ozone concentrations averaged higher during this seven-hour period than during the 12-hour daytime period.

3.1.9 Diurnal Ozone

Figure 3.31 displays the mean diurnal ozone for both 1988 and 1989. This plot provides further support that ozone concentrations were much lower in 1989 than in 1988. Both curves are typical of the diurnal ozone cycle at low elevations^{9,18,27}. Figures 3.32 and 3.33 are diurnal cycles displayed by seasons. All plots show midmorning minima and midafternoon maxima.

3.1.10 Monthly Average Ozone

Figure 3.34 shows monthly average ozone concentrations for both years. This plot strikingly contrasts the low summer ozone of 1989 with the more normal values of 1988. These low values can also be seen in Table 3.3 below.

Table 3.3: Monthly Mean and Maximum 24-Hour Ozone for 1988 and 1989, in ppb.

| | 1988 | | 1989 | | % Difference 1989 vs 1988 | |
|-------|-------------|----------------|-------------|----------------|------------------------------|----------------|
| | <u>Mean</u> | <u>Maximum</u> | <u>Mean</u> | <u>Maximum</u> | <u>Mean</u> | <u>Maximum</u> |
| April | 43 | 59 | 45 | 65 | +5 | +10 |
| May | 51 | 72 | 46 | 64 | -10 | -11 |
| June | 58 | 82 | 31 | 59 | -47 | -28 |
| July | 47 | 74 | 33 | 61 | -30 | -18 |
| Aug | 43 | 68 | 32 | 52 | -26 | -24 |
| Sept | 36 | 56 | 25 | 53 | -31 | -5 |
| Oct | 33 | 48 | 33 | 54 | 0 | +12 |
| Nov | - | - | 28 | 43 | - | - |

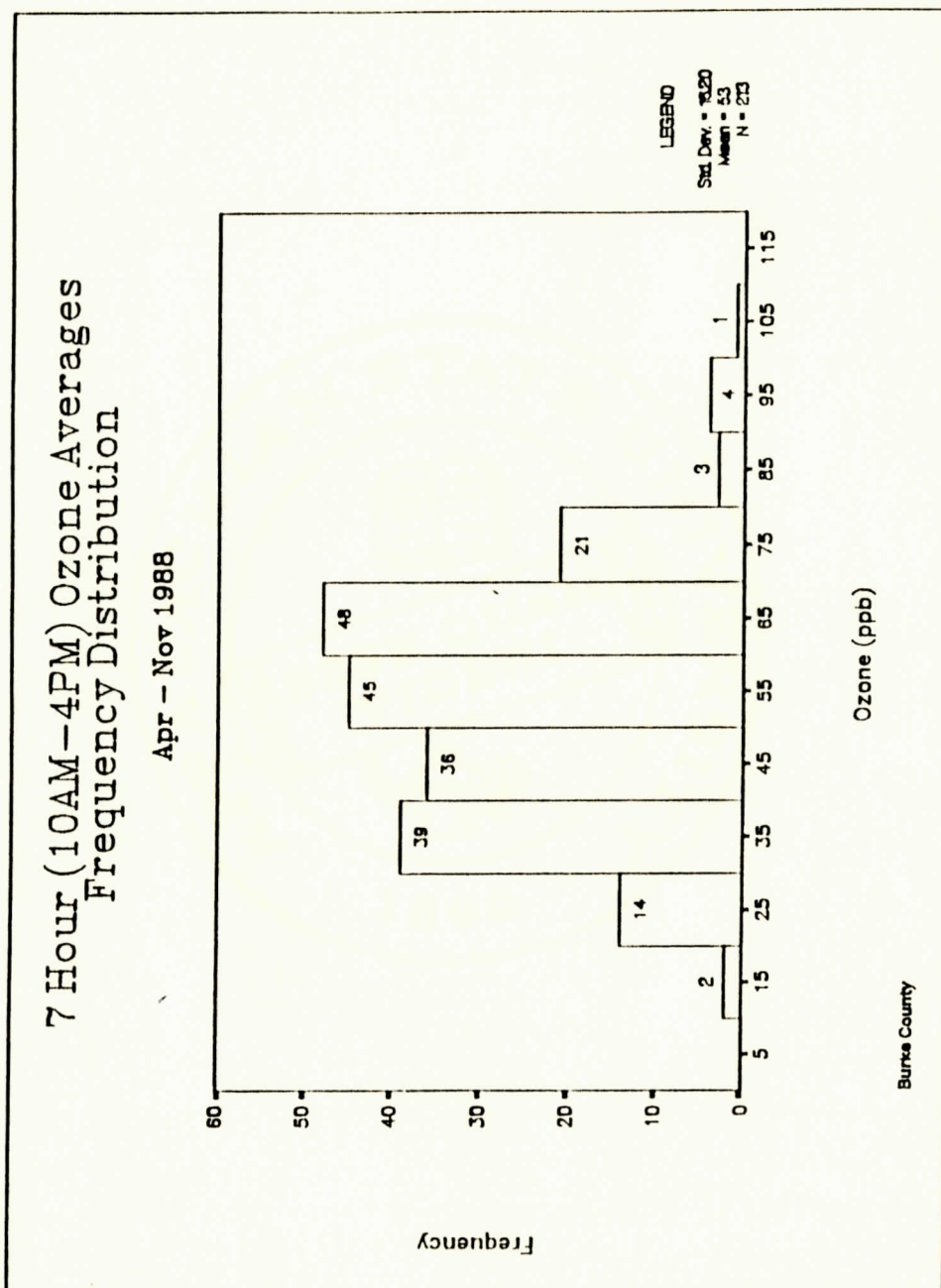


Figure 3.29: Seven-hour ozone averages frequency distribution for 1988.

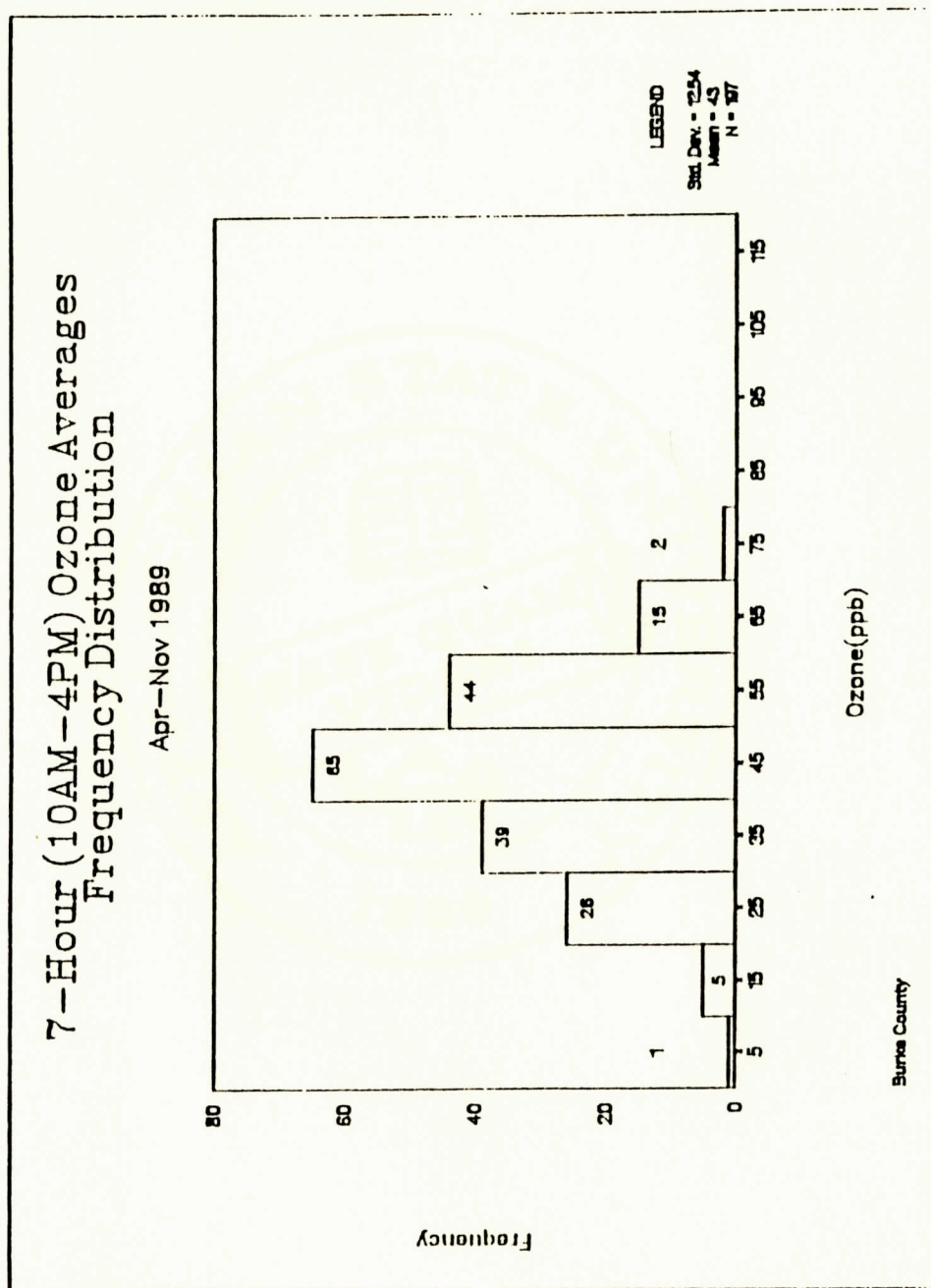


Figure 3.30: Seven-hour ozone averages frequency distribution for 1989.

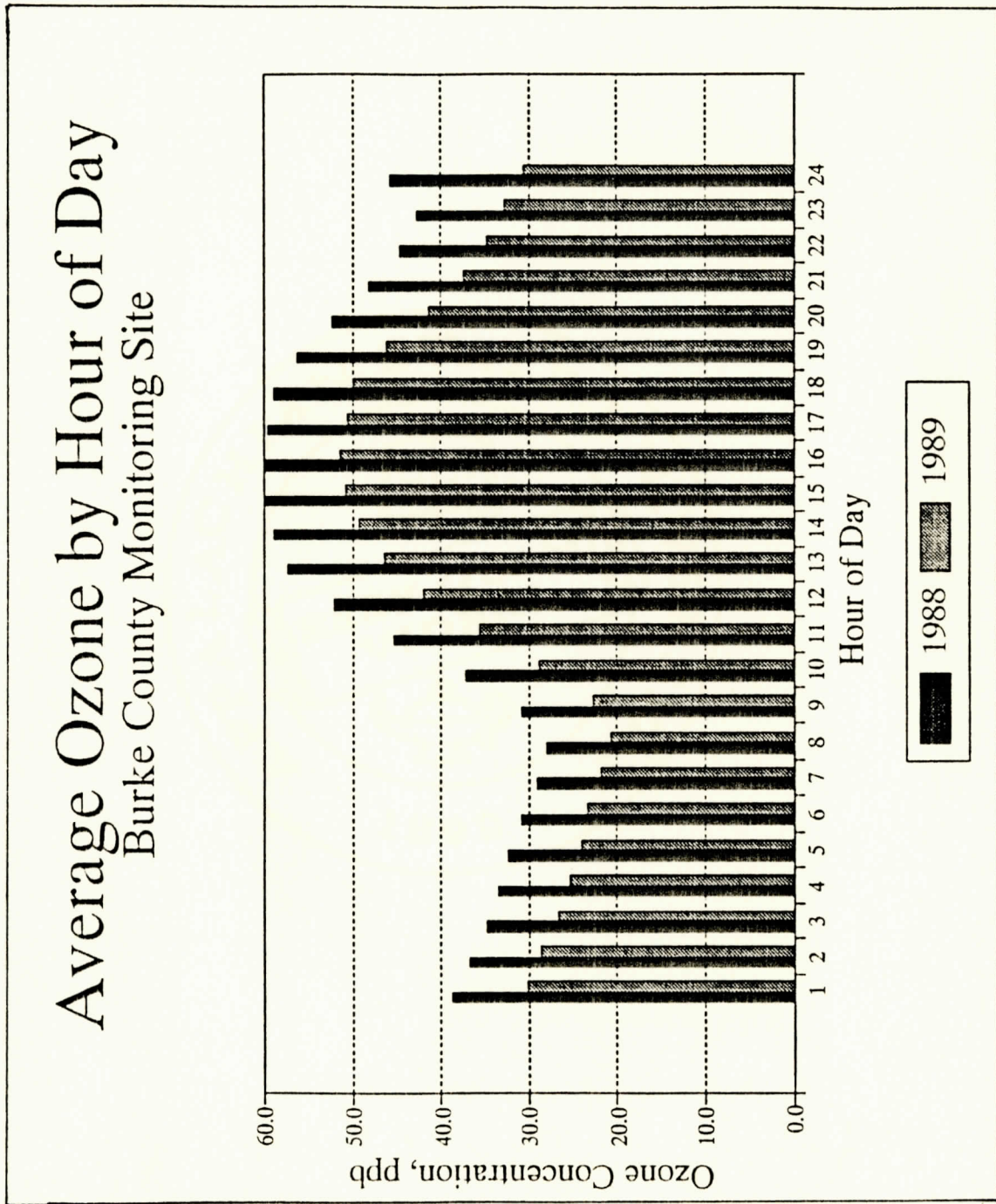


Figure 3.31: 1988 and 1989 Overlays of the mean diurnal cycles for Burke County, NC.

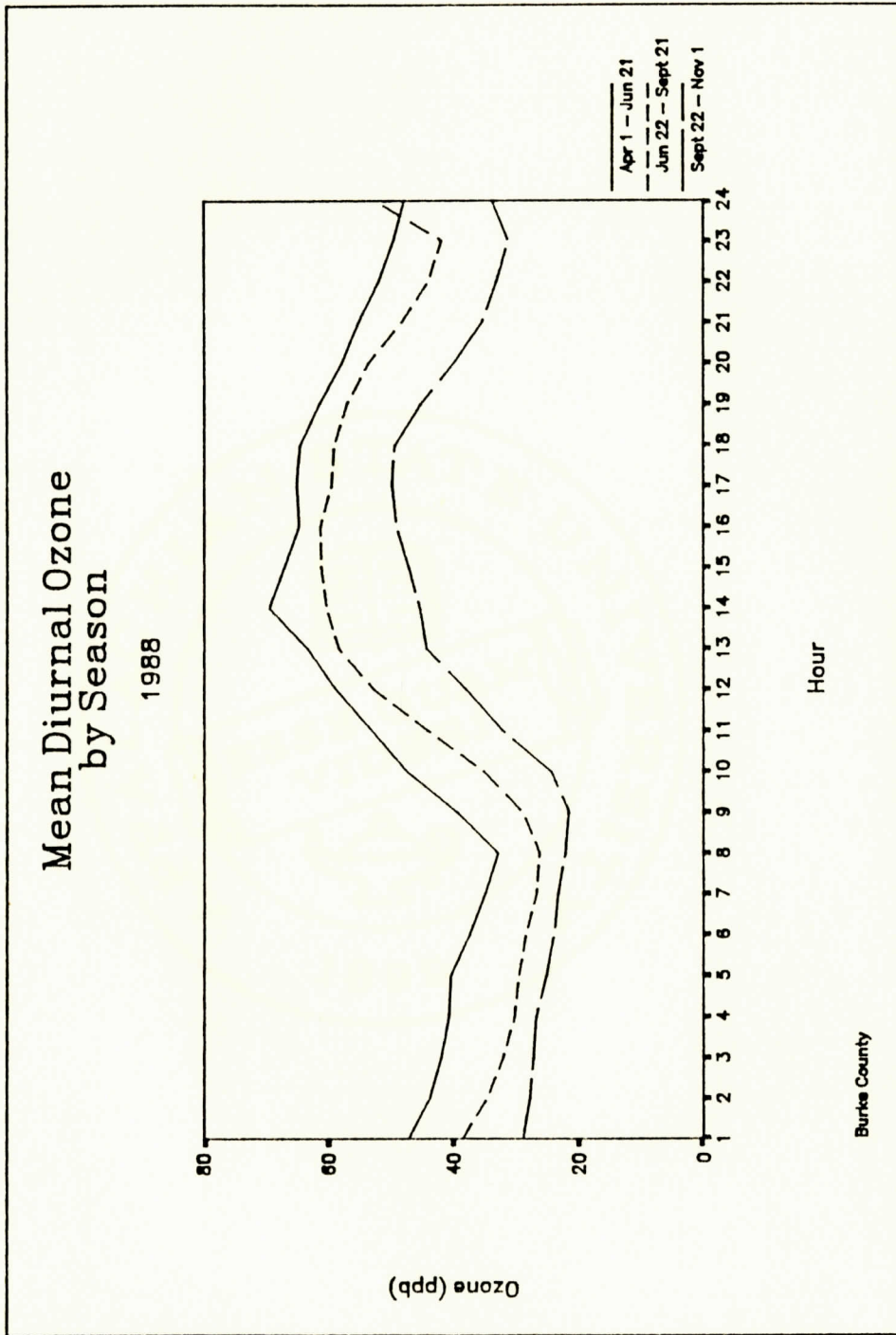


Figure 3.32: Mean diurnal ozone, by season, for 1988.

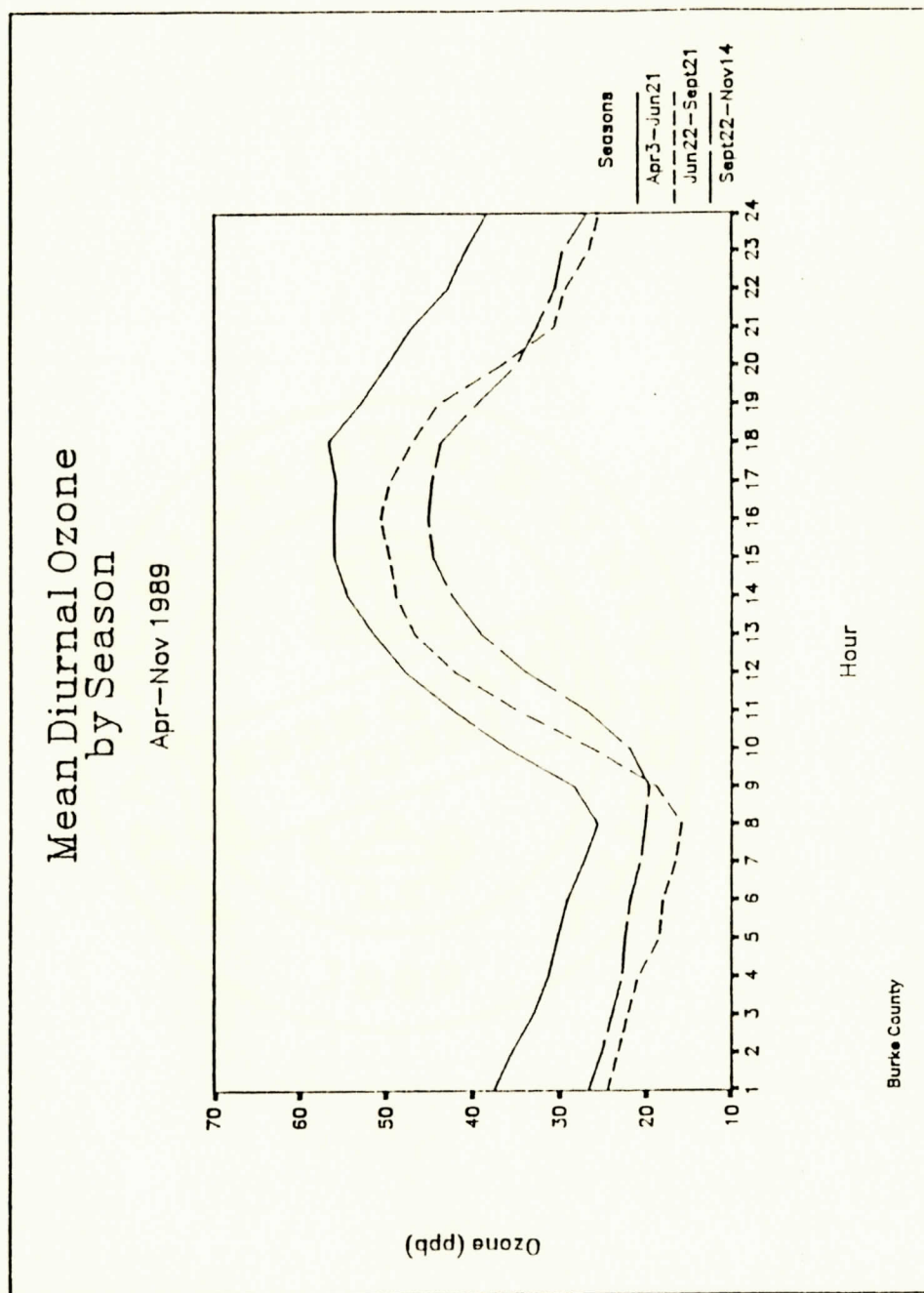


Figure 3.33: Mean diurnal ozone, by season, for 1989.

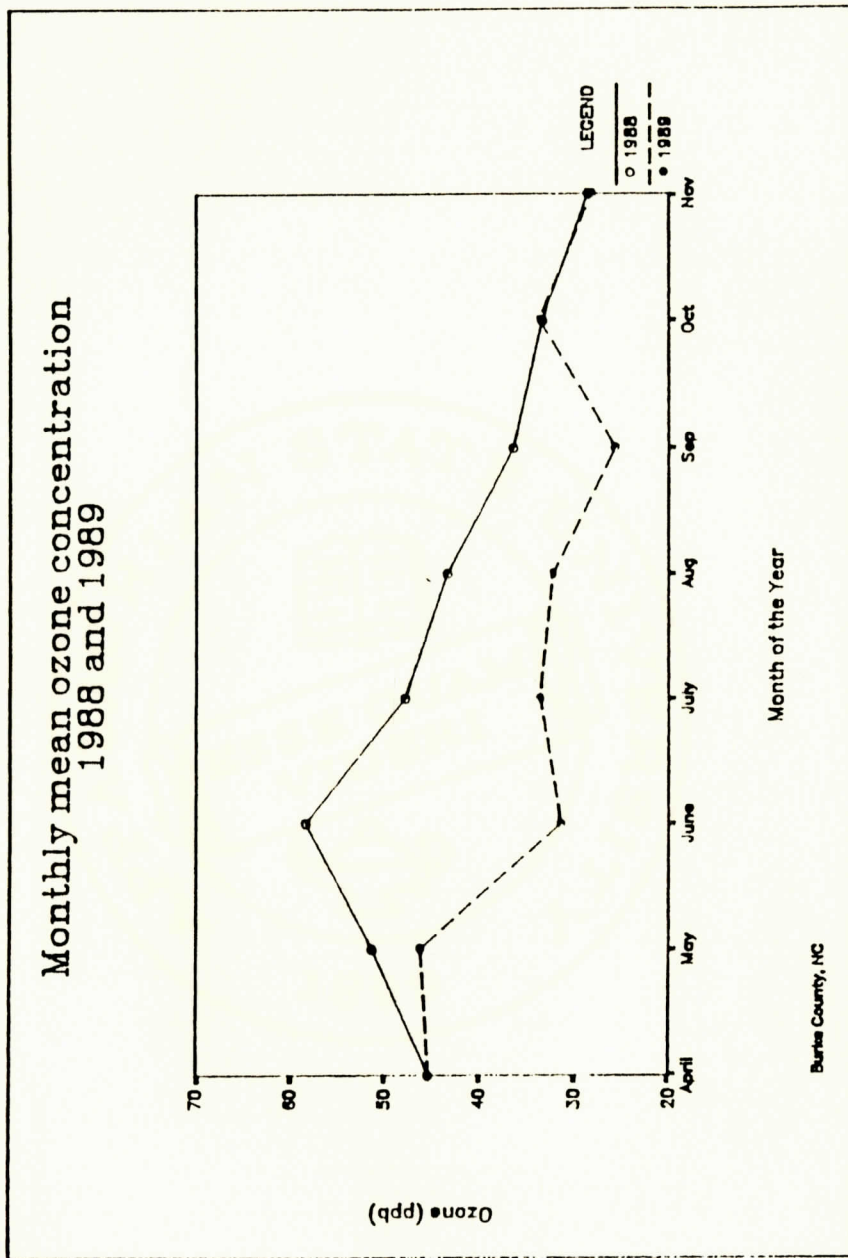


Figure 3.34: Monthly mean ozone concentrations for 1988 and 1989.

3.2 Meteorological Data for 1988 and 1989

Meteorological data were obtained from the National Weather Service at the Hickory Regional Airport. The airport is approximately 23 miles due east of the sampling site. Meteorological conditions were assumed to be similar at the site and the airport, since they are at approximately the same elevation, and there are no major geographical features (such as mountain ranges) between the two locales. Each has a lake adjacent to the area, and both are in the Catawba River Valley. Weather conditions for the two years were very different, 1988 being unusually dry and 1989 relatively cool and wet.

3.2.1 Average Daily and 24-Hour Average Ambient Temperatures

Figure 3.35 displays the average daily ambient temperatures for 1988 and 1989. Both years show the usual maximizing in late summer, but 1989 clearly had more cool days. Figures 3.36 and 3.37 are 24-hour average ambient temperatures, smoothed by a weighted least-square technique available on SPSS. This smoothing technique is very similar to spline fit smoothing. In 1988 ambient temperatures occurring in the summer averaged about 3 °C higher than in 1989.

3.2.2 Twenty-four-Hour Average Water in the Atmosphere

Water is considered the most important of the trace gases in the atmosphere. Water vapor comprises about three percent of atmospheric gas by volume and is the only constituent that varies significantly in concentration³⁴. In most mathematical models of the atmosphere, water vapor is included as relative humidity. Another indication of the amount of water vapor in the atmosphere is the difference between the ambient and dewpoint temperatures^{**}. According to W. D. Bach of the Army Research Office, Research Triangle Park, NC²⁵, when the difference is small (< 3 °C), the air is nearly saturated. When the separation is large (> 15 °C), the air is dry²⁵.

^{**} Dewpoint temperature is defined as the temperature to which air must be cooled at constant pressure in order for it to become saturated with respect to a plane surface of water^{35,36}

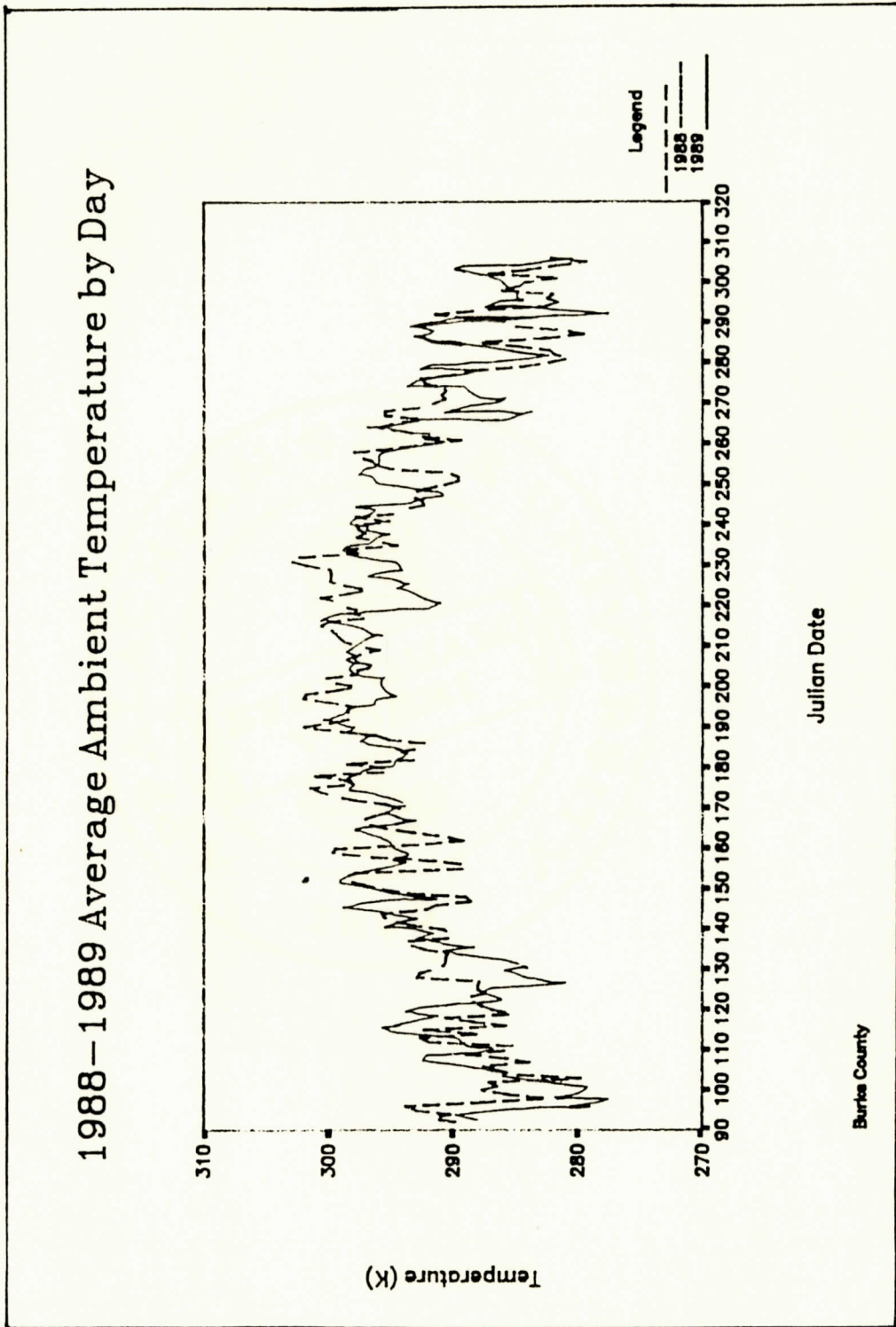


Figure 3.35: 1988 and 1989 average ambient temperatures by day.

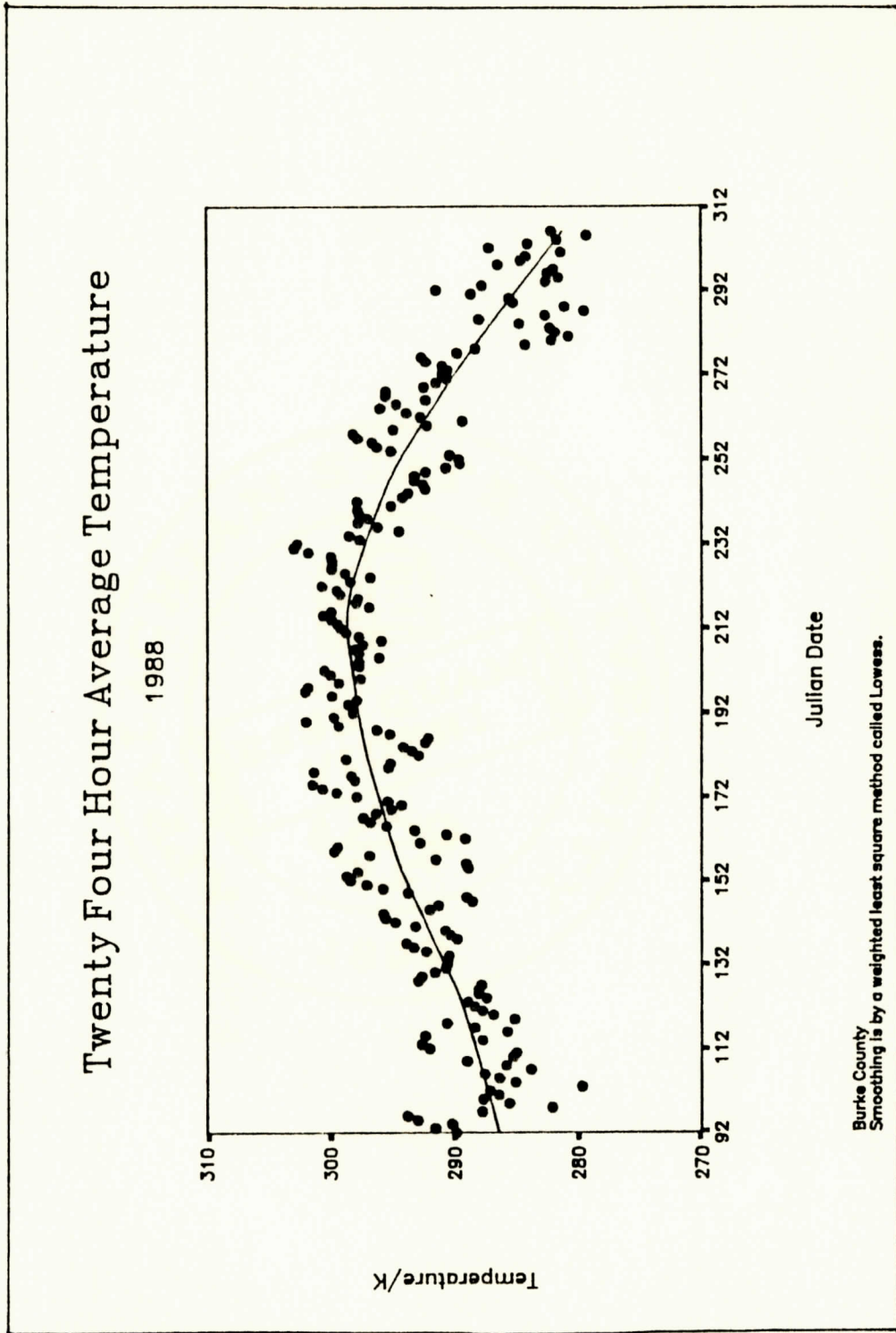


Figure 3.36: Twenty-four-hour average ambient temperature for 1988, using a weighted least square smoothing curve with smoothing parameter 33.3.

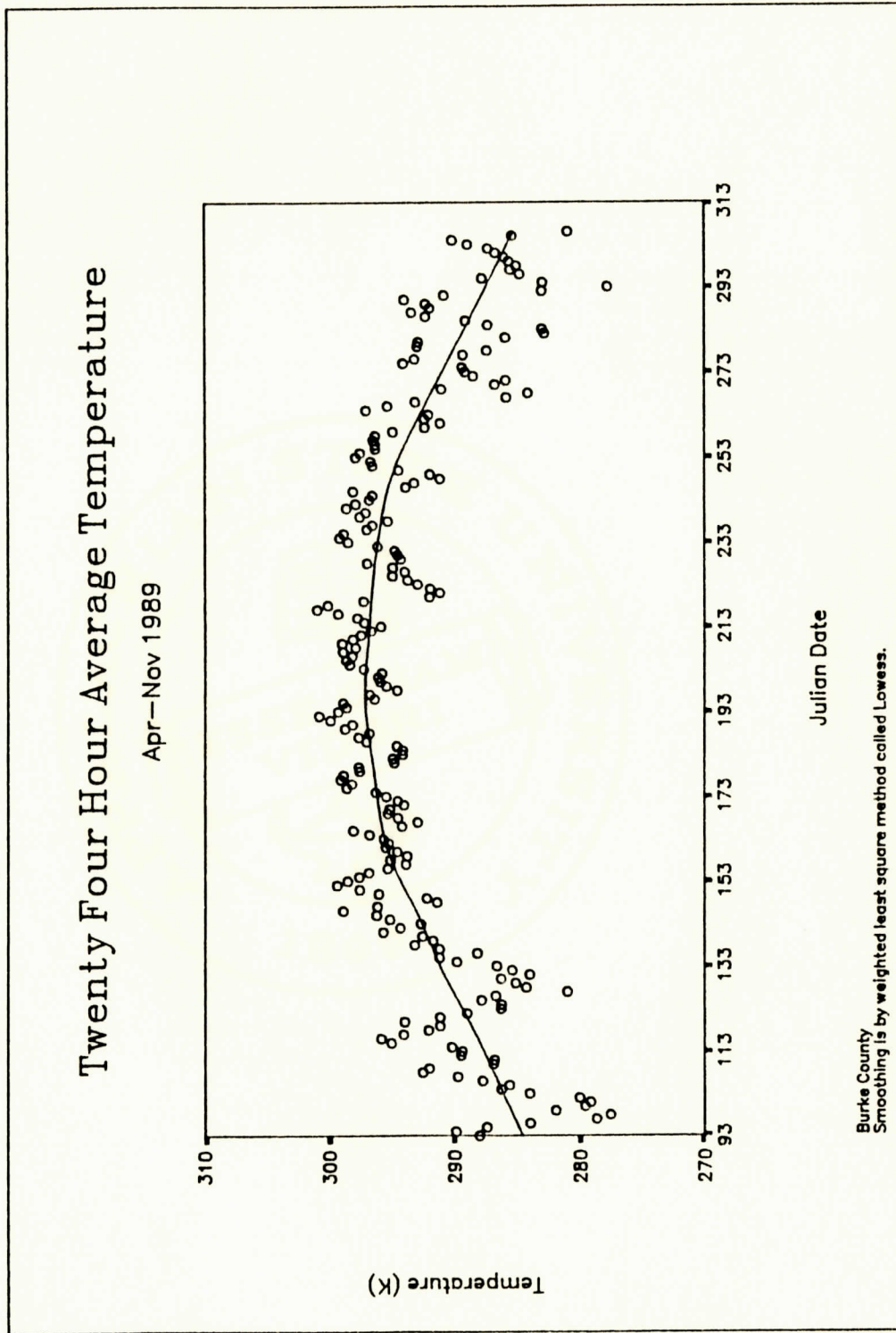


Figure 3.37: Twenty-four-hour average ambient temperature for 1989, using a weighted least square smoothing curve with smoothing parameter 33.3.

Figures 3.38 and 3.39 are charts of the average ambient and the dewpoint temperatures spread. It is clear that 1989 was a wetter year than 1988.

Bach suggested that a parameter to represent the absolute amount of water vapor should be included in any model attempting to predict ozone concentrations³⁷. This is accomplished using the integrated exponential form of the Clausius-Clapeyron equation,

$$P = C \exp(-\Delta H/RT) \quad (31)$$

where P is the water vapor pressure; C is a constant; ΔH is the enthalpy of vaporization of water; R is the universal gas constant; and T is the temperature of the gas. Assuming a constant value of ΔH over the temperature range³⁸ of -10 °C to 40 °C and taking the natural logarithm of equation 31 gives an equation for the absolute vapor pressure of water as a function of dewpoint temperature, T_d .

$$\ln P = -5352.42/T_d + 21.11 \quad (32)$$

Figures 3.40 and 3.41 are plots of the 24-hour average water vapor in the atmosphere for the two years as calculated using equation 32. These plots support Figures 3.38 and 3.39, showing that there were longer periods where the atmosphere was saturated in 1989 than in 1988. In 1988, peak water vapor occurred in late summer. In 1989 there was a broad maximum for water vapor pressure during all summer months.

3.2.3 Twenty-four-Hour Average Cloud Cover

Figures 3.42 and 3.43 are 24-hour average cloud cover for the two years, recorded in percentages. Both curves are of the same general shape. However, the 1989 data indicate that skies were approximately ten percent more obscured. Average cloud cover was about 55 percent during the summer period for 1988, and 65 percent in 1989.

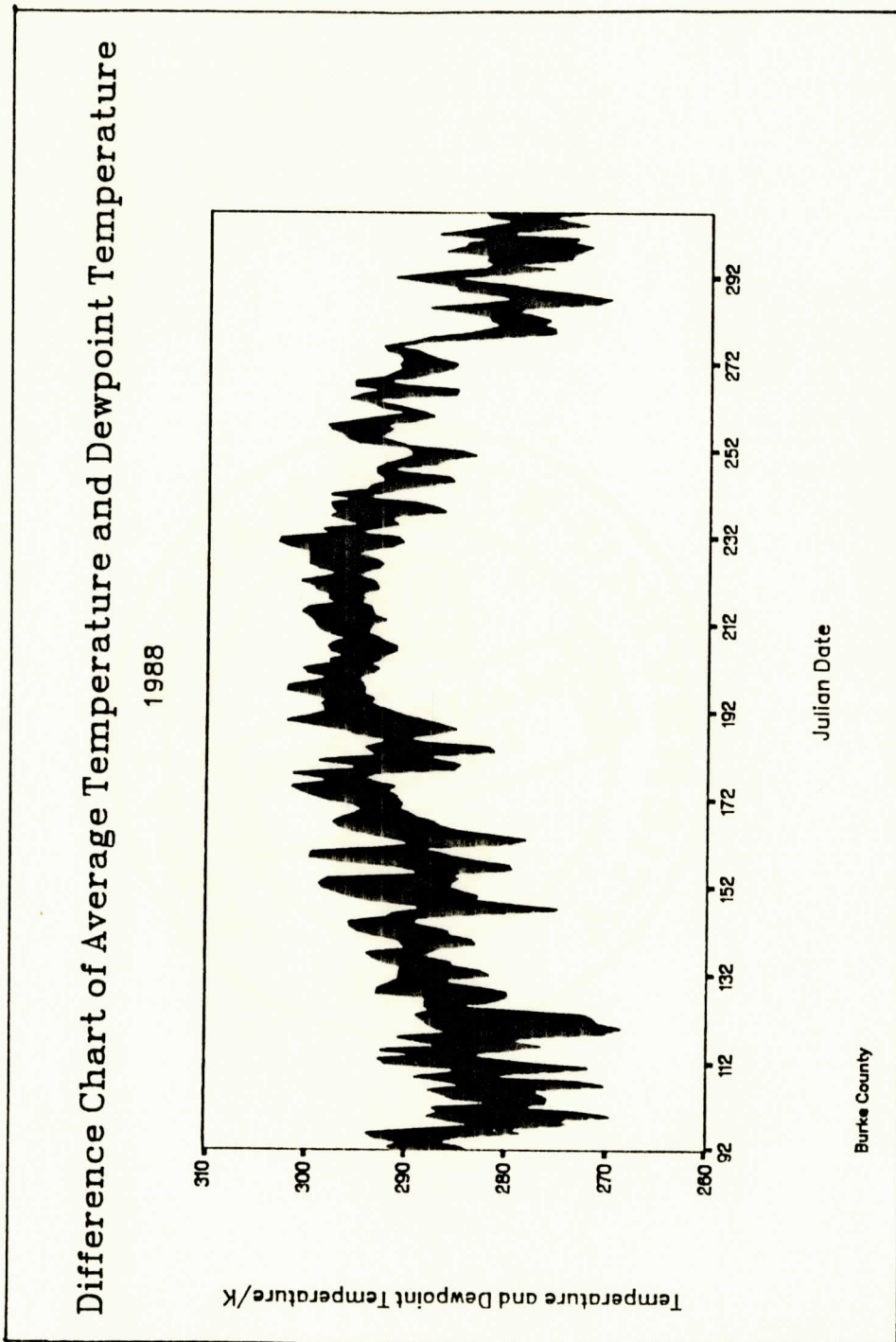


Figure 3.38: Difference chart of average ambient and dewpoint temperatures for 1988.

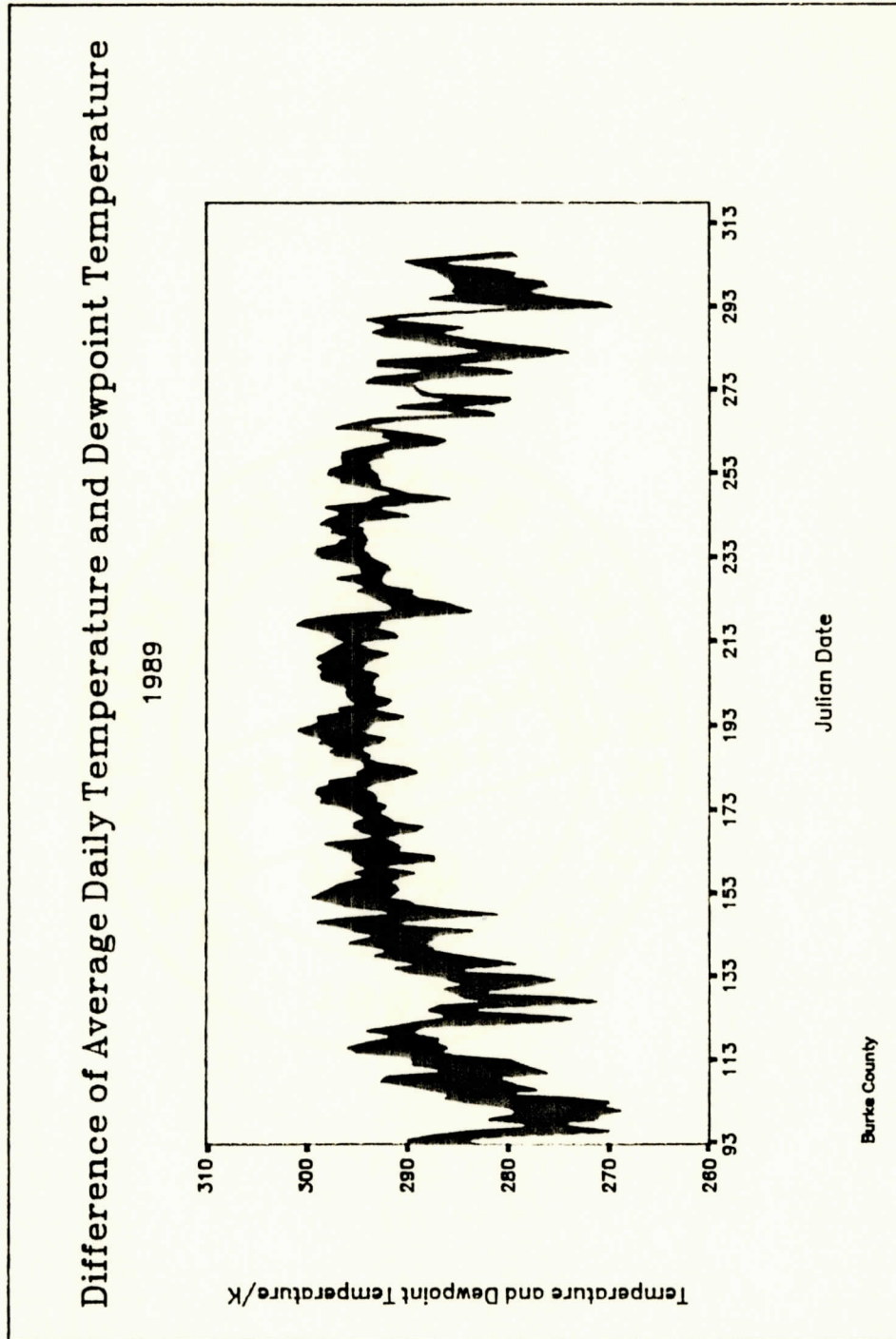


Figure 3.39: Difference chart of average ambient and dewpoint temperatures for 1989.

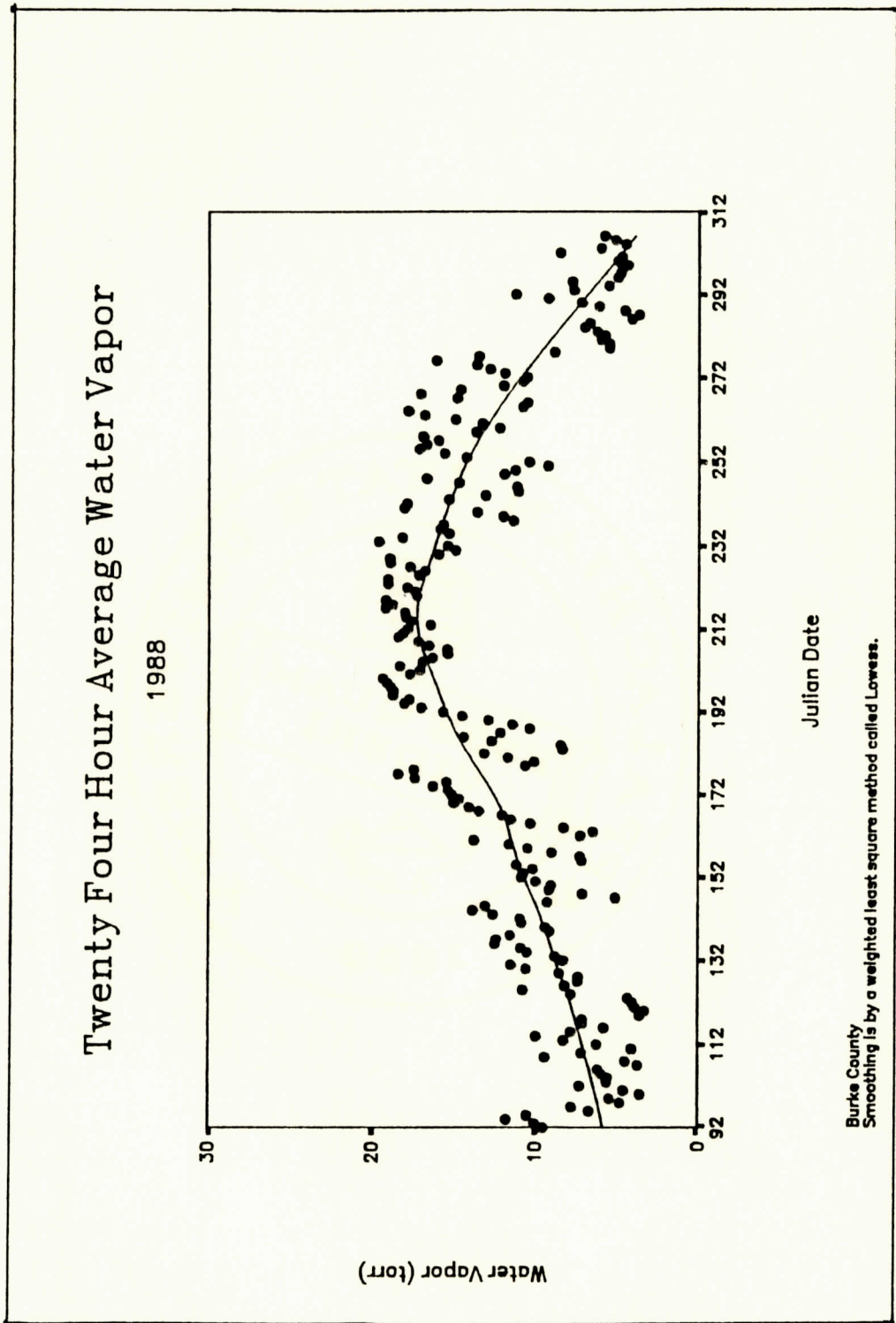


Figure 3.40: Twenty-four-hour average water vapor for 1988, in torr, using a weighted least square smoothing curve with smoothing parameter 33.3.

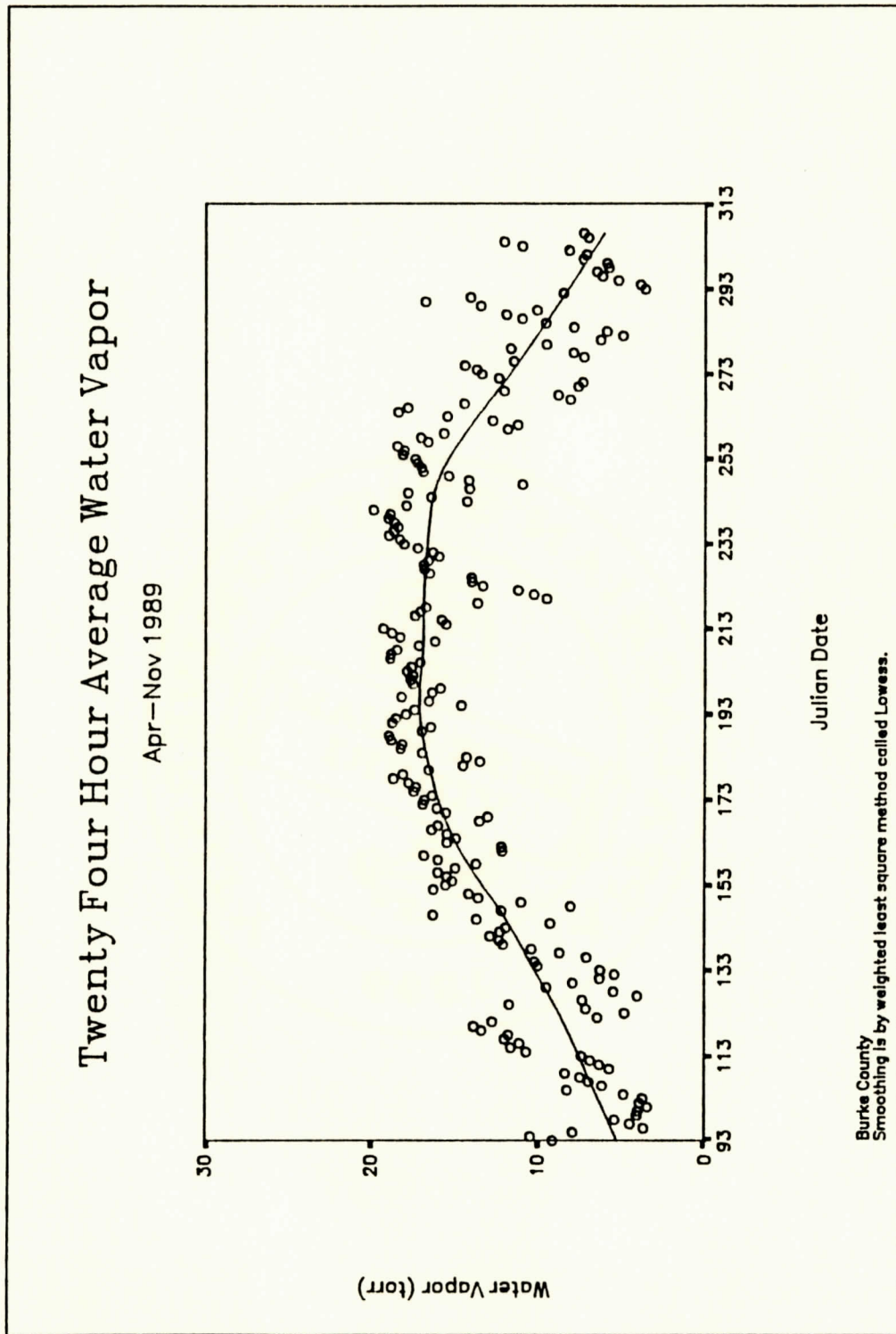


Figure 3.41: Twenty-four-hour average water vapor for 1989, in torr, using a weighted least square smoothing curve with smoothing parameter 33.3.

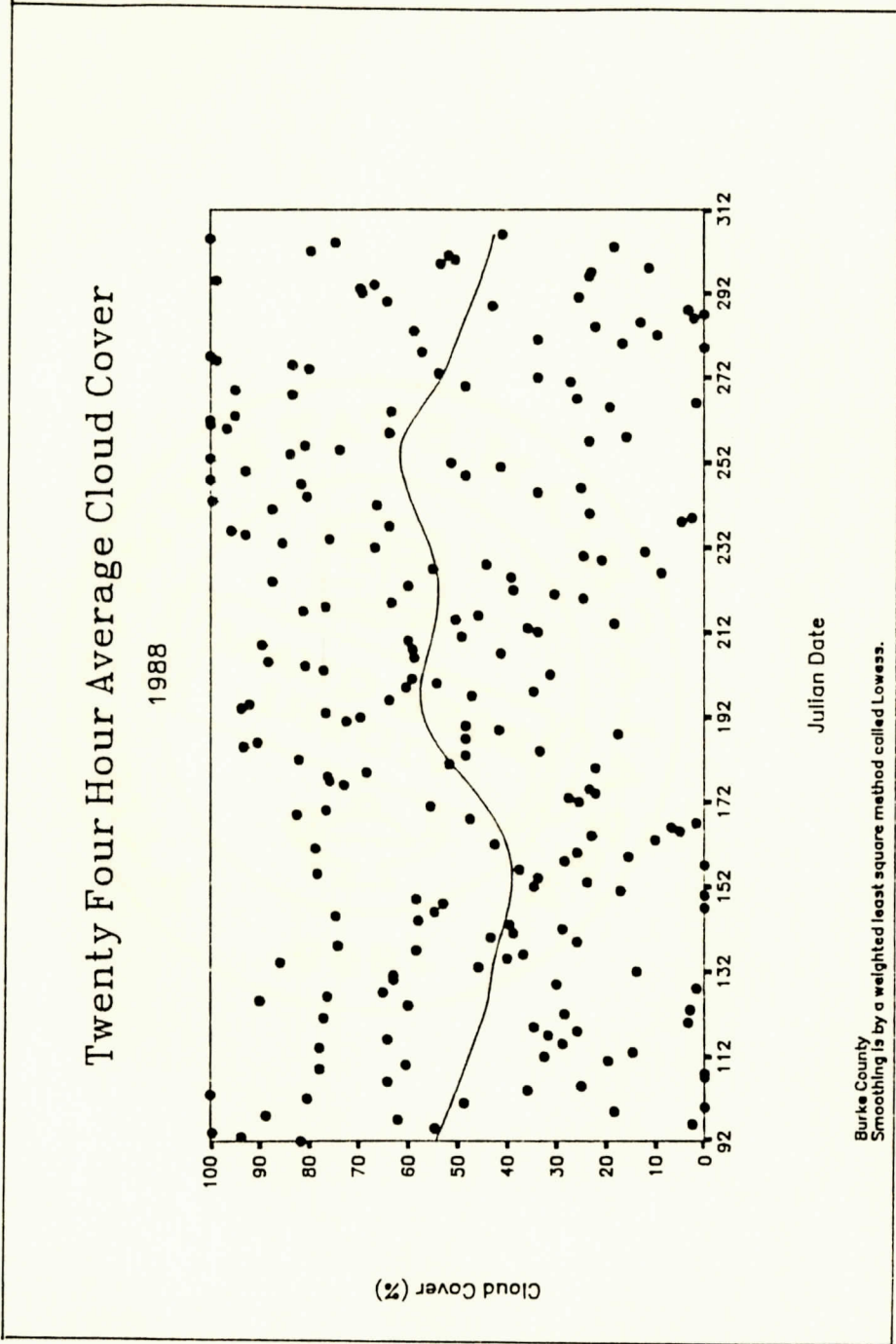


Figure 3.42: Twenty-four-hour average cloud cover in percent by day, for 1988.

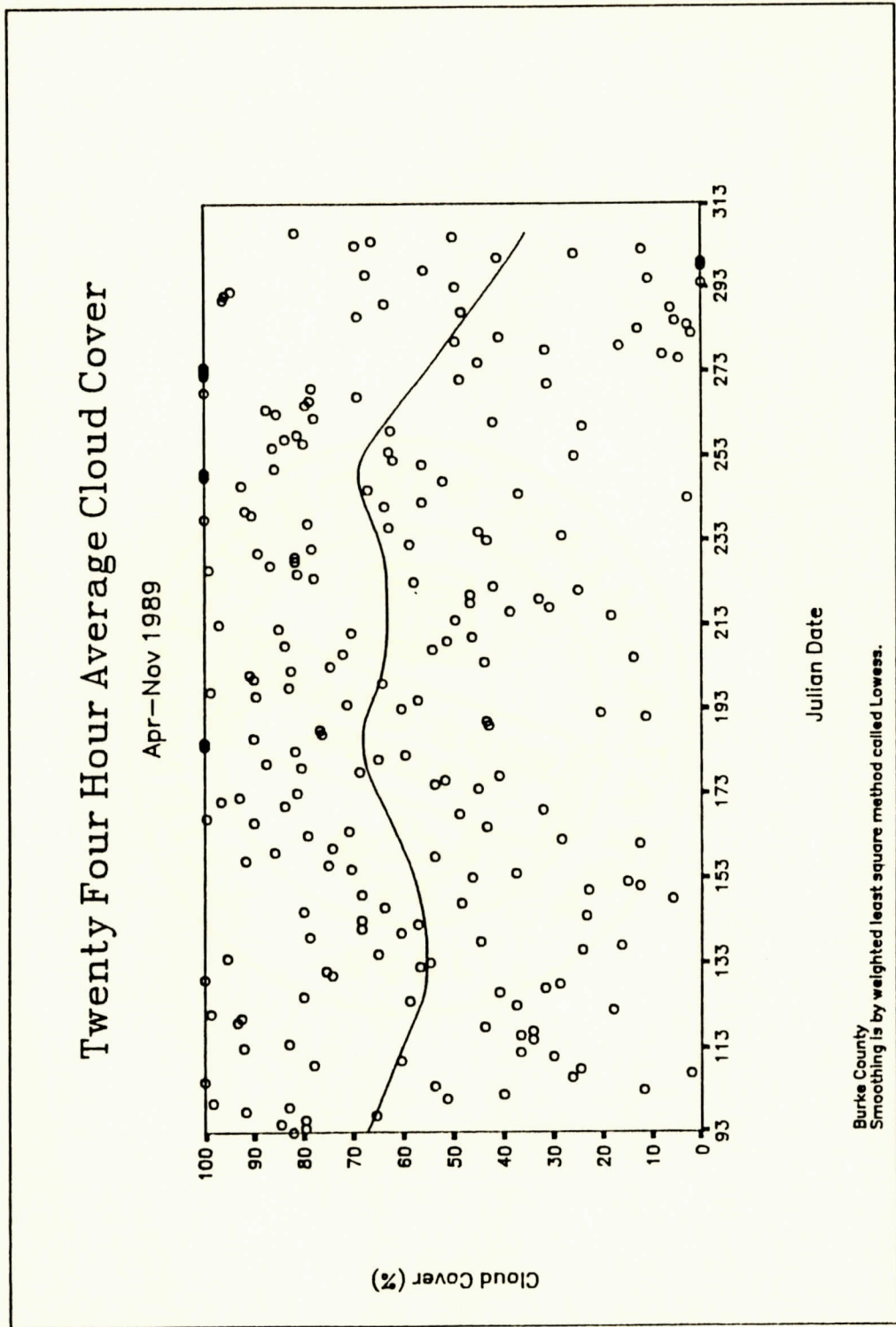


Figure 3.43: Twenty-four-hour average cloud cover in percent by day, for 1989.

3.3 Simple Linear Comparisons

Simple linear correlations of ozone versus weather variables were conducted. Figures 3.44 to 3.55 display average ozone versus average 24-hour temperature, water vapor, and cloud cover for 1988 and 1989. Figures 3.44, 3.45, 3.46, 3.47, 3.48, and 3.49 are plots of ozone versus temperature, water vapor and cloud cover by day, all without smoothing. Since there is a large amount of variability in the data these plots are difficult to interpret. The weighted least-squares smoothing technique was then applied to the data to see what relationships existed. Figures 3.50, 3.51, 3.52, 3.53, 3.54, and 3.55 display the various plots with the smoothing technique applied.

3.3.1 Twenty-Four-Hour Ozone versus Ambient Temperature, Water Vapor and Cloud Cover.

The smoothed temperature and ozone plots of Figures 3.50 and 3.51 do not show the positive relationship expected from earlier studies^{14,15,25,33}. Rather, there appears to be a decrease in ozone at higher average temperatures. Figure 3.51 clearly indicates an inverse relationship existing between ambient temperature and ozone. Figures 3.52 and 3.53 display smoothed overlays of ozone and water vapor. A clear inverse relationship exists between these variables, for both years. When cloud cover was correlated with ozone in the smoothed plots (Figures 3.54 and 3.55) the most significant aspect was the inverse relationship.

3.4 Multiple Linear Regression to Predict Ozone

Multiple linear regression (MLR) equations were generated from their respective yearly databases. The computerized stepwise search described in section 2.2.4 yielded an equation with coefficients of determination (R squared) for years and seasons. Table 3.4 displays these

coefficients of determination (R squared) for all the seasonal and yearly equations generated.

Highest coefficients obtained were for the Fall seasons.

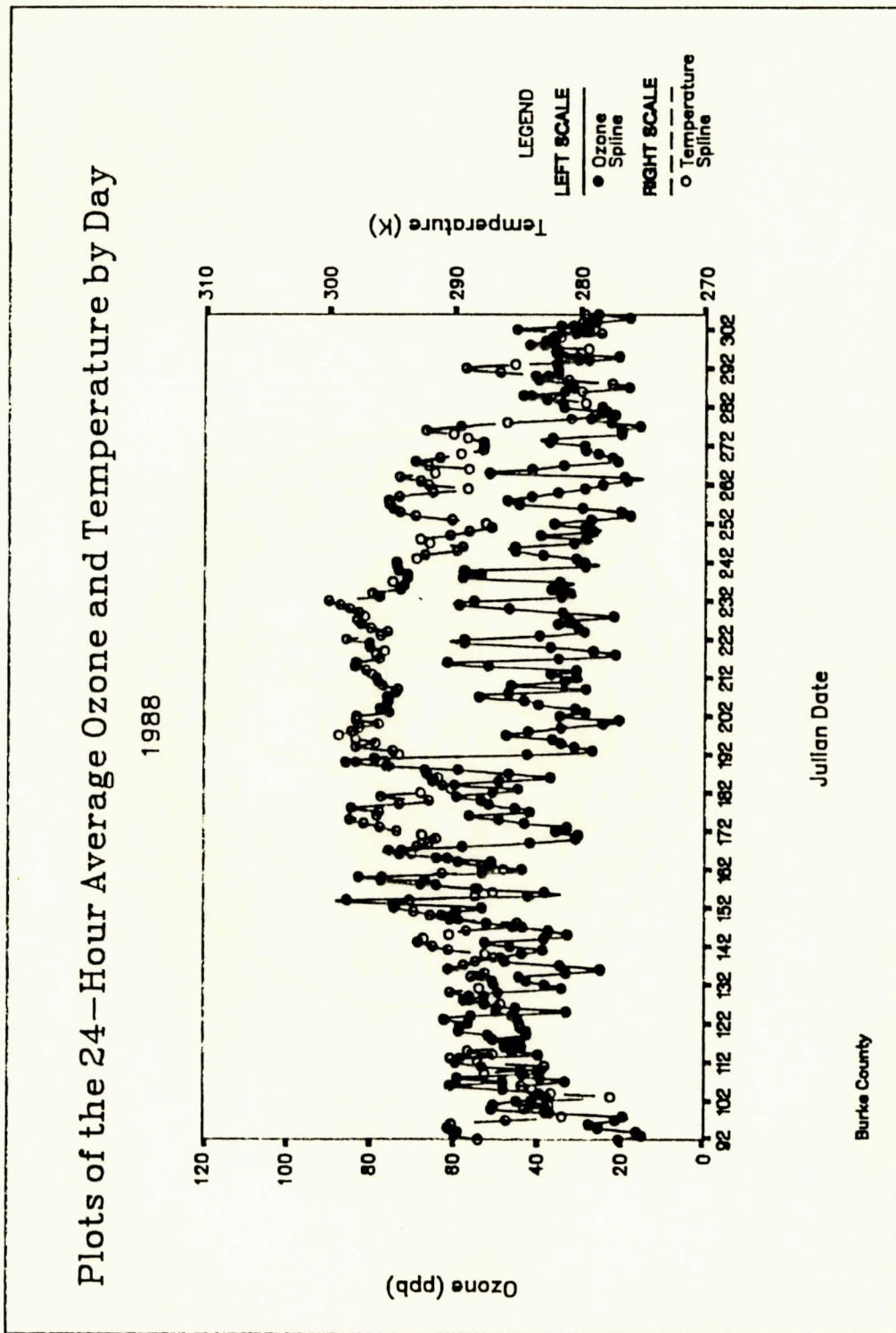


Figure 3.44: Twenty-four-hour average ozone and ambient temperature by day, for 1988, using a spline fit with S_m parameter 1.

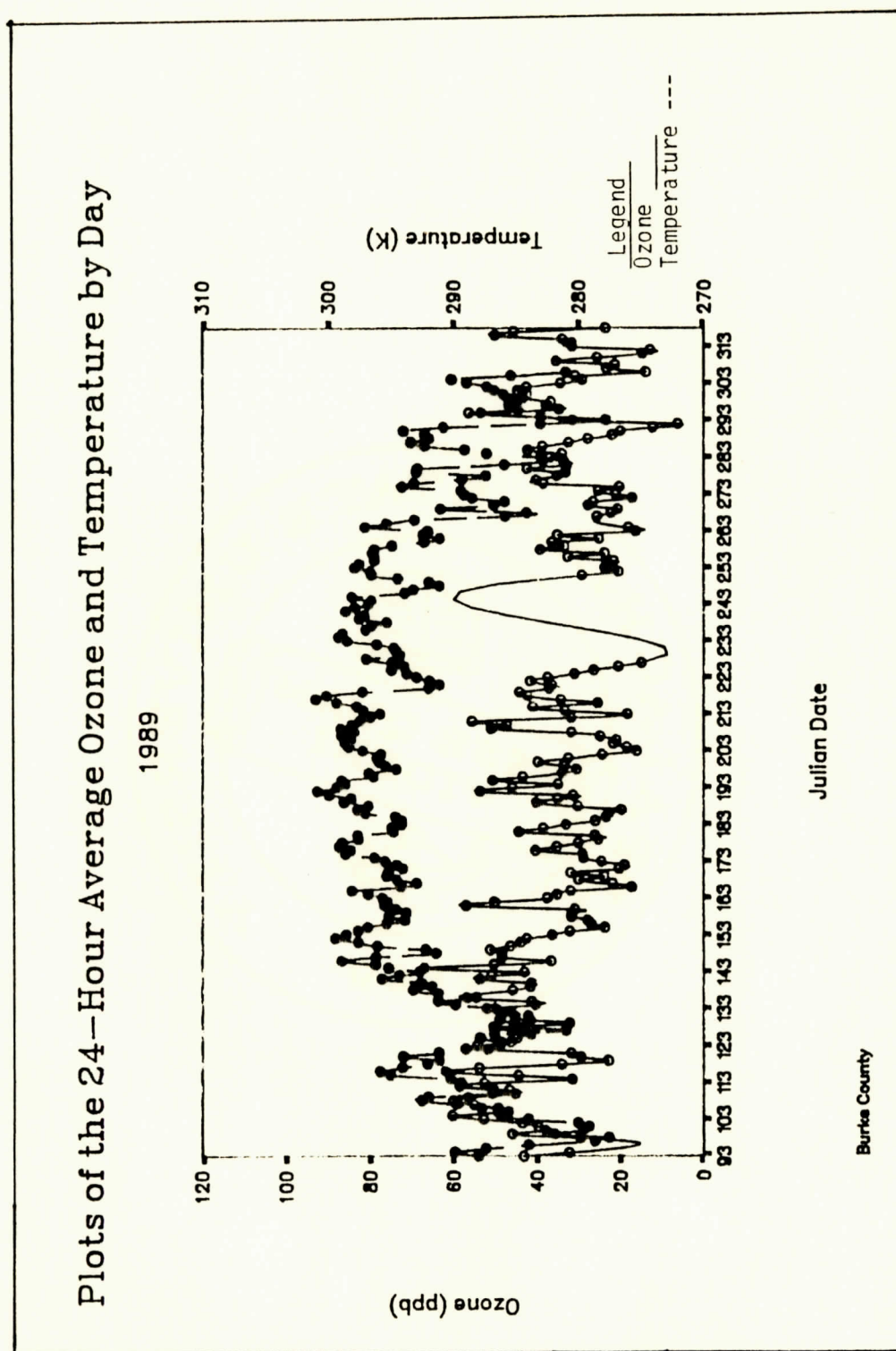


Figure 3.45: Twenty-four-hour average ozone and ambient temperature by day, for 1989, using a spline fit with S_m parameter 1.

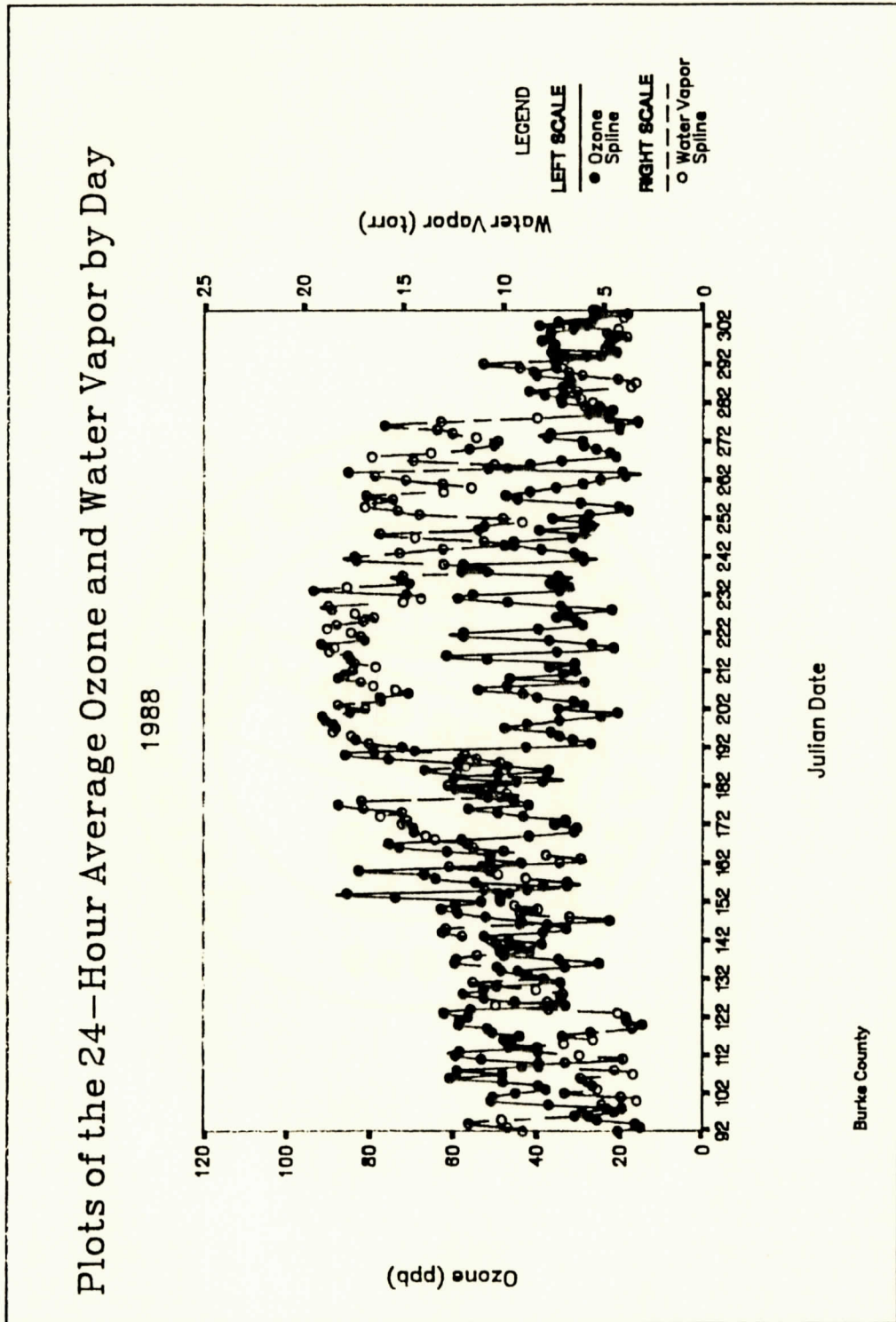


Figure 3.46: Twenty-four-hour average ozone and water vapor by day, for 1988, using a spline fit with S_m parameter 1.

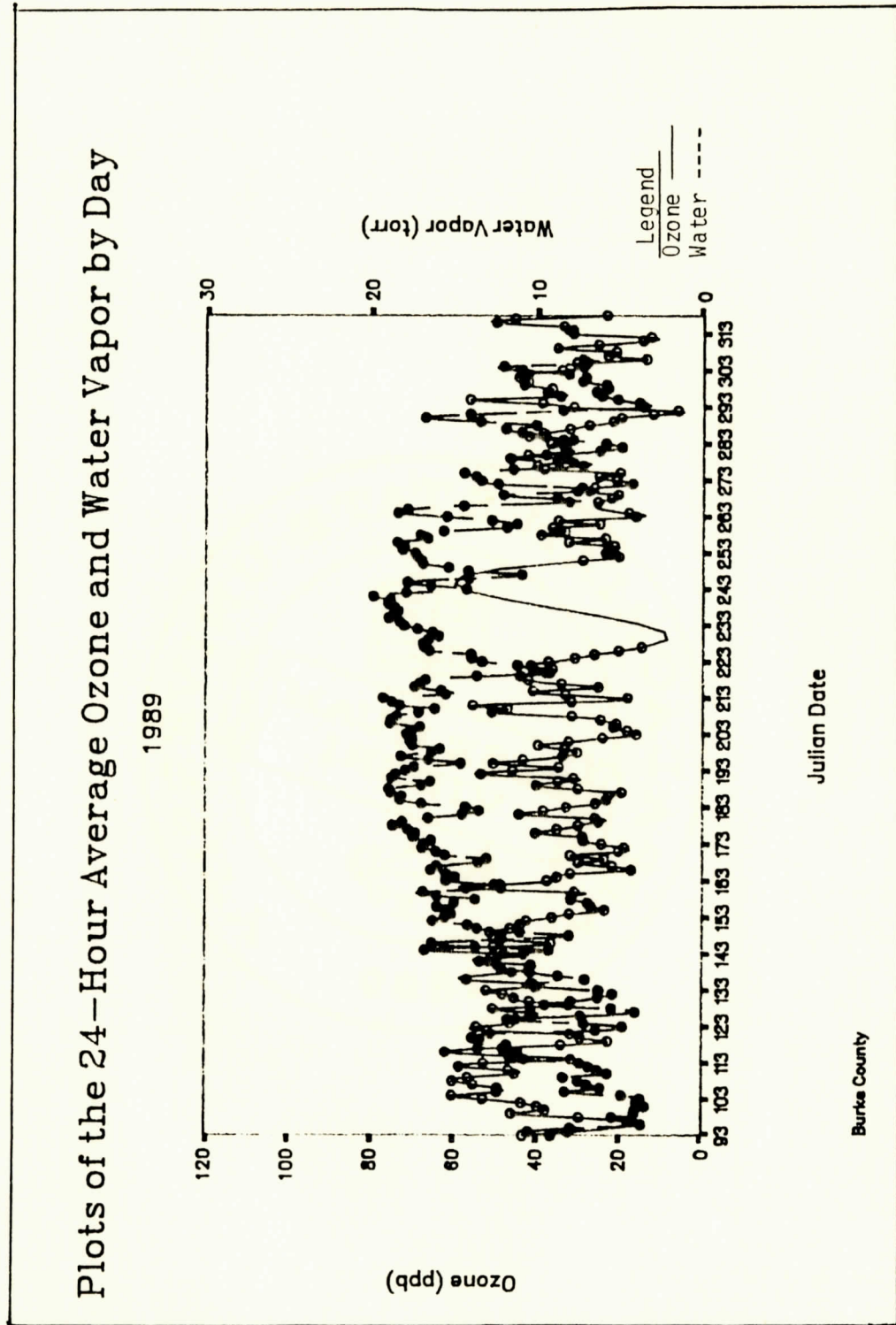


Figure 3.47: Twenty-four-hour average ozone and water vapor by day, for 1989, using a spline fit with S_m parameter 1.

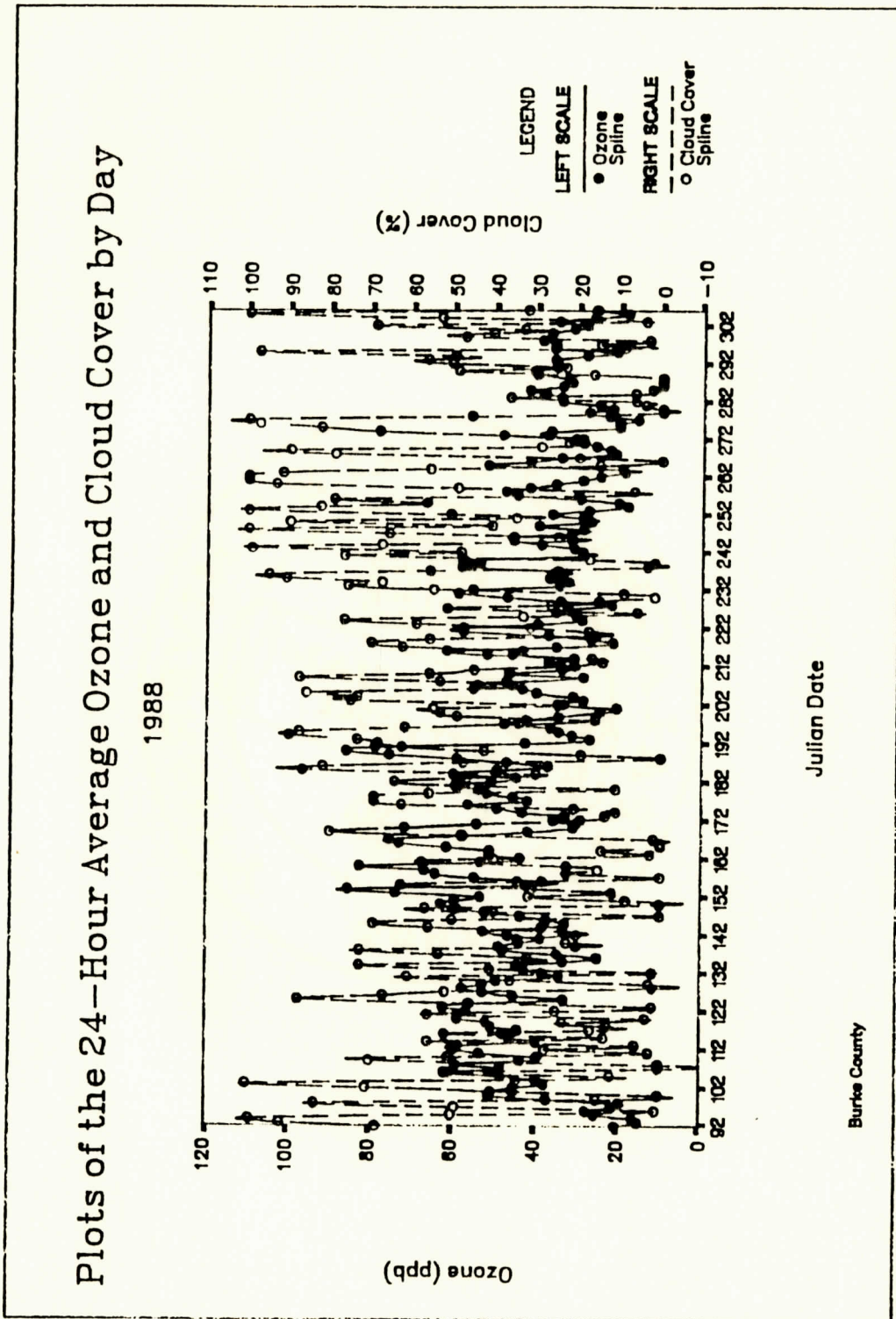


Figure 3.48: Twenty-four-hour average ozone and cloud cover in percent by day, for 1988, using a spline fit with Sm parameter 1.

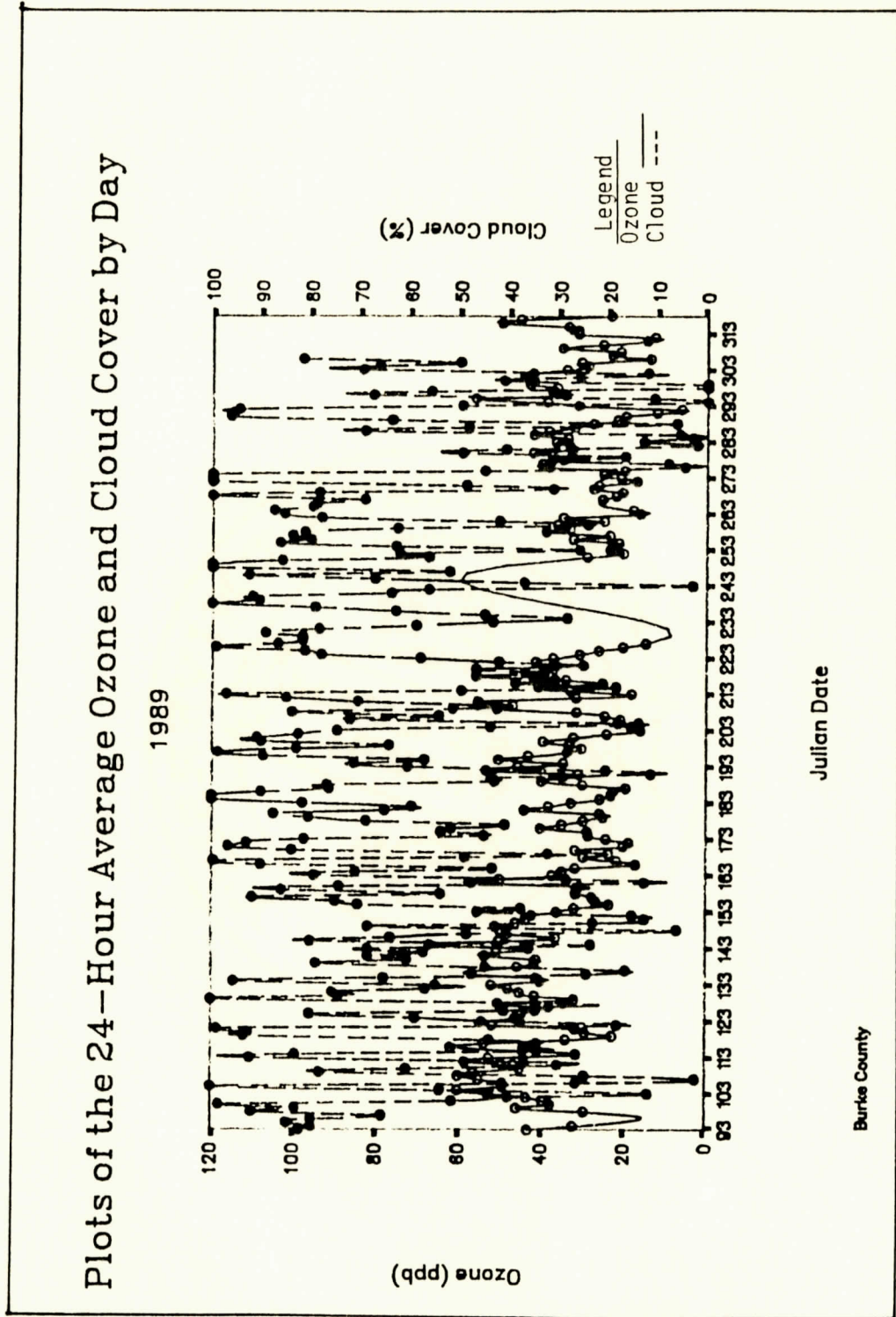


Figure 3.49: Twenty-four-hour average ozone and cloud cover in percent by day, for 1989, using a spline fit with Sm parameter 1.

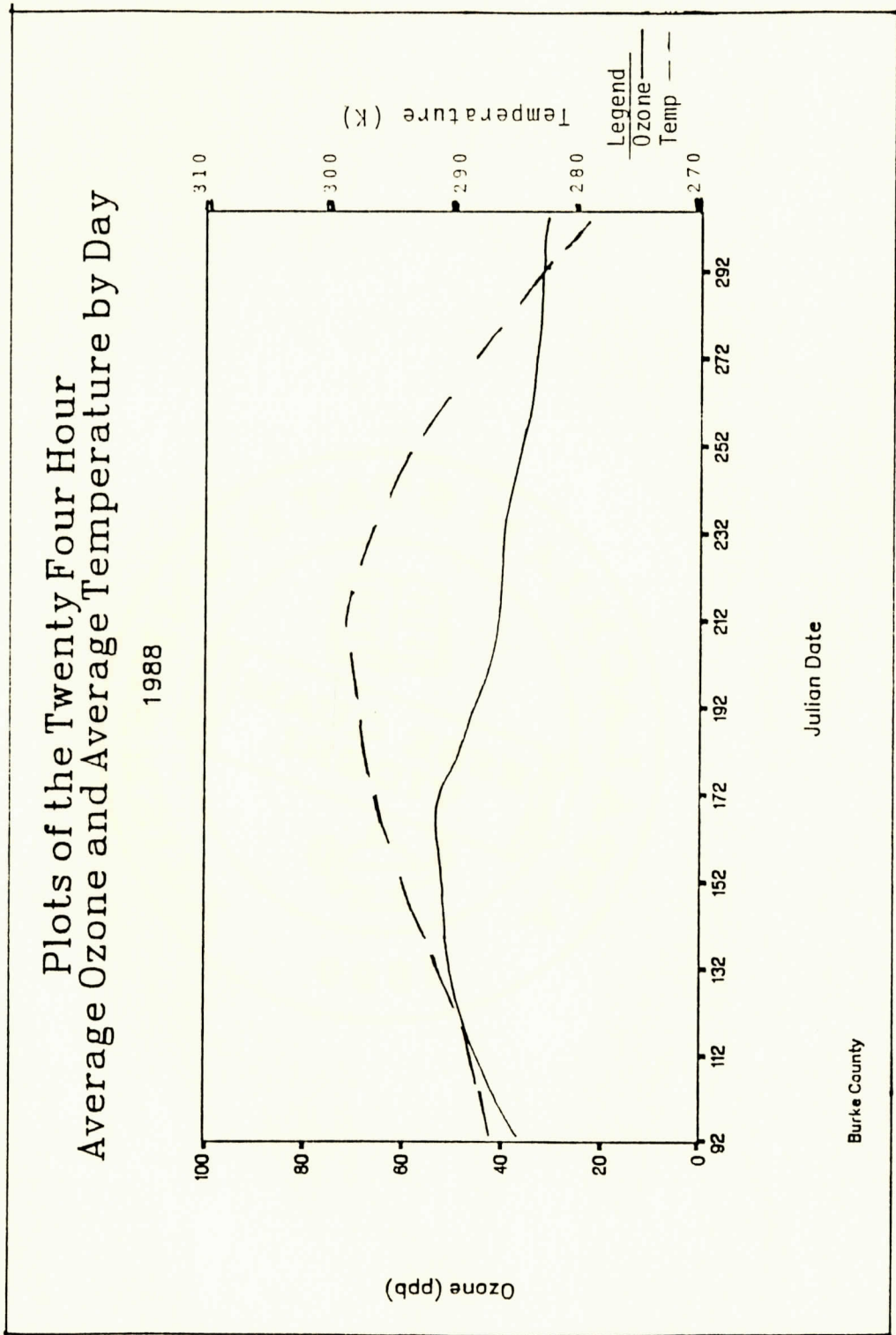


Figure 3.50: Twenty-four-hour average ozone and average temperature by day, for 1988, with a weighted least square smoothing parameter of 33.3.

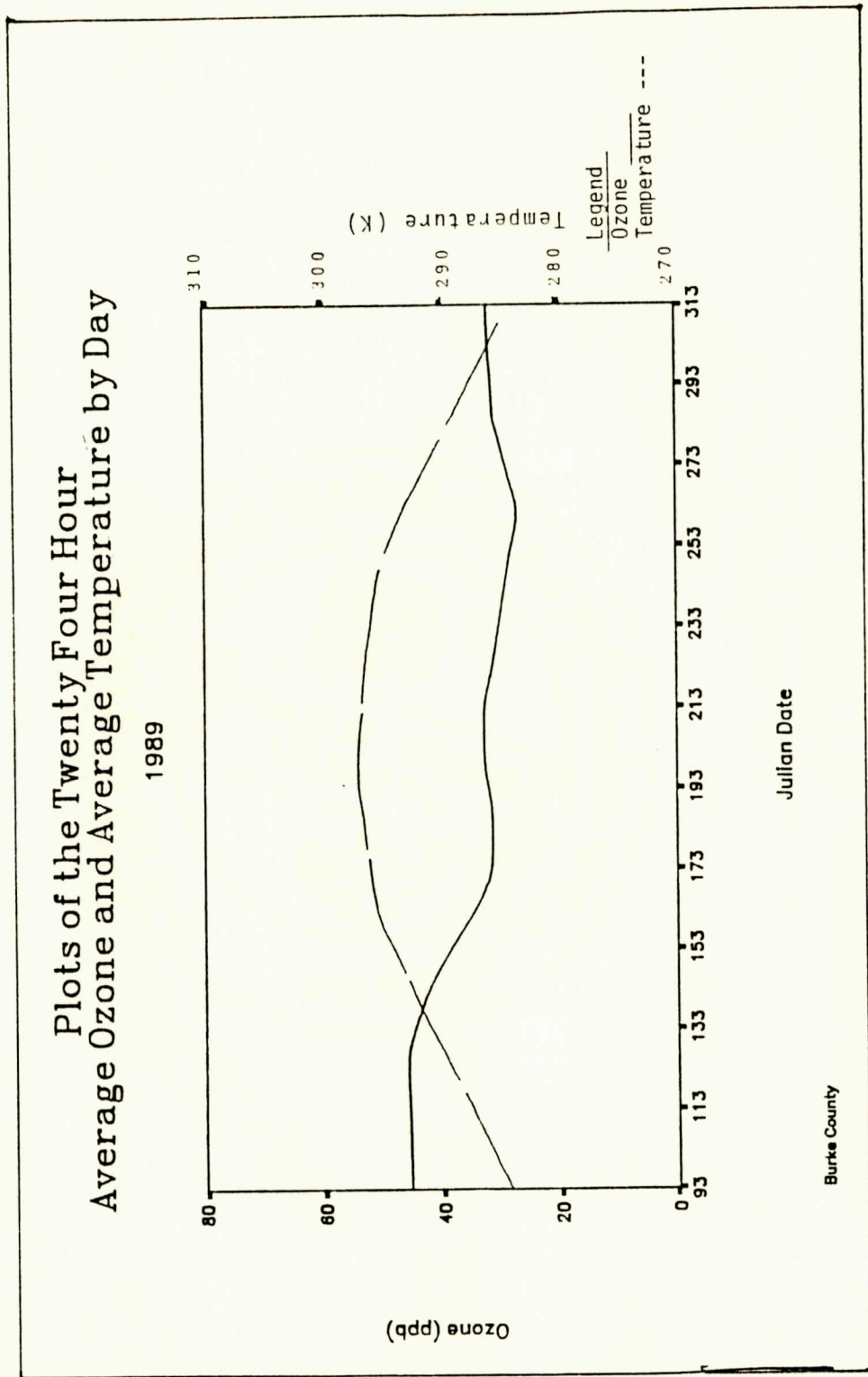


Figure 3.51: Twenty-four-hour average ozone and average temperature by day, for 1989, with a weighted least square smoothing parameter of 33.3.

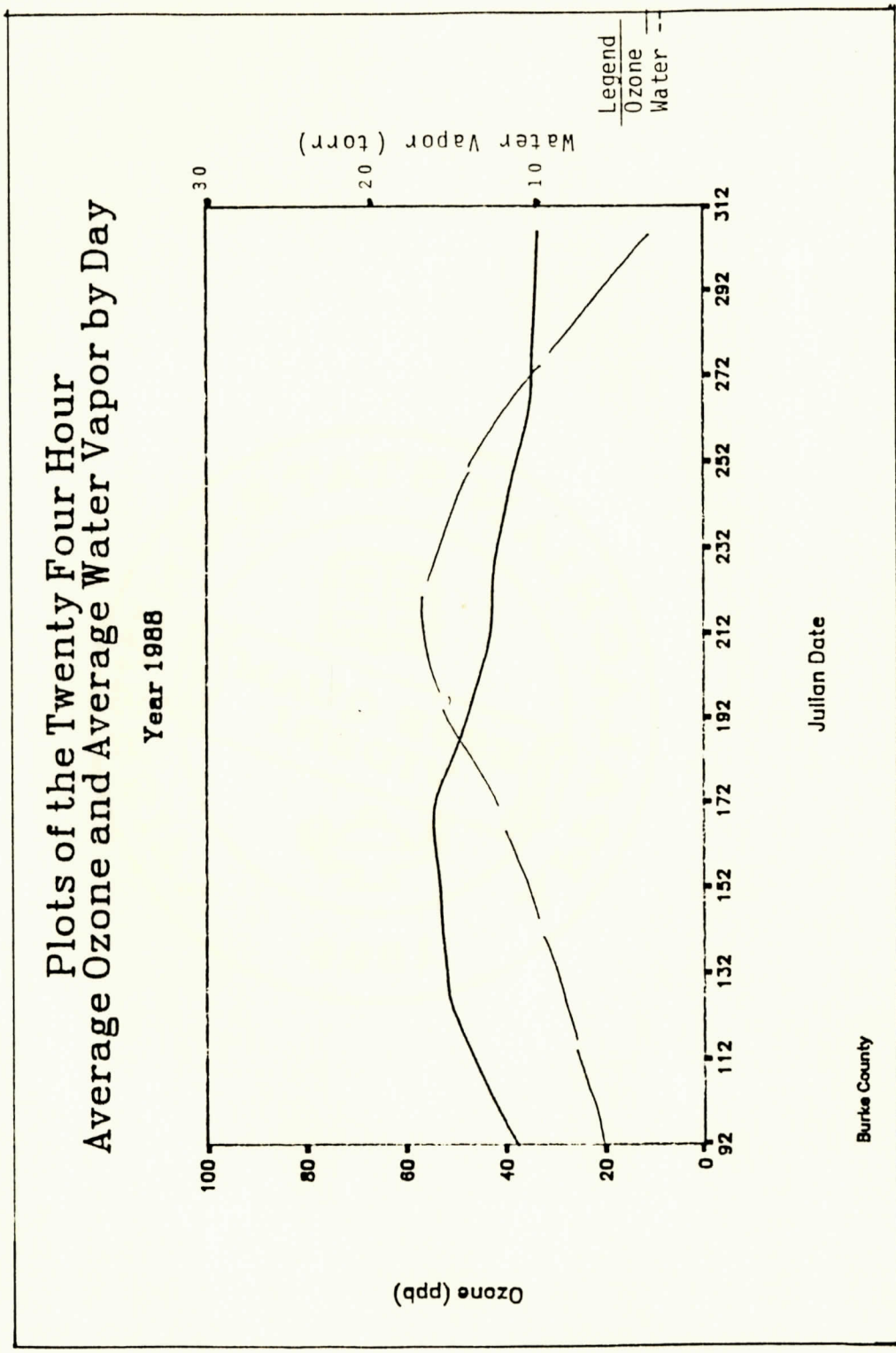


Figure 3.52: Twenty-four-hour average ozone and average water vapor by day, for 1988, with a weighted least square smoothing parameter of 33.3.

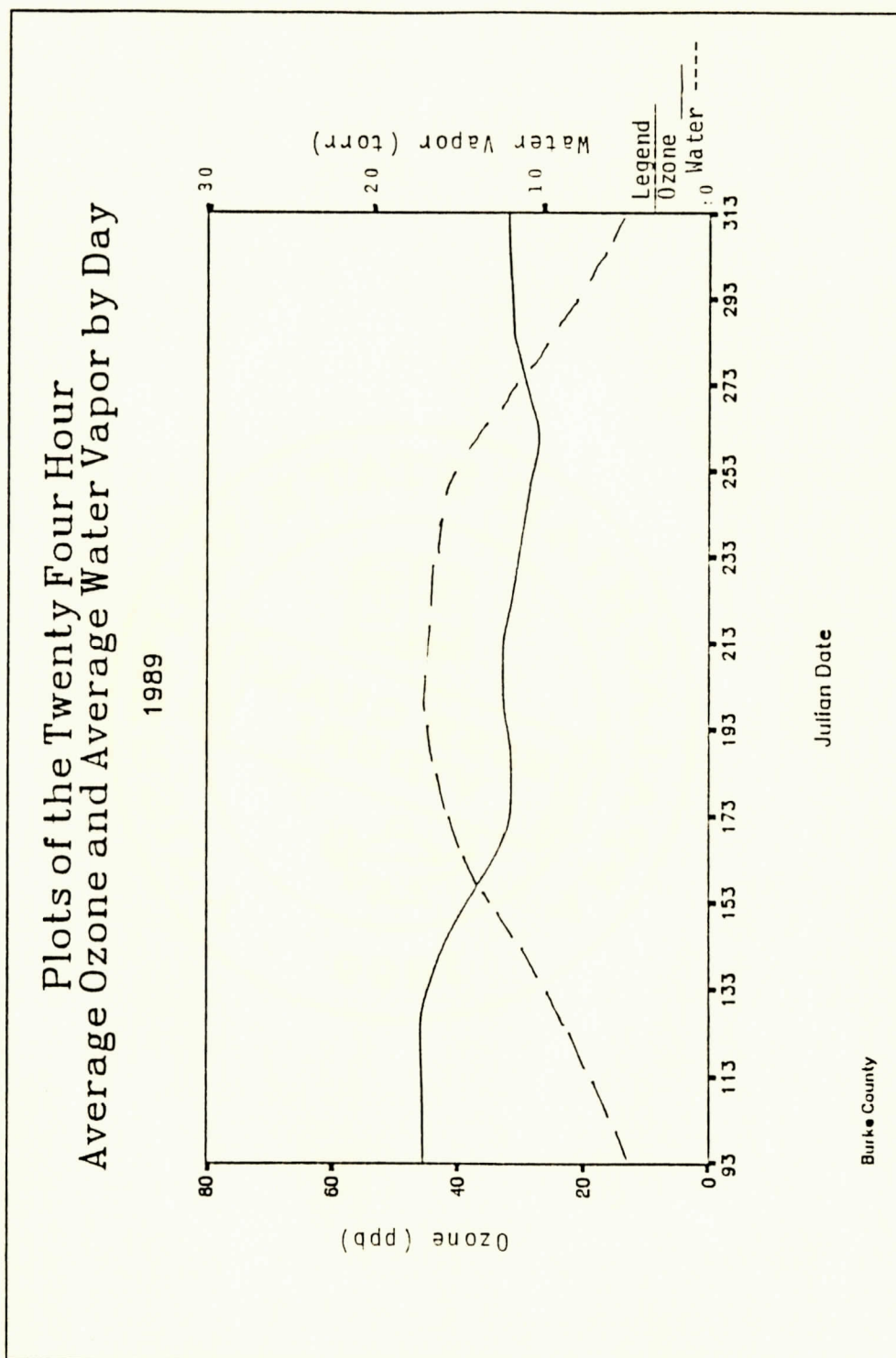


Figure 3.53: Twenty-four-hour average ozone and water vapor by day, for 1989, using a weighted least square smoothing parameter of 33.3.

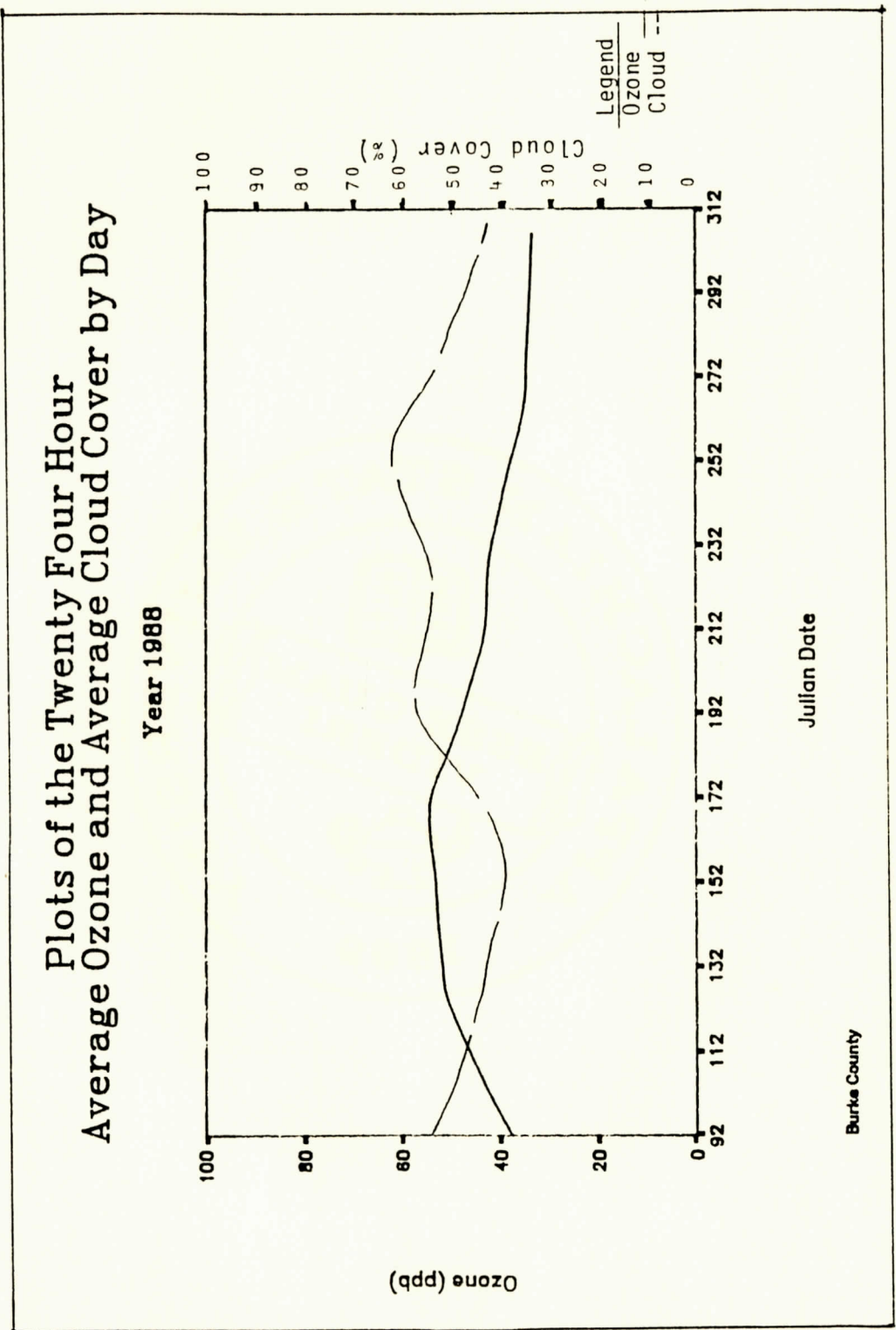


Figure 3.54: Twenty-four-hour average ozone and cloud cover by day, for 1988, with a weighted least square smoothing parameter of 33.3 .

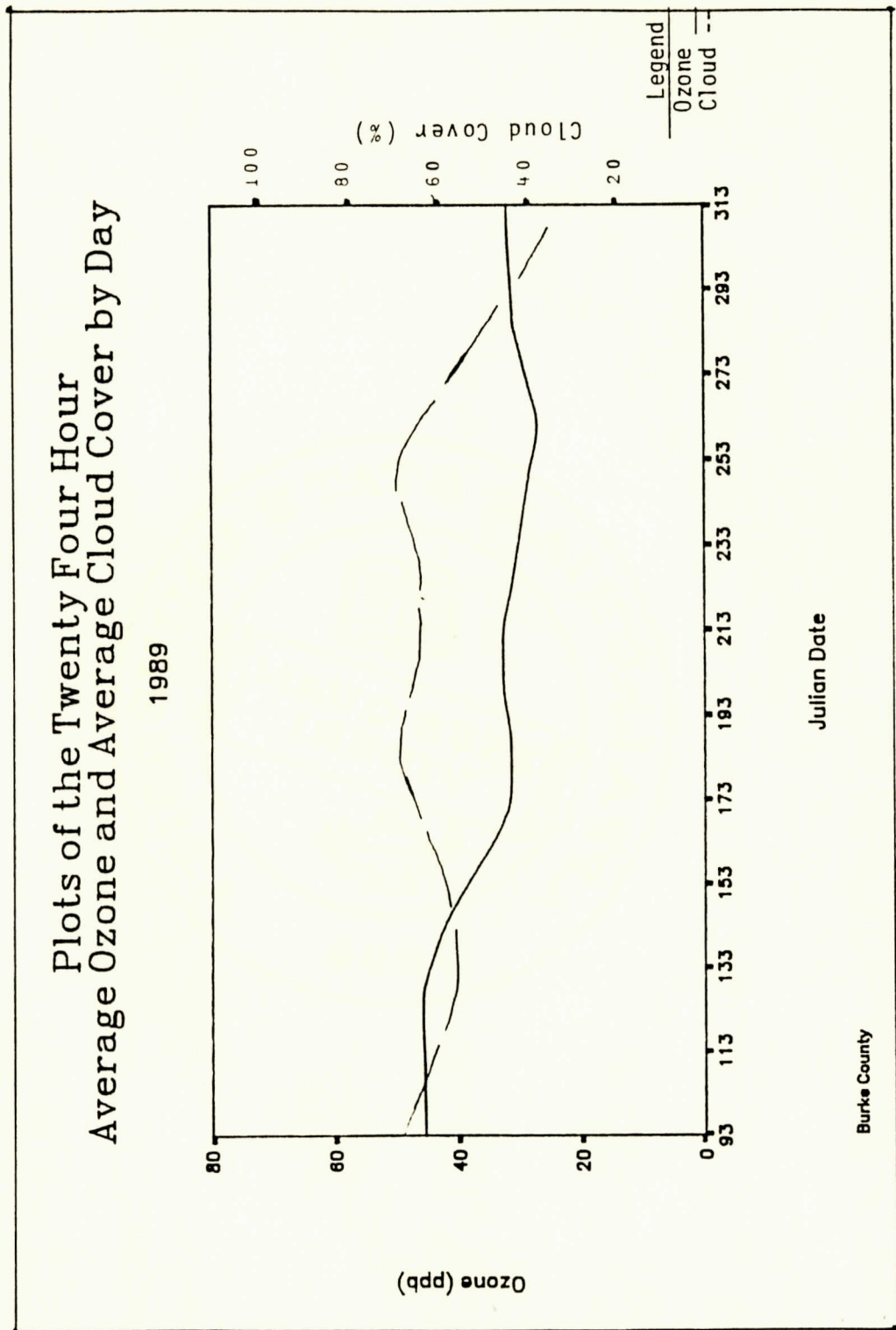


Figure 3.55: Twenty-four-hour average ozone and cloud cover by day, for 1989, using a weighted least square smoothing parameter of 33.3.

Table 3.4: Seasonal Coefficients of Determination (R squared) for 1988 and 1989 Daytime and 24-Hour Seasonal Periods.

| | 1988 | |
|--------|----------------|-------------------------|
| | <u>Daytime</u> | <u>Twenty Four Hour</u> |
| Spring | 0.37 | 0.40 |
| Summer | 0.54 | 0.51 |
| Fall | 0.62 | 0.55 |
| Year | 0.51 | 0.57 |
| | 1989 | |
| | <u>Daytime</u> | <u>Twenty Four Hour</u> |
| Spring | 0.65 | 0.71 |
| Summer | 0.13 | 0.42 |
| Fall | 0.74 | 0.65 |
| Year | 0.56 | 0.58 |

The independent meteorological variables chosen for the model equations were mean temperature, water vapor, and cloud cover. The equations generated had the general form

$$\text{OZONE} = \beta_0 + \beta_1 \text{temp} + \beta_2 \text{VP} + \beta_3 \% \text{cloud} \quad (30)$$

Where β_0 is the intercepts and $\beta_{1,2,3}$, are the respective variable coefficients. Temp is the mean daily ambient temperature in Kelvin, VP is the mean daily vapor pressure as calculated using the Clausius-Clapeyron Equation in torr (See page 67) and the mean dewpoint temperature, and %cloud is the mean daily cloud cover in percent. Table 3.5 is a composite of the coefficients generated and the intercept terms for the 1988 and 1989 equations. R squared for each equation were 57 and 58 percent for 1988 and 1989, respectively.

Table 3.5: Independent Variable Coefficients and Intercept Terms for 1988 and 1989.

| <u>Beta</u> <u>Coefficient</u> | <u>1988</u> | <u>1989</u> |
|-----------------------------------|-------------|-------------|
| 0 | -922.54 | -890.22 |
| 1 | +3.46 | +3.36 |
| 2 | -3.89 | -4.77 |
| 3 | +0.006 | +0.048 |

Magnitudes of the independent variable coefficients can be used as an indication of each variable's importance. Temperature showed a significant, positive correlation with ozone. Water

vapor was negatively correlated and showed larger coefficients than temperature. Cloud cover contributed negligibly to the prediction of ozone concentrations.

3.4.1 1988 and 1989 MLR Equations as Predictor Model

Figures 3.56 and 3.57 display the daytime 12-hour mean predicted and actual (measured) ozone for 1988 and 1989, respectively. Figures 3.58 and 3.59 are the respective 1988 and 1989 24-hour mean actual and predicted ozone. In each case, predicted ozone corresponds well with actual ozone. This result was expected, since Neter and Wasserman state that all equations generated by multiple linear regression handle their corresponding databases well³¹. The significant test of any regression equation is its predicting ability with a different database.

Figure 3.60 displays the results when testing the 1988 MLR equation by using 1989 weather variables to predict 1989 ozone concentrations. The results are disappointing. The model generally overestimates ozone concentrations by as much as 50 ppb. When testing the 1989 multiple linear regression equation, using the 1988 weather variables to predict 1988 ozone, the correspondence between predicted and measured ozone values was generally very close (See Figure 3.61).

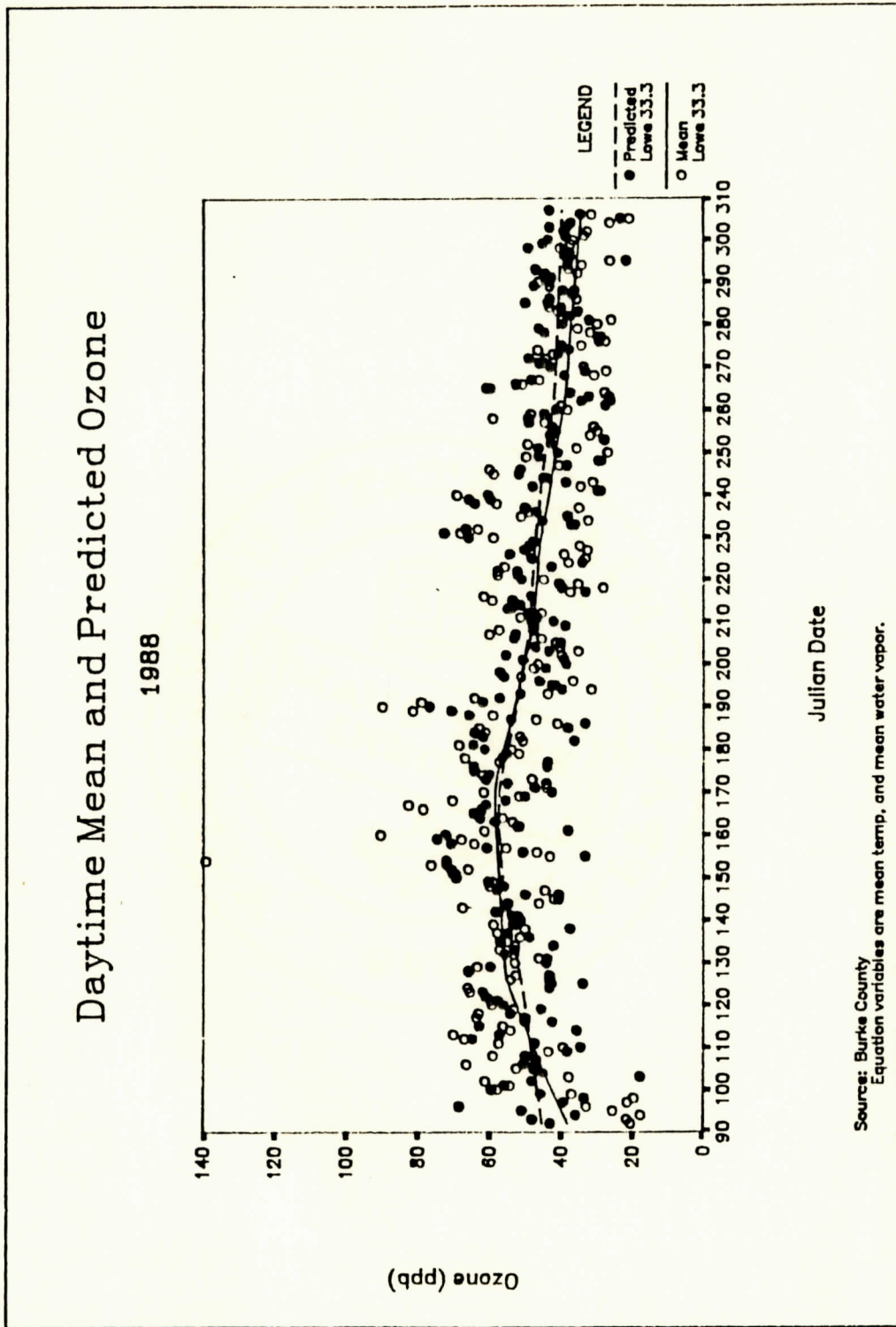


Figure 3.56: Daytime mean and predicted ozone for 1988, with a weighted least square smoothing parameter of 33.3.

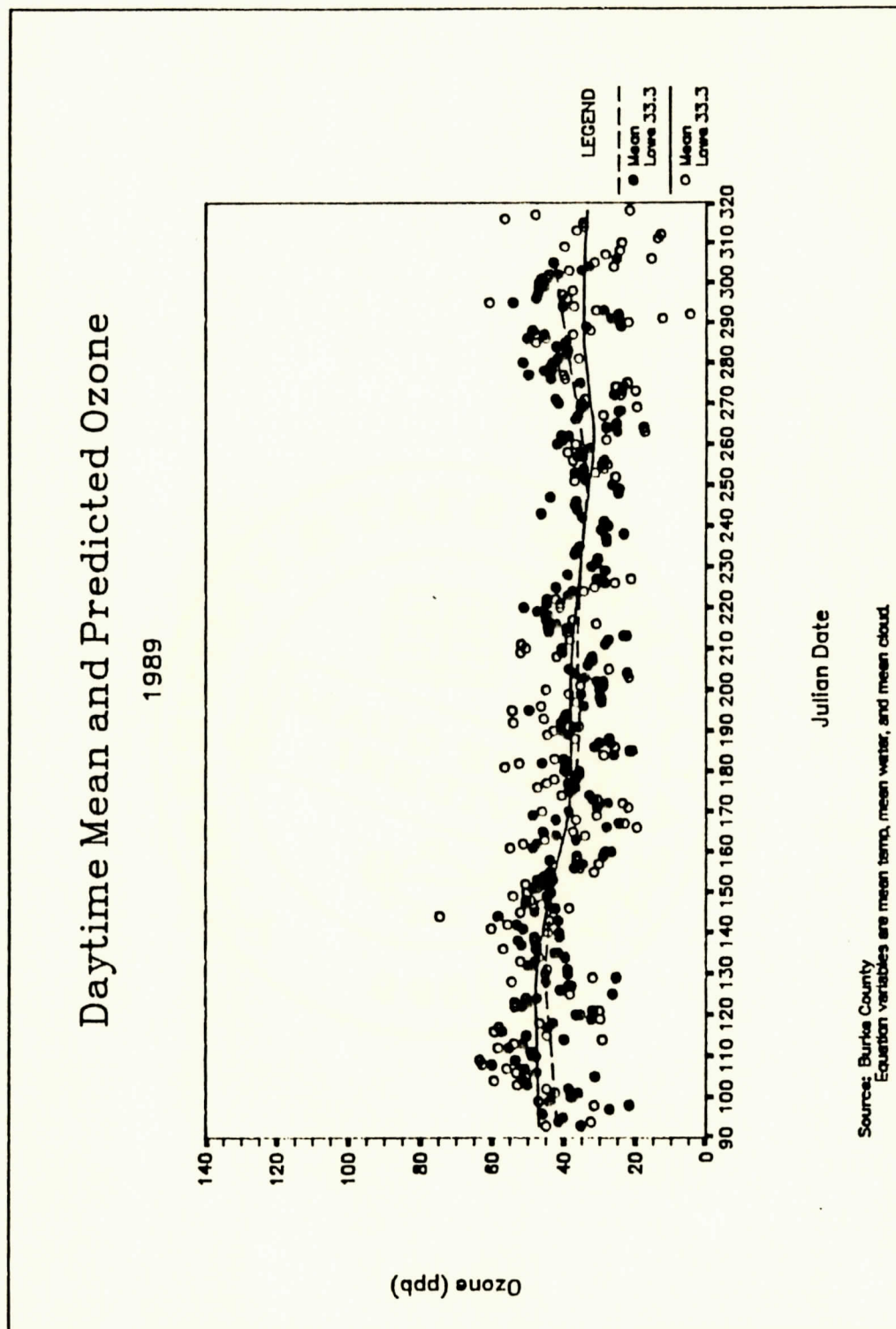


Figure 3.57: Daytime mean and predicted ozone for 1989, with a weighted least square smoothing parameter of 33.3.

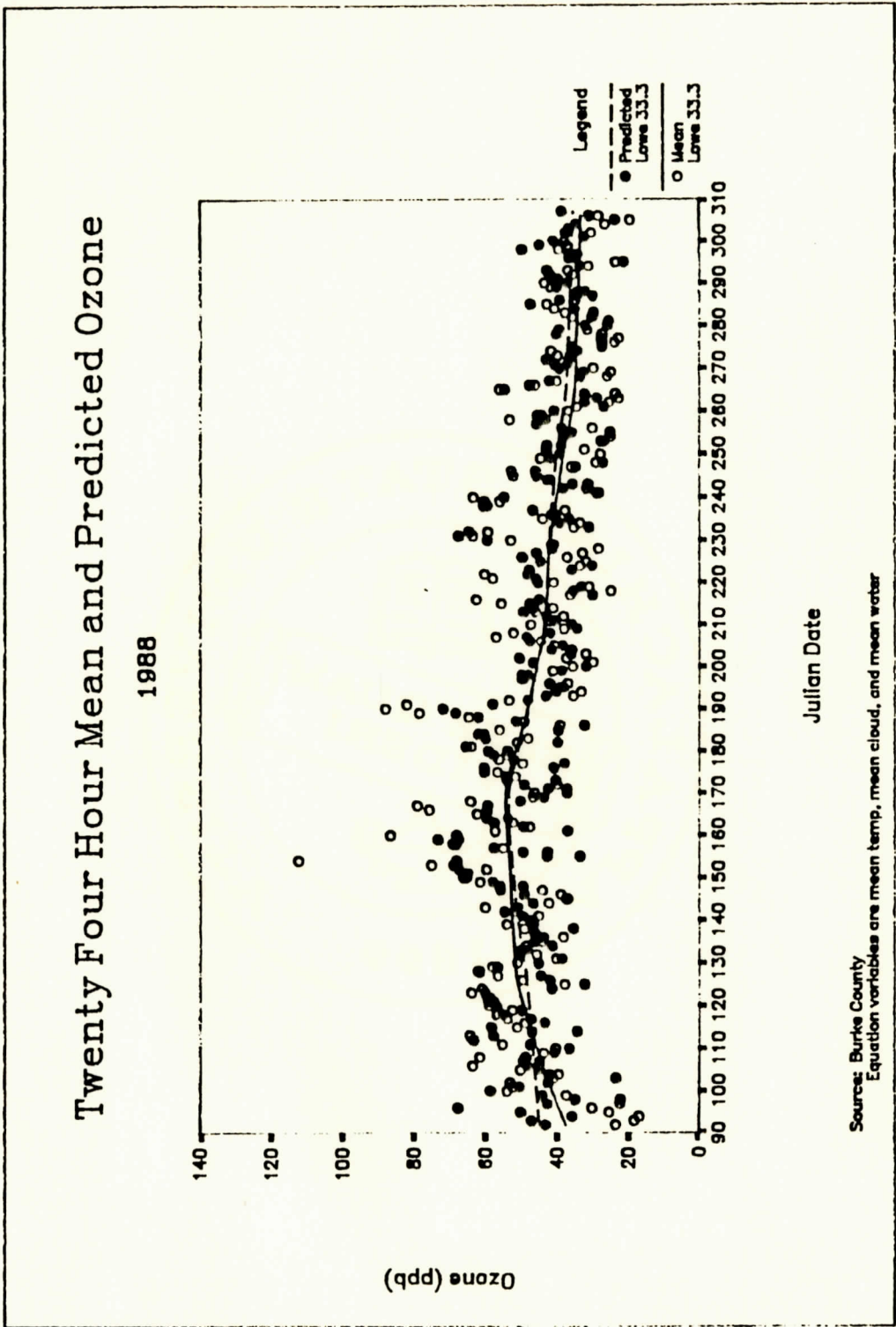


Figure 3.58: Twenty-four-hour mean and predicted ozone for 1988, with a weighted least square smoothing parameter of 33.3.

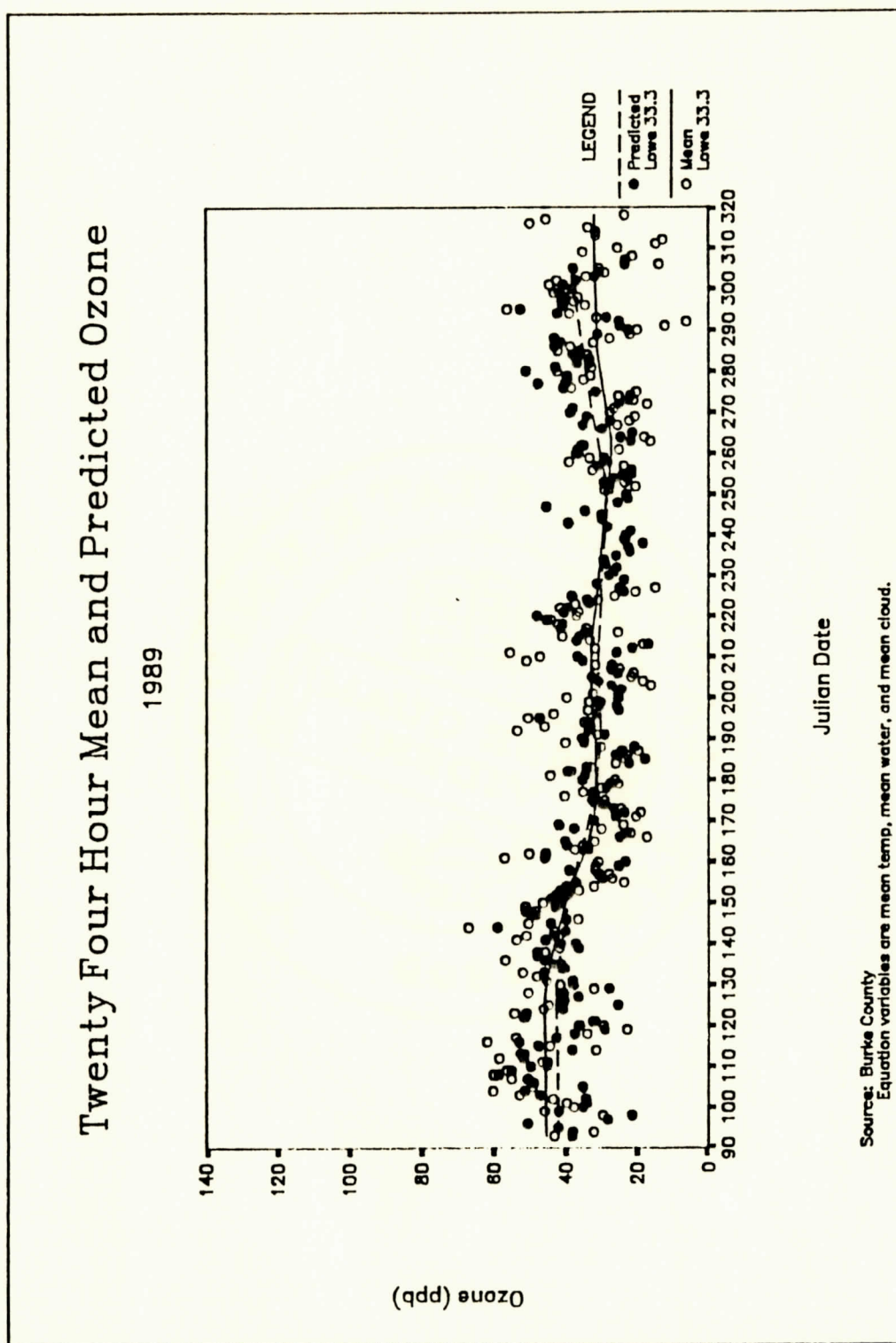


Figure 3.59: Twenty-four-hour mean and predicted ozone for 1989, with a weighted least square smoothing parameter of 33.3.

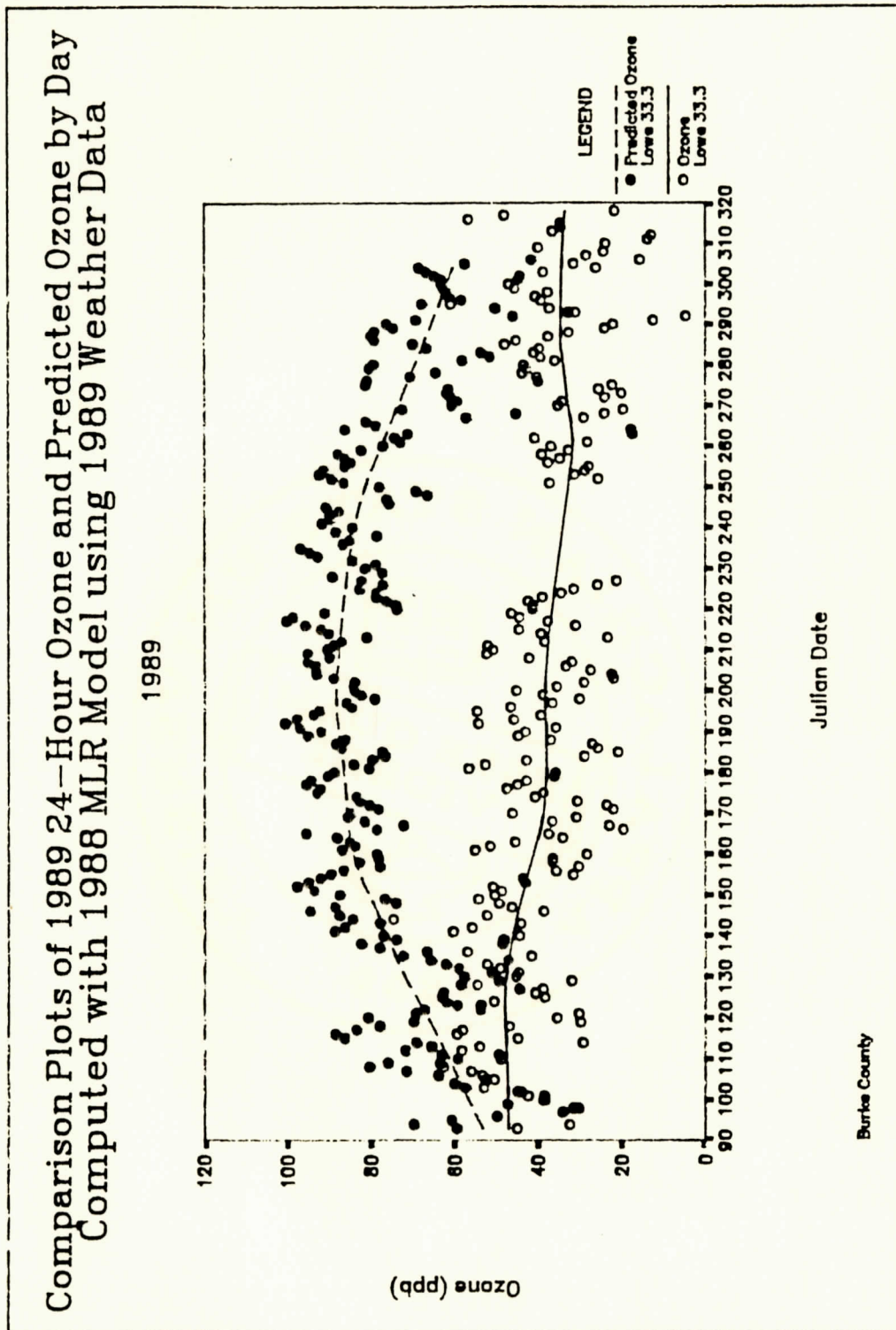


Figure 3.60: Comparison plots of the 1989 24-hour ozone and predicted ozone, computed with the 1988 multiple linear regression equation and using 1989 weather data. A weighted least square smoothing parameter of 33.3 is used.

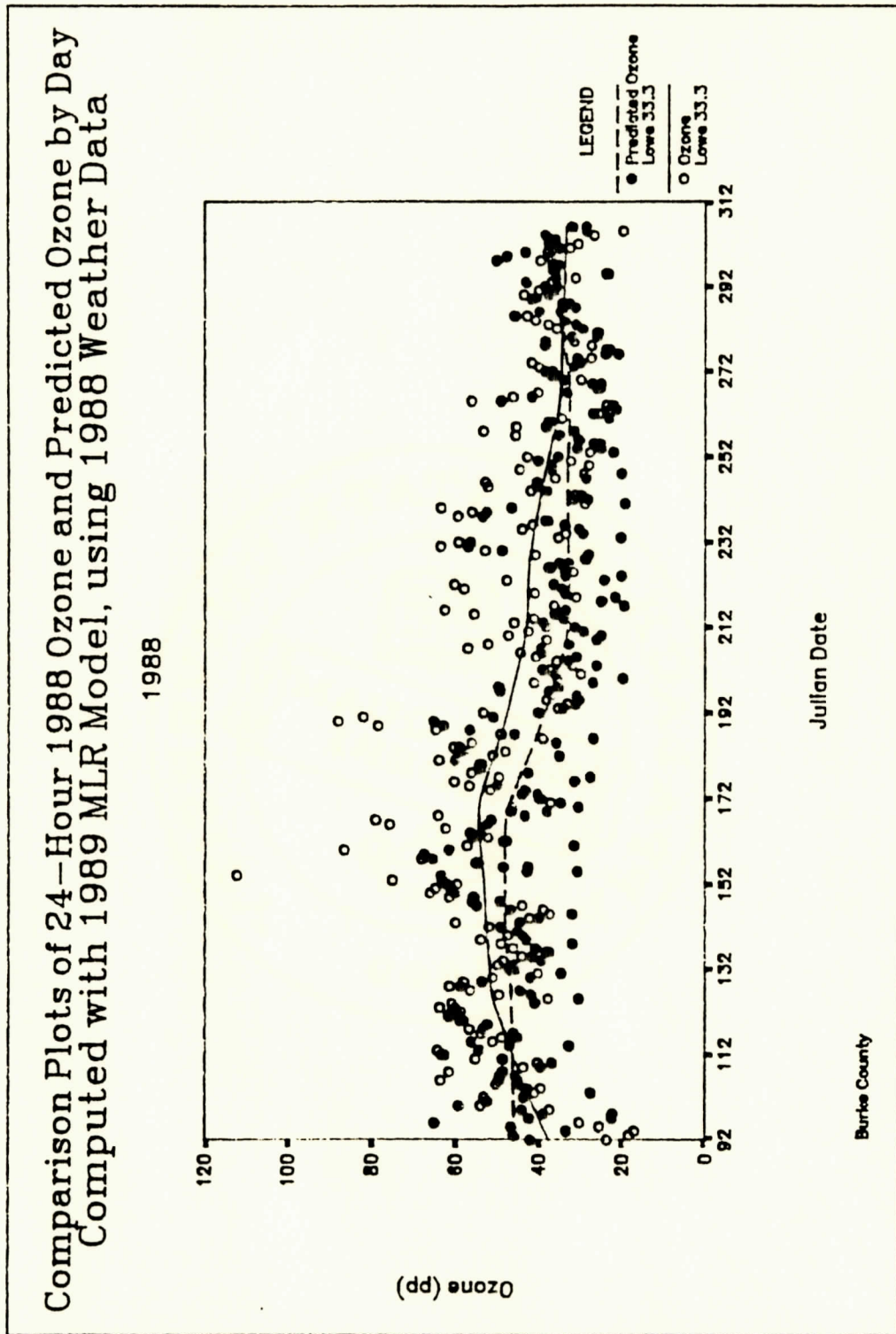


Figure 3.61: Comparison plots of the 1988 24-hour ozone and predicted ozone, computed with the 1989 multiple linear regression equation and using 1988 weather data. A weighted least square smoothing parameter of 33.3 is used.

Chapter 4

DISCUSSION AND CONCLUSIONS

Strong correlations exist between ozone and various weather variables, with more than 58 percent of the variance of ozone concentration being accounted for by the independent variables of temperature, water vapor, and cloud cover (See Table 3.4) from multiple linear regression. Cloud cover was much less important than temperature and water vapor, this might have been anticipated since cloud elevation and type vary greatly (See page 67).

The negative relationship between ozone and water vapor as shown by the independent variable coefficients (Table 3.5) was obvious and strong. Magnitudes of the coefficients generated in the 1989 multiple linear regression equation indicates that water vapor is the most important contributor to ozone prediction.

Aqueous phase reactions contribute significantly to a photochemical model suggested by Lelieveld and Crutzen²⁰. As a test of their model, we compared the annual mean hourly average ozone concentrations with hourly concentrations when ambient and dewpoint temperature differed by either zero or one degree Fahrenheit. Table 4.1 indicates that hourly ozone concentrations were reduced by 44-45 percent relative to the seasonal mean when moisture was present, just as predicted by Lelieveld and Crutzen.

Table 4.1: Reduction in Hourly Ozone from the Annual Mean, as a Function of Days when the Mean Atmosphere was saturated with Water Vapor.

| | <u>Hours Saturated/Total Hrs</u> | <u>% Reduction from Annual Mean</u> |
|------|----------------------------------|-------------------------------------|
| 1988 | 606/5019 | 45 |
| 1989 | 793/4692 | 44 |

In 1989, there were 187 more hourly averages taken in a saturated atmosphere than in 1988, again demonstrating the wetness of the 1989 season. Since the 1989 regression is a good predictor of 1988 ozone, but the reverse is not true, it appears that water vapor may be a stronger predictor of ozone than temperature. The current literature indicates ambient temperature as the most important meteorological parameter for estimating ozone^{14,15,25}.

Other factors which can affect ozone concentrations such as motor vehicle traffic and local emissions from the industrial environment were considered. From traffic reports as reported by NC Department of Transportation the daily traffic count for the area did not affect ozone concentrations. The major pollutant from industrial sources as reported by the NC Department of Natural Resources was a substantial amount of hydrocarbons. This information was considered, however, while we did not measure for hydrocarbons levels we were unable to draw any valid conclusions from this data concerning ozone concentrations.

This project has demonstrated a quantitative relationship between ozone and the weather variables temperature, water vapor, and cloud cover. The statistical model equation developed here uses simple variables, and no knowledge of ozone chemistry is required. Using weather variables is simple, and obtaining the data is inexpensive. Considering the simplicity of this model, it is satisfying that its predicting ability appears to be reasonably good. Further study is required to see if the equation will maintain its predicting ability for other years and at other sites.

References

1. Lefohn, A. S.; Pinkerton, J. E. *J. Air Pollution Control Assoc.* **1988**, *38*, 1504-1511.
2. Lefohn, A. S.; Runeckles, V. C.; Krupa, S. V.; Shadwick, D. S. *J. Air Pollution Control Assoc.* **1989**, *39*, 1039-1045.
3. Lefohn, A. S.; Runeckles, V. C. *Atmos. Environ.* **1987**, *21*, 561-568.
4. Yang, Y.S.; Skelly, J. M.; Chevone, B. I. *Environ. International* **1983**, *9*, 265-269.
5. Peterson, D. L.; Arbaugh, M. J. *J. Air Pollution Control Assoc.* **1988**, *38*, 921-927.
6. Altshuller, A. P. *J. Air Pollution Control Assoc.* **1987**, *37*, 1409-1417.
7. "Ozone and Forest Health", Electric Power Research Institute: Palo Alto, CA, 1988.
8. Chock, D. P. *J. Air Pollution Control Assoc.* **1989**, *39*, 1063-1072.
9. Aneja, V. P.; Businger, S.; Li, Z.; Claiborn, C.; Murthy, A., submitted for publication in *J. Geophys. Res.*
10. *Air Quality Criteria for Ozone and other Photochemical Oxidants*, U. S. Environmental Protection Agency, Research Triangle Park, NC, 1979; EPA-600/8/78-004.
11. Meagher, J. F.; Lee, N. T.; Valente, R. J.; Parkhurst, W. J. *Atmos. Environ.* **1987**, *21*, 605-615.
12. Chameides, W. L.; Davis, D. D. "Chemistry in the Troposphere", *Chemical and Engineering News*, Oct **1982**, 39-52.
13. Ching, J. K. S.; Shipley, S. T.; Browell, E. V.; Brewer, D. A. "Cumulus Cloud Venting of Mixed Layer Ozone", U. S. Environmental Protection Agency, Research Triangle Park, NC, 1985; EPA-600/D-84-299.
14. Finlayson-Pitts, B. J.; Pitts, J. N. *Atmospheric Chemistry: Fundamentals and Experimental Techniques.*, John A. Wiley: New York, 1986.
15. Fishman, J. PhD Dissertation, Saint Louis University, 1977.

16. Seinfeld, J. H. *Atmospheric Chemistry and Physics of Air Pollution*, John A. Wiley: New York, 1986.
17. Tingey, D. T.; Manning, M. *Plant Physiol.* **1980**, 797-801.
18. Worth, J. J.; Ripperton, L. A. *Rural Ozone-Source and Transport*, Research Triangle Institute, Research Triangle Park, NC.
19. Schwartz, S. E. *Nature* **1990**, 343, 209-210.
20. Lelieveld, J.; Crutzen, P. J. *Nature*, **1990**, 343, 227-233.
21. Finlayson-Pitts, B. J.; Pitts, J. N. *Atmospheric Chemistry: Fundamentals and Experimental Techniques.*, John A. Wiley: New York, 1986; Graedel, T. E., *Rev. Geophys Space Phys.*, 1979, 17, 937.
22. Trainer, M.; Williams, E. J.; Parrish, D. D.; Buhr, M. P.; Allwine, E. J.; Westburg, H. H.; Fehsenfeld, F. C.; Liu, S. C. *Nature* **1987**, 329, 705-707.
23. Bufallini, J. J.; Arnts, R. R. *Atmospheric Biogenic Hydrocarbons*, Ann Arbor Science, MI, 1981.
24. Altshuller, A. P. *Atmos. Environ.* **1983**, 17, 2131-2165.
25. Bach, W. D. *Investigation of Ozone and Ozone Precursor Concentrations at NonUrban Locations in the Eastern United States Phase II, Meteorological Analysis*, U. S. Environmental Protection Agency, Research Triangle Park, NC, 1975; EPA-450/3-74-034.
26. Pagnotti, V. J. *Air Waste Manage. Assoc.* **1990**, 40, 206-210
27. McRae, G. J.; Seinfeld, J. H. *Atmos. Environ.* **1983**, 17, 501-522
28. *Thermo Electron Model 49/49PS Instruction Manual*, Thermo Electron Corporation, Environmental Instruments Division, Mass. 1987.
29. *SX-405 Data Acquisition System-Operation Manual*, Austin, Tx, SX405-840131-03.
30. Buchanan, J. W.; Callahan, K. M., Final Report of Ozone Data Collection and Analysis in Burke County, NC, 1988.

31. Neter, J.; Wasserman, W. *Applied Linear Statistical Models*, Richard D. Irwin: Georgetown, Ontario, 1974.
32. Norusis, M. J. *SPSS-X Advanced Statistics Guide* 1988, Chpt 2.
33. Buchanan, J. W.; Thomas, T. L., Final Report of Ozone Data Collection and Analysis in Burke County, NC, 1989.
34. Wallace, J. M.; Hobbs, P. V. *Atmospheric Science, An Introductory Survey*, Academic Press: New York, 1977.
35. Byers, H. R. *General Meteorology*, 4th ed.; McGraw-Hill: New York, 1974, Chpt 5.
36. Holton, J. R. *Introduction Geophysic Series*, Miegheem, J. V., Ed.; Academic Press: New York 1972; 16.
37. Bach, W. D., Army Research Office at Research Triangle Park, personal communication, 1989.
38. Barrow, G. M. *Physical Chemistry*, 4th ed.; McGraw-Hill: New York, 1979, 314.

Vita

Terry Lee Thomas was born in Fort Bragg, North Carolina, on December 4, 1952. He attended Broadway Elementary and Broadway High School, where he graduated in May 1971. Mr. Thomas enlisted in the US Navy and served four years as a Hospital Corpsman Second Class. In 1975 he was honorably discharged from the Navy and entered Campbell College. He graduated with a Bachelor of Science degree in Chemistry in May, 1978. He accepted a Reserve Commission in the US Air Force in 1979 and served as Staff Weather Officer until April 1987. Mr. Thomas attended the University of Utah in 1980, and received 26 credit hours in Meteorology. He was honorably discharged from the US Air Force at the rank of Captain. In August, 1987, Mr. Thomas entered Appalachian State University and accepted a teaching assistantship. His thesis research was done under the supervision of Dr. James Buchanan. Mr. Thomas received a Master of Arts in Chemistry in August, 1990.

Mr. Thomas' address is P. O. Box 2, Broadway, North Carolina. His parents are Mr. Edward Warren Thomas (deceased), and Mrs. Nellie S. Thomas.